Dissertation

Submitted to the
Combined Faculties for the Natural Sciences and for Mathematics
of the Ruperto-Carola University of Heidelberg, Germany

For the Degree of
Doctor of Natural Sciences

Presented by
Melanie Marianne Barra (M.Sc.)
Born in Saarlouis, Germany

Oral Examination: 20.11.2014

Transcription factor 7 limits regulatory T cell generation and influences peripheral T cell subsets

Referees

1st Referee: Prof. Dr. Viktor Umansky

2nd Referee: Dr. Markus Feuerer

This dissertation was performed and written during the period from May 2011 to September 2014 in the German Cancer Research Center (DKFZ) under the supervision of Prof. Dr. Viktor Umansky and direct supervision of Dr. Markus Feuerer. The dissertation was submitted to the Combined Faculties for the Natural Sciences and for Mathematics of the Ruperto-Carola University of Heidelberg, Germany in September 2014.

German Cancer Research Center (DKFZ)
Immune Tolerance (D100)
Im Neuenheimer Feld 280
69120 Heidelberg, Germany

Confirmation

Hereby, I confirm that I have written this thesis independently, using only the results of my investigation unless otherwise stated. Furthermore I declare that I have not submitted this thesis for a degree to any other academic or similar institution.

Parts of this dissertation have been submitted for publishing:

> Transcription factor 7 limits regulatory T cell generation in the thymus
> Melanie M. Barra, David M. Richards, Jenny Hansson, Ann-Cathrin Joschko, Michael Delacher, Jan Hettinger, Jeroen Krijgsveld, and Markus Feuerer

Quantitative differential proteomics experiments in this dissertation were performed in collaboration with:

> Genome Biology Unit, EMBL, Heidelberg
> Dr. Jenny Hansson & Dr. Jeroen Krijgsveld

Heidelberg, 18th September 2014

Melanie M. Barra

Table of content

1 Summary

Regulatory T (T_{reg}) cells are generated in the thymus and are involved in the regulation of self-tolerance, immune homeostasis and immune responses. So far the mechanisms behind the T_{reg} cell differentiation and their function are not fully understood. The work of this thesis aimed to gain insight into these processes. We used a quantitative differential proteomics approach and identified 164 proteins that were differentially expressed in T_{reg} cells compared to conventional T cells. Among these transcription factor 7 (TCF7) was identified as a promising candidate for further investigations of its role in T_{reg} cells. Using a *Tcf7*-deficient mouse model we observed elevated frequencies of T_{reg} cells among CD4 single-positive and CD4 CD8 double-positive thymocytes in the absence of TCF7. Quite surprisingly, we also found a fraction of CD4 CD8 double-negative cells that expressed the T_{reg} cell transcription factor forkhead box P3 (FOXP3) independent of previous T cell receptor engagement, indicating that TCF7 prevents premature FOXP3 expression. *In vitro* T_{reg} precursor differentiation assays showed that the reduction of TCF7 levels was beneficial for the T_{reg} cell generation capacity and that TCF7 activation through the β-catenin/Wnt pathway had the opposite effect. Furthermore, our results indicated that FOXP3 supports down regulation of TCF7, as FOXP3 expression in thymocytes was accompanied by decreased levels of TCF7 and enforced expression of FOXP3 in T cells caused reduced expression levels of TCF7.

In addition to its role in thymic T_{reg} cell differentiation, we found that TCF7 was involved in regulating the balance between T_{reg} and T_H17 cells and the survival of NKT cells. TCF7 deficiency also changed the typical expression patterns of T_{reg} and T cell markers.

In summary, we propose that TCF7 is involved in limiting the access into the T_{reg} cell lineage and that TCF7 influences peripheral T cell subsets.

2 Zusammenfassung

Regulatorische T (T_{reg}) Zellen entstehen im Thymus und sind beteiligt an der Regulierung der Immunantwort, der Selbsttoleranz und der Immunhomöostase im Gewebe. Zurzeit sind die Mechanismen der T_{reg} Zellentstehung und ihrer Funktion noch nicht vollständig aufgeklärt. Zielsetzung dieser Doktorarbeit war es diese Mechanismen weiter zu untersuchen. Mithilfe einer quantitativ differentiellen massenspektroskopischen Herangehensweise war es uns möglich 164 Proteine zu identifizieren, die in T_{reg} Zellen im Vergleich zu konventionellen T Zellen differentiell exprimiert wurden. Zur weiteren Untersuchung seiner Funktion in T_{reg} Zellen wurde der Transkriptionsfaktor 7 (TCF7) als ein vielversprechender Kandidat befunden. Durch die Verwendung eines *Tcf7*-defizienten Mausmodells konnten wir beobachten, dass die Abwesenheit von TCF7 die Anteile von T_{reg} Zellen unter den CD4 einzelpositiven und CD4 CD8 doppeltpositiven Zellen erhöhte. Überraschender Weise konnten wir auch einen Anteil von CD4 CD8 doppeltnegativen Zellen feststellen, die den T_{reg} Zell Transkriptionsfaktor forkhead box P3 (FOXP3) unabhängig von vorangegangener T Zell Rezeptor Interaktion exprimierten. Dies deutet darauf hin, dass TCF7 die frühzeitige Expression von FOXP3 verhindert. *In vitro* Versuche zur T_{reg} Vorläuferdifferenzierung zeigten, dass sich verringerte TCF7 Level positiv auf deren Differenzierungspotential auswirkten und dass die Aktivierung von TCF7 durch den β-catenin/Wnt Signalweg den gegenteiligen Effekt hatte. Darüber hinaus deuteten unsere Ergebnisse darauf hin, dass FOXP3 die Herabregulierung von TCF7 unterstützt, da die Expression von FOXP3 in T Zellen und T_{reg} Vorläufen zeitgleich mit der verringerter TCF7 Expression auftrat.

Neben seiner Rolle bei der Differenzierung von T_{reg} Zellen haben wir herausgefunden, dass TCF7 an der Regulierung der Balance zwischen T_{reg} und T_H17 Zellen, sowie dem Überleben von NKT Zellen beteiligt war. TCF7 Defizienz veränderte außerdem die typischen Expressionsmuster von T_{reg} und T Zell Markern.

Zusammenfassend implizieren unsere Daten, dass TCF7 an der Limitierung des Zugangs zur T_{reg} Zelllinie beteiligt ist und dass TCF7 zusätzlich periphere T Zelluntergruppen beeinflusst.

3 Introduction

3.1 The immune system

3.1.1 General overview

The mammalian immune system consists of different tissue, cellular and molecular components that all work together to protect from disease. Various pathogens like viruses, bacteria, fungi or parasites can cause disease and are found in our environment. Pathogens greatly differ in their surface structures, their way of replication and their mechanisms of pathogenesis. Once the microorganism enters the body, the immune system is challenged to recognize, contain and eliminate the infection. Besides these environmental threats the immune system is faced with autoreactive, damaged or transformed cancerous cells of the host itself. Impaired function of the immune system can cause allergies, autoimmune disease or infection with opportunistic pathogens (Murphy et al., 2008).

The immune system can be subdivided into two major components: the innate and the adaptive immune responses. These two arms of the immune system are equipped with a diverse set of mechanisms to defend the body. The innate response represents the first line of immediate host defense against pathogens and most infections are cleared within hours by the defense mechanisms of the innate system. Once the innate response fails to contain the infection the adaptive immune response comes into play. Adaptive immunity relies on the clonal expansion of antigen specific cells that target the microorganisms and on the generation of long-lasting memory cells that prevent reinfection. For an effective clearing of disease, cooperation of both the innate and the adaptive systems is essential (Murphy et al., 2008).

3.1.2 The innate immune response

The first barriers that prevent pathogens from invading the body and replicating are the skin and mucosal epithelia. But these surface epithelia are not only a physical barrier, they also produce chemical components, so called antimicrobial peptides (Ganz, 2003) or enzymes to prevent pathogens from growing. The surface pH of the epithelia is often changed to a milieu in which the pathogens do not replicate and the mucosal epithelia secrete mucus that keeps pathogens from adhering. In addition, most epithelia are covered by a layer of nonpathogenic commensal bacteria that compete with pathogenic bacteria for nutrition and space (Murphy et al., 2008).

Once the pathogens overcome this first barrier they can be recognized and phagocytosed by tissue resident macrophages, dendritic cells (DCs) or if they enter the blood stream by neutrophils. After phagocytosis, the pathogens are destroyed by a mixture of toxic products and enzymes. Phagocytic cells use different specialized receptors to recognize pathogens and induce a proper immune response. Some receptors recognize repeating patterns found on the surface of microorganisms, others help to distinguish different types of pathogens. Receptor ligation can trigger different effects: phagocytosis, complement activation or induction of cytokines, chemokines and co-stimulatory molecules (Akira et al., 2006; Murphy et al., 2008).

The release of cytokines and chemokines results in local inflammation which then induces the expression of cell-adhesion molecules on the endothelial cells of local blood vessel cells. Movement of blood leukocytes, e.g. neutrophils and monocytes, is slowed down by the cell-adhesion molecules and the chemokines attract the cells to the site of inflammation. Depending on the signals they receive monocytes can either differentiate into macrophages or DCs (Murphy et al., 2008).

The complement system is one of the major components of the innate immune response. The complement system consists of plasma proteins that get activated directly by the pathogen or indirectly through pathogen bound antibodies. Activation of complement leads to a cascade of reactions and generates effector components with different functions. Fragments of the complement components are involved in opsonization of pathogens, chemotactic attractions of phagocytic cells, activation of leukocytes and cytolysis of pathogens through the membrane attack complex (Murphy et al., 2008; Rus et al., 2005).

Natural killer (NK) cells are the effector lymphocytes of the innate response. They are activated by interferons and macrophage-derived cytokines as a response to intracellular infections, especially by viruses. NK cells are able to discriminate healthy from infected cells through a variety of cell surface activating and inhibitory receptors. The activating NK cell receptors sense alert ligands that mark cells under distress. Inhibitory NK cell receptors detect constitutively expressed major histocompatibility complex (MHC) class I molecules and other "self-signals". Signaling from the inhibitory receptors usually overwrites the signal from the activating receptors. MHC class I is a receptor that randomly presents self-peptides produced within the cell. Expression of MHC class I and other self-ligands is often lost upon cellular stress. Once the absence of the self-ligands is detected, this induces killing of the target cell though cytotoxic granules. NK cells serve to contain the infection until the adaptive immune response, and in particular cytotoxic T lymphocytes (CTLs), clear the infection (Murphy et al., 2008; Vivier et al., 2008).

3.1.3 The adaptive immune response

If the innate immune response fails to eliminate the pathogen, adaptive immunity gets induced. T cells are the central cells of the adaptive immunity. After their development in the thymus the naïve T cells start to circulate in the bloodstream and the peripheral lymphoid organs. The naïve T cells continue to recirculate until they meet their specific antigen presented as a peptide:MHC complex by an antigen presenting cell (APC). MHC class I molecules are found on almost every nucleated cell, including APCs, and serve to present peptides from cytosolic produced proteins to T cells. MHC class II molecules are normally expressed by APCs and present peptides of extracellular proteins mainly derived from phagocytosed and digested pathogens. DCs are by far the most important APCs for the activation of T cells. After contact to the pathogen at the side of infection, DCs will migrate to lymph nodes (LN) and spleen, where they present the pathogen-peptide:MHC complexes to the T cells. T cells recognize the peptide:MHC complex with their surface T cell receptor (TCR) and CD4/CD8 molecules. In addition to the specific antigen, the T cells need CD28-dependent co-stimulation through CD80 or CD86 and cytokines to differentiate and proliferate into effector T cells that help to remove the pathogen. Depending on

the kind of pathogen, the T cells will differentiate into different effector T cells subtypes (Murphy et al., 2008).

$CD8^+$ naïve T cells recognize a complex of MHC class I and intracellular peptide. $CD8^+$ T cells are specialized in the detection of intracellular pathogens, in particular viruses. Upon stimulation they will differentiate into CTLs, which kill infected host cells through the release of cytotoxic granules that contain among others granzymes and perforin (Jenkins and Griffiths, 2010).

The TCR of $CD4^+$ T cells recognizes a complex of a pathogen peptide and a MHC class II molecule. Upon stimulation naïve $CD4^+$ T cells can differentiate into different CD4 effector subsets. Currently, CD4 effector subsets are mainly differentiated into T helper (T_H) 1, T_H2 and T_H17.

The T_H1 subset is induced through the cytokines interleukin 12 (IL-12) and interferon γ (IFNγ) and is characterized by the expression of the transcription factor T-bet and the release of IL-2 and IFNγ. T_H1 cells are associated with cell-mediated immunity and have two different functions. Certain bacteria, such as mycobacteria can upon phagocytosis through macrophages evade the usual killing mechanisms and instead replicate inside the macrophages. One role of T_H1 cells is to detect such infected macrophages, stimulate them further and thereby enable killing of the intracellular bacteria. The second function of T_H1 cells is to stimulate antibody production and also class switching of B cells. B cells activated through T_H1 cells will produce opsonizing antibodies, primary Immunoglobulin G (IgG).

IL-4 induces T_H2 cells, which are characterized by the expression of the transcription factor GATA3 and the secretion of IL-4 and IL-5. T_H2 cells are also involved in the activation and class switching of B cells. The humoral immune response induced by T_H2 leads to the production of IgM, IgA and IgE antibodies by B cells. Besides interaction with T cells, B cells need prior contact with their specific antigen via their B cell receptor molecule to get activated. The activating T cells need to have the same antigen specificity as the activated B cells. Upon activation, B cells proliferate and differentiate either into antibody-secreting plasma cells or into memory B cells. Antibodies secreted by B cells serve different functions: they can neutralize a pathogen, facilitate uptake by phagocytes or activate the complement system (Murphy et al., 2008).

A combination of the cytokines transforming growth factor β (TGFβ) and IL-6 leads to differentiation into the T_H17 lineage. T_H17 cells are characterized by the expression

of RORγT and the secretion of IL-17. T_H17 cells are usually the first T cells that emerge during infections. They induce massive tissue inflammation, recruit neutrophils to the side of infection and thereby help to clear infection with different pathogens (Korn et al., 2009).

NKT cells are innate-like mostly $NK1.1^+CD4^+$ thymocytes that develop in the thymus and express a TCR. Development of these cells in the thymus is independent of MHC class I and II molecules but instead dependent on MHC–like CD1d molecules which bind self- and microbial-glycosphingolipids. NKT cells proliferate and acquire an effector/memory phenotype prior to the emigration from the thymus. The stimulation of NKT cells through glycosphingolipids leads to the secretion of IFNγ, IL4 and chemokines and to the activation of DCs. DCs in turn prime adaptive CD4 and CD8 T cell responses. In addition, NKT cells can activate NK cells and activate antibody production by B cells (Bendelac et al., 2007).

T_H1, T_H2, T_H17 and NKT cells all carry a TCR consisting of one α- and one β-chain. In contrast to those cells, γδT cells have a TCR consisting of a γ- and δ-chain. γδT cells are especially found within epithelial tissues, e.g. skin, but also in lymphoid tissues. These T cells have been described as innate-like since their TCRs have only a limited diversity compared to the αβTCRs and it seems that they are not depending on MHC interaction for activation. It was suggested that those cells recognize molecules that are derived from the epithelia themselves as a result of cellular stress (Murphy et al., 2008; Thedrez et al., 2007).

Last but not least, regulatory T (T_{reg}) cells have to be introduced as an important part of the adaptive immune system. These cells maintain the tolerance towards self-antigens, regulate immune reactions and immune homeostasis through their suppressive mechanisms (Vignali et al., 2008). T_{reg} cells are characterized by high surface expression of the IL-2 receptor molecule CD25 and by expression of the transcription factor forkhead box P3 (FOXP3), which was identified as essential for proper T_{reg} cell function (Fontenot et al., 2003; Hori et al., 2003; Khattri et al., 2003). T_{reg} cells are in the focus of this dissertation and their generation and function will be explained in the following chapters of this introduction.

3.2 Generation of T cells

3.2.1 The multi-step process of thymic T cell selection

All T cells are thymus derived. T cell progenitors develop from pluripotent hematopoietic stem cells in the bone marrow and migrate to the thymus where they differentiate into the different types of mature T cells. At first, these multi lymphoid progenitors do not express the TCR or the surface co-receptors CD4 and CD8. Due to the lack of CD4 and CD8 surface expression these precursors are termed double-negative (DN) cells. The DN precursors are divided into DN1-DN4 developmental stages depending on their CD44 and CD25 expression. Between the DN2 and DN3, stages the first gene rearrangement takes place, which results in the expression of TCRβ, TCRγ and TCRδ chains. At this point, commitment to either αβT or γδT cell lineage takes place and the development of γδT cell branches off from the αβT cell development (Ceredig and Rolink, 2002). TCRβ rearrangement leads to the expression of a pre-TCR complex, composed of the TCRβ chain, a pre-Tα molecule and CD3. Successful signaling of the pre-TCR allows the precursors to pass the DN3 checkpoint and leads to proliferation at the late DN3 and early DN4 stage (von Boehmer, 2005). Finally the cells start to rearrange their *Tcra* gene resulting in the expression of an αβTCR on the cell surface. In addition, expression of CD4 and CD8 co-receptors is induced. These $CD4^+CD8^+$ T cell precursors are referred to as double-positive (DP) cells. For further maturation into specialized CD4 or CD8 single-positive (SP) cells, the DP cells need to undergo positive and negative selection processes (von Boehmer and Melchers, 2010). During positive selection, cortical thymic epithelial cells (cTECs) present MCH class I and II molecules to the DP cells. DP cells that fail to recognize MHC molecules with their TCR are eliminated through apoptosis. This selection step also decides whether the cells will commit to the CD4 or CD8 T cell lineage. DP precursors that interact well with MHC class II will commit to a CD4 T cell fate, the ones interacting well with MHC class I will commit to the CD8 T cell lineage (Taniuchi, 2009). Once the cells have been positively selected, medullary thymic epithelial cells (mTECs) and other thymic APCs will present them with a broad range of self-peptide:MHC complexes. mTECs are capable of promiscuous gene expression, which is facilitated by the transcription factor AIRE. If

the affinity of a TCR toward these self-antigens is too strong, the precursor will be driven into apoptosis. Thereby negative selection helps to eliminate potentially autoreactive T cells (Klein et al., 2014). To escape negative selection, conventional $CD4^+$ or $CD8^+$ T cells need to express a TCR with low to moderate affinity towards self-antigen, while $CD4^+$ T cells committed to the T_{reg} cell lineage typically express a TCR with a higher affinity for self-antigens (Hogquist, 2001).

3.2.2 Thymic T_{reg} cell generation

The majority of the T_{reg} cell population is thymic derived. The importance of thymic derived T_{reg} (tT_{reg}) cells was first noted in thymectomy experiments. Thymectomy in newborn mice on day 3 but not day 7 resulted in severe autoimmune disease. This observation was later explained by the fact that T_{reg} cells which start to migrate from the thymus into the periphery after day 3 are essential for inducing and maintaining self-tolerance (Asano et al., 1996; Fontenot et al., 2005a). Hence the thymus establishes immune tolerance not only by eliminating potentially autoreactive T cells from the conventional T (T_{conv}) cell pool, but also by generating the tolerance inducing population of tT_{reg} cells (Hsieh et al., 2012). Different molecular and cellular aspects contribute to the differentiation of T_{reg} cells in the thymus and will be introduced in the following paragraphs.

In the past years several experimental approaches addressed the question if TCR self-reactivity is the driving force behind tT_{reg} generation with differing results. The first hints for a role of TCR specificity came from experiments that used mice which only expressed a transgenic TCR with specificity for chicken ovalbumin. $CD4^+CD25^+$ T_{reg} cells were completely absent from the thymi of these mice (Itoh et al., 1999). Later studies showed that for the generation of tT_{reg} cells, the matching cognate antigen needs to be present in the TCR-transgenic mouse (Apostolou et al., 2002; Jordan et al., 2001; Knoechel et al., 2005). Comparative analysis of the TCR hyper variable complementarity determining region 3 (CDR3) repertoires between T_{conv} and T_{reg} cells from mice with limited TCR diversity showed only little overlap of the sequences from the two subsets, also indicating an important role of TCR specificity in tT_{reg} cell selection (Hsieh et al., 2004; Pacholczyk et al., 2006; Wong et al., 2007). In line with the hypothesis that part of tT_{reg} TCRs cells recognize self-antigen, one study identified a T_{reg} TCR that appears to be specific for skin antigen (Killebrew et

al., 2011). Controversially, studies using other TCR-transgenic mouse models detected that expression of the tT_{reg} TCRs resulted in negative selection rather than tT_{reg} cell generation or increased frequencies of tT_{reg} cells due to preferential survival of tT_{reg} cells (Shih et al., 2004; van Santen et al., 2004). In contrast to the reports mentioned above, one other study of TCR repertoires detected a large overlap of the T_{conv} and T_{reg} cell TCR sequences and suggested that several T_{reg} cell TCRs recognize foreign antigens (Pacholczyk et al., 2007). As an alternative route to the selection by TCR specificity it was proposed that induction of the tT_{reg} cell lineage could at least partially occur at the DN cell level (Pennington et al., 2006). Although controversially discussed for years, the current evidence is in favor of a role of TCR specificity in tT_{reg} cell selection.

Besides TCR specificity, intraclonal competition is a factor described to play a role in tT_{reg} cell differentiation. Studies using transgenic mice that express the naturally occurring TCRs of tT_{reg} cells showed that the factors required for tT_{reg} cell development are limited (Bautista et al., 2009; Leung et al., 2009). These results suggested that access to the tT_{reg} cell lineage is in part restricted by the number of thymic APCs and the amount of antigen presented.

Another factor that determines tT_{reg} cell selection is TCR signaling strength. The current model suggests that the interaction avidity that drives commitment into the tT_{reg} cell lineage lies higher than that of T_{conv} cell selection and even slightly overlaps the area of negative selection. It was observed in a TCR-transgenic mouse model that recognized an expressed cognate antigen with either high or low affinity, that the antigens recognized with a low affinity did not drive T_{reg} cell development (Cozzo Picca et al., 2011). These results demonstrated the importance of the interaction affinity between TCR and peptide-MHC in tT_{reg} cell selection. Experiments using a transgenic mouse with green fluorescent protein (GFP) under the control of the *Nr4a1* promoter gave interesting insights into the signaling strength required for tT_{reg} cells differentiation. In these mice, TCR stimulation results in activation of the *Nr4a1* gene. Hence, GFP expression is directly correlated with the TCR signaling strength. GFP levels detected in $Foxp3^+$ T_{reg} cell were higher than those detected in the $Foxp3^-$ cells indicating that differentiation into the tT_{reg} cell lineage requires higher signaling strength (Moran et al., 2011).

In addition to the TCR signaling strength itself, co-stimulation via CD28 seems to be involved in the generation of T_{reg} cells. Frequencies of generated tT_{reg} cells were

massively decreased under CD28-deficient conditions (Salomon et al., 2000; Tai et al., 2005).

Based on the current knowledge, a two-step model of T_{reg} cell differentiation was proposed (Figure 1) (Lio and Hsieh, 2008). It was previously noted that CD4SP $CD25^+FOXP3^-$ cells preceded the generation of CD4SP $CD25^+FOXP3^+$ cells and that CD4SP $CD25^+FOXP3^-$ precursors did not depend on TCR stimulation to up regulate FOXP3 (Fontenot et al., 2005b; Lio and Hsieh, 2008). While up regulation of FOXP3 in the CD4SP $CD25^+FOXP3^-$ precursors is independent of TCR signaling, the two common-γ-chain cytokines, IL-2 and IL-15 are essentially needed factors (Lio and Hsieh, 2008; Wirnsberger et al., 2009). In conclusion, during the first step, the "early" precursor defined as CD4SP $CD69^+CD25^-FOXP3^-$ differentiates in a TCR and co-stimulation-dependent manner into the "late" precursor characterized as CD4SP $CD69^+CD25^+FOXP3^-$. The second step involves the TCR independent, but IL-2- and IL-15-dependent differentiation of the late T_{reg} precursor into a mature CD4SP $CD25^+FOXP3^+$ tT_{reg} cell (Lio and Hsieh, 2008; Wirnsberger et al., 2009).

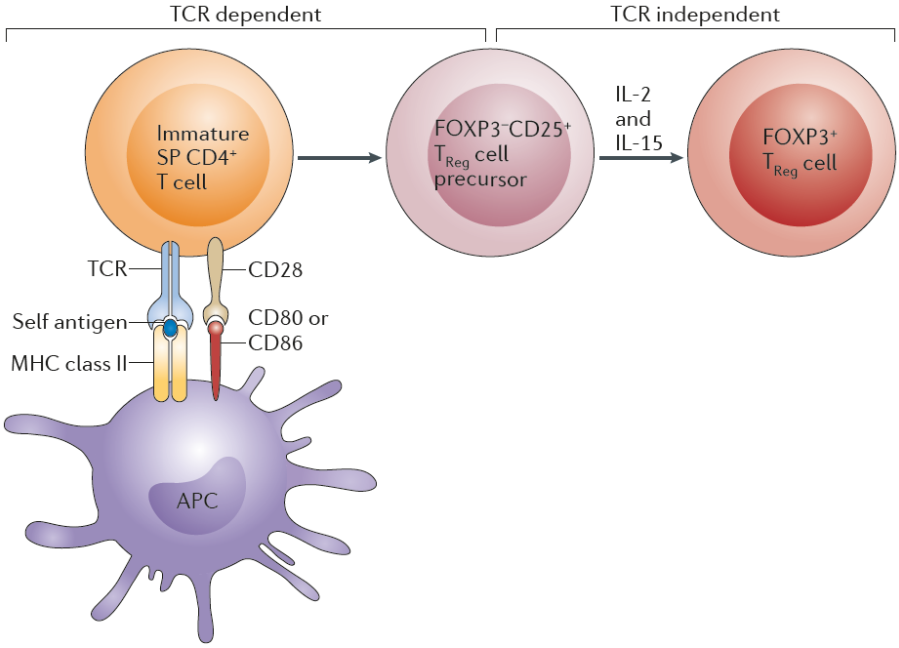

Figure 1: A two-step model for tT_{reg} cell differentiation. Recognition of self-peptide–MHC class II complexes with sufficiently high per cell avidity for tT_{reg} cell selection, in the presence of co-stimulation leads to differentiation of the "early" precursor cells (CD4SP $CD69^+CD25^-FOXP3^-$; here immature SP $CD4^+$ T cell) into the "late" precursors (CD4SP $CD69^+CD25^+FOXP3^-$; here $FOXP3^-CD25^+$ T_{reg} cell precursors). At this point, the late T_{reg} precursor does not require further TCR stimulation for the expression of FOXP3. Instead, cytokine signals mediated by IL-2 and IL-15, facilitate the induction of FOXP3 expression. Reprinted by permission of Macmillan Publishers Ltd: Nat Rev Immunol, March 2012 (doi: 10.1038/nri3155) (Hsieh et al., 2012).

The molecular mechanisms downstream of TCR signaling are crucial for tT_{reg} differentiation since the expression of *Foxp3* is essential for the suppressive function of T_{reg} cells. Several pathways get activated downstream of TCR signaling and are involved in *Foxp3* gene regulation (Delacher et al., 2014). Activation of the AKT-mTOR pathway was demonstrated to have an inhibitory effect on *Foxp3* initiation (Haxhinasto et al., 2008). While Ca^{2+} signaling seems to be involved in tT_{reg} differentiation (Oh-Hora et al., 2013), its downstream transcription factor, the nuclear factor of activated T cells (NFAT) which binds to the *Foxp3* promoter, seems to be mainly important in the generation of TGFβ induced peripheral T_{reg} cells (Vaeth et al., 2012). The NF-κB pathway on the other hand was identified as crucial for the initiation of *Foxp3*. cREL, a transcription factor of the NF-κB family was suggested as a pioneer transcription factor that binds to the conserved non-coding sequence 3 (CNS3) promoter region and thereby initiates *Foxp3* expression (Schuster et al., 2012; Zheng et al., 2010). The members of the Nr4a family were recently identified as critical transcription factors for the regulation of *Foxp3*, as the triple knock-out of *Nr4a1*, *Nr4a2* and *Nr4a3* resulted in the complete loss of *Foxp3* expression. It was suggested that these factors help to translate TCR signaling strength into *Foxp3* induction (Sekiya et al., 2013).

3.2.3 Generation of peripheral T_{reg} cells

A small part of the T_{reg} cell population is generated in the periphery. These so called peripheral derived T_{reg} (pT_{reg}) cells are former $FOXP3^-$ T_{conv} cells that converted to the T_{reg} cell lineage. Induction of pT_{reg} cells involves soluble factors in the microenvironment like TGFβ and IL-2, in combination with activation through specialized APCs (Yadav et al., 2013). pT_{reg} cells participate in the control of immune responses at sites of inflammation and are thought to complete the T_{reg} pool through the induction of tolerance against non-pathogenic foreign antigens, including commensal bacteria, food and fetal antigens (Josefowicz et al., 2012; Samstein et al., 2012; Yadav et al., 2013). The transcription factor HELIOS of the Ikaros family was suggested as a marker that distinguishes tT_{reg} from pT_{reg} cells, as it is only expressed by the thymic derived tT_{reg} cells (Thornton et al., 2010).

3.3 Features of T_{reg} cells

3.3.1 Functional mechanisms of T_{reg} cells

T_{reg} cells which represent about 10 percent of the $CD4^+$ T cell population have emerged as an essential part of the immune system more than a decade ago. Their relevance became clear when the human immunodysregulation polyendocrinopathy, enteropathy X-linked (IPEX) autoimmune diseases was connected to a mutation in the *Foxp3* gene, the transcription factor that drives T_{reg} cell development (Bennett et al., 2001). Likewise, scurfy mice that carry a mutated *Foxp3* gene suffer from a lethal autoimmune disease (Brunkow et al., 2001). Furthermore impaired function of T_{reg} cells was linked to other autoimmune conditions, including lupus, type 1 diabetes, rheumatoid arthritis and multiple sclerosis (Ehrenstein et al., 2004; Horwitz, 2010; Lindley et al., 2005; Viglietta et al., 2004). T_{reg} cells are important for the maintenance of immune tolerance throughout life. Depletion of T_{reg} cells from healthy adult mice results in catastrophic autoimmune disease and death within weeks (Kim et al., 2007). But how do T_{reg} cells mediate immune tolerance? The following chapter will explain some of the basic mechanisms used by T_{reg} cells that induce tolerance at different levels.

T_{reg} cell-mediated suppressive mechanisms can be divded into four different categories: 1) suppression by inhibitory cytokines, 2) suppression by cytolysis, 3) suppression by metabolic disruption and 4) suppression by modulation of DC maturation and function (Figure 2) (Vignali et al., 2008).

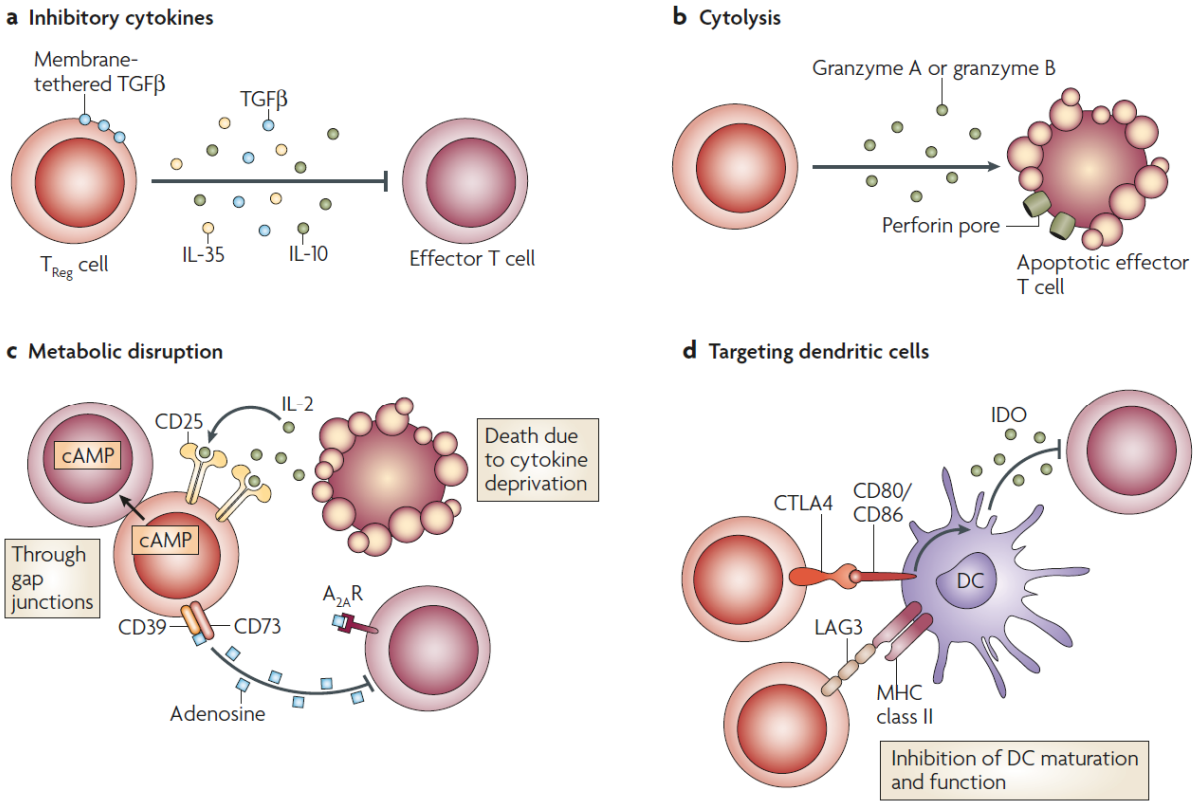

Figure 2: Basic mechanisms used by T_{reg} cells. Depiction of the various T_{reg} cell mechanisms centered around four basic modes of action. a) Inhibitory cytokines include IL-10, IL-35 and TGFβ. b) Cytolysis includes granzyme A- and B-dependent and perforin-dependent killing mechanisms. c) Metabolic disruption includes high-affinity CD25-dependent cytokine deprivation mediated apoptosis; cAMP mediated inhibition; CD39 and/or CD73 generated adenosine and A2AR mediated immunosuppression. d) Targeting DCs includes mechanisms that modulate DC maturation and/or function such as LAG3–MHC-class-II mediated suppression of DC maturation; and CTLA-4–CD80/CD86 mediated induction of IDO, which is an immunosuppressive molecule made by DCs. Reprinted by permission of Macmillan Publishers Ltd: Nat Rev Immunol, Jul 2008 (doi: 10.1038/nri2343) (Vignali et al., 2008).

Release of inhibitory cytokines including IL-10, IL-35 and TGFβ is one of the T_{reg} cell suppressive mechanisms. Release of IL-10 by T_{reg} cells has inhibitory effects on T_{conv} cells and it was demonstrated to be particularly important for the control of inflammatory disease in barrier tissue such as colon and lungs (Rubtsov et al., 2008). The T_{reg} cell-mediated suppression by soluble TGFβ or surface-tethered TGFβ is a controversial topic. The role of TGFβ seems to depend on the specific disease and experimental settings (Vignali et al., 2008). Glycoprotein-A repetitions predominant (GARP) was identified as the molecule that tethers TGFβ in a latent form to the surface of T_{reg} cells (Probst-Kepper and Buer, 2010). Surface-tethered TGFβ was

suggested to induce tolerance by converting T_{conv} into $FOXP3^+$ pT_{reg} cells with suppressive functions (Andersson et al., 2008). The inhibitory cytokine IL-35 is preferentially expressed and secreted by T_{reg} cells and has an inhibitory effect on T_{conv} cells. It was suggested that IL-35 is required for maximal T_{reg} cell suppressive function (Collison et al., 2007).

Another mechanism of T_{reg} cell-mediated suppression is induction of apoptosis in target cells by cytolysis. Human T_{reg} cells were demonstrated to kill target cells in a granzyme A and perforin-dependent manner (Grossman et al., 2004), while mouse T_{reg} cells were shown to induce granzyme B-dependent apoptosis in T_{conv} but also B cells (Gondek et al., 2005; Zhao et al., 2006).

Among the different suppressive mechanisms of metabolic disruption, CD25 expression has been well studied. High surface expression of CD25 is one of the T_{reg} cell phenotypical hallmarks and CD25 expression might also contribute to the T_{reg} cell suppressive capacity by consuming local IL-2 and thereby starving other T_{conv} cells that depend on IL-2 for survival (Oberle et al., 2007). The cell surface ectoenzymes CD39 and CD73 are preferentially expressed by T_{reg} cells and mediate T_{reg} cell suppression. The ectoenzymes generate pericellular adenosine which can suppress T_{conv} cell and DC function through binding and activating the adenosine receptor 2A ($A_{2A}R$) (Deaglio et al., 2007). In addition, T_{reg} cells can inhibit T_{conv} cells by transferring the second messenger cyclic adenosine monophosphate (cAMP) directly through gap junctions into T_{conv} cells (Bopp et al., 2007).

DC cells are required for the activation of T_{conv} cells and T_{reg} cell-mediated inhibition of DC maturation and function thereby indirectly suppresses T_{conv} cells. The T cell surface molecule cytotoxic T lymphocyte associated protein 4 (CTLA-4) is an essential molecule for T_{reg} cell-mediated suppression of DCs. T_{reg} cell specific loss of CTLA-4 results in multi organ autoimmunity (Wing et al., 2008). It was suggested that interaction between CTLA-4 and CD80/CD86 leads to trans-endocytosis of the co-stimulatory molecules CD80 and CD86 by T_{reg} cells (Qureshi et al., 2011). In addition, CTLA-4 engagement of T_{reg} cells with DCs was shown to induce expression and release of indoleamine 2, 3-dioxygenase (IDO), which results in the suppression of T_{conv} cells (Mellor and Munn, 2004). Another cell surface molecule of T_{reg} cells involved in the control of DC function is the CD4 homologue lymphocyte activation gene 3 (LAG3). LAG3 interacts with MHC class II molecules on DCs and thereby blocks DC maturation (Liang et al., 2008). Furthermore, most T_{reg} cells express the

surface molecule neuropilin 1 (NRP1). NRP1 is involved in mediating prolonged interactions between T_{reg} cells and DCs. The prolonged interaction period compared to T_{conv} cells might give them an advantage for the modulation of DC cell function (Sarris et al., 2008). Indeed, blocking of NRP1 leads to reduced T_{reg} cell suppressive function (Solomon et al., 2011).

T_{reg} cells are equipped with a variety of different immunosuppressive mechanisms, which they can use for the regulation of inflammatory conditions or immune homeostasis. The importance of these different mechanisms always depends on the character of the inflammation and the specific tissue environment (Campbell and Koch, 2011).

3.3.2 T_{reg} cell stability and plasticity

The T_{reg} cell phenotype is mainly defined by suppressive capacity and high expression of CD25 and FOXP3. Under physiological conditions these markers are stably expressed, but T_{reg} cells have been reported to lose the expression of FOXP3 under inflammatory or pathogenic conditions and acquire a T_H cell phenotype (Zhou et al., 2009). When $CD25^{low}$ $Foxp3^+$ T_{reg} cells are transferred into a lymphopenic host, a part of the cells also lose expression of CD25 and FOXP3 and differentiate into T_H cells (Duarte et al., 2009; Komatsu et al., 2009). Upon TCR stimulation, such ex-T_{reg} cells are capable of re-expressing FOXP3 and re-gaining suppressive capacity (Miyao et al., 2012). Human and mouse T_{conv} cells have been demonstrated to transiently express FOXP3 following activation (Hori, 2011; Sakaguchi et al., 2010). But the fact that these cells express FOXP3 does not turn them into a T_{reg} cell with suppressive capacities. While FOXP3 is essential, evidence suggests that other transcription factors are needed for the manifestation of the characteristic T_{reg} cell phenotype (Fu et al., 2012).

T_{reg} cells also show the ability for further differentiation following initial activation. T_{reg} cells can use the same transcription factors used by naïve T_{conv} cells for differentiation into effector T cells. Expression of T-bet allows T_{reg} cells to traffic into areas of T_H1 inflammation and to suppress T cells of the T_H1 phenotype (Koch et al., 2009). Similarly, expression of the transcription factors IRF4 and STAT3 by T_{reg} cells was needed for efficient T_H2- and T_H17-mediated inflammation respectively (Chaudhry et al., 2009; Zheng et al., 2009). These reports suggest that T_{reg} cells

have the ability to adapt to special microenvironments by using mechanisms comparable to those of T_{conv} cells.

Recently, epigenetics have come more into the focus of T_{reg} cell research. Demethylation patterns are inheritable, stable and linked to gene expression. During T_{reg} cell differentiation in the thymus characteristic demethylation patterns are induced upon TCR stimulation. tT_{reg} cells retain a specific demethylation pattern, particularly in T_{reg} cell function-associated genes like *Foxp3*, *Helios* or *Ctla-4* (Ohkura et al., 2012). Stable expression of the Foxp3 gene has been linked to demethylation of CpG islands within the regulatory CNS2 region of the *Foxp3* locus (Polansky et al., 2008; Zheng et al., 2010). One of the differences between tT_{reg} and pT_{reg} cells lies within the methylation status of the CNS2 region of the *Foxp3* gene. pT_{regs} that fail to demethylate the CNS2 region eventually lose FOXP3 (Hori, 2011; Miyao et al., 2012).

3.4 Transcription factor 7 and the immune system

3.4.1 The TCF7/LEF1 family

The high mobility group (HMG) box family member, transcription factor 7 (TCF7), also known as T cell specific transcription factor 1 (TCF1) was first identified as a possible candidate for the T cell maturation process in 1991 (van de Wetering et al., 1991). Several TCF7 isoforms exist, which can be roughly subdivided into short (25-40 kDA) and long (42-60 kDA) isoforms. The long isoforms consist of: 1) a nuclear localization sequence (NLS), 2) a 5'-TCAAAG consensus sequence recognizing HMG domain, 3) a Groucho protein binding domain known to mediate transcriptional repression and 4) a β-catenin binding domain which mediates transcriptional activation. Short TCF7 isoforms lack the β-catenin binding domain and are therefore constant transcriptional repressors (Maier et al., 2011; Van de Wetering et al., 1996).

Another member of the HMG box family lymphoid enhancer binding factor 1 (LEF1) shares a nearly identical HMG domain and shows, in general, a high level of sequence homology with TCF7 (Van de Wetering et al., 1996). Binding sites for TCF7 and LEF1 have been identified in transcriptional control regions of different genes, including CD4, TCRβ and TCRγ (Okamura et al., 1998). Both TCF7 and LEF1

are expressed during T cell differentiation and in mature T cells (Verbeek et al., 1995).

3.4.2 TCF7 and T cell development

The essential role of TCF7 in thymic T cell development was first noticed when *Tcf7*-deficient (*Tcf7*$^{-/-}$) mice showed greatly reduced numbers of thymocytes (Verbeek et al., 1995). Originally a *neo* gene insertion was performed at 2 different locations within the *Tcf7* gene site, but only the insertion into exon 7 *Tcf7*$^{\Delta VII}$, which encoded for the HMG domain, resulted in the severe phenotype. Since the generation of *Tcf7*$^{-/-}$ mice, several defects in thymocyte development from the DN to the SP stage have been reported. Otherwise healthy young *Tcf7*$^{-/-}$ mice have an incomplete block of thymocyte differentiation at DN and immature SP stages, as β-selection and maturation to the DP stage are compromised. Several month old mice have a complete block probably at the DN1 stage (Schilham et al., 1998; Staal et al., 2008; Verbeek et al., 1995). A double knock-out of *Tcf7* and *Lef1* resulted in complete block of T cell differentiation and demonstrated that TCF7 and LEF1 have partially redundant function during thymocyte development (Okamura et al., 1998). The importance of the interaction between TCF7 and β-catenin for T cell development was experimentally shown. Reconstitution of *Tcf7*$^{-/-}$ mice with different forms of TCF7 that can or cannot interact with β-catenin showed that only reconstitution with β-catenin interacting forms restored T cell development (Ioannidis et al., 2001). Furthermore, Cre driven conditional deletion of β-catenin resulted in impaired T cell development at the DN stage (Xu et al., 2003). Clearly, β-catenin/TCF7 signaling has an important role in T cell development and activation of β-catenin/TCF7 during T cell development was implicated downstream of the Notch, Wnt and TCR signaling pathways (Kovalovsky et al., 2009; Staal et al., 2008; Weber et al., 2011). In early T cell precursors, TCF7 expression is induced through Notch signals and is involved in T cell fate imprinting (Weber et al., 2011). Expression of TCF7 at the DP stages contributes to the survival of T cell precursors (Ioannidis et al., 2001). To specifically look at the influence of the TCF7 and LEF1 in the DP to SP transition, a recent study used a *Cd4*-Cre induced double loss of TCF7 and LEF1 transcription factors. The results demonstrated that the double loss impaired CD4 SP generation and promoted CD8 SP fate (Steinke et al., 2014). Older *Tcf7*$^{-/-}$ mice are prone to develop thymic

malignant transformations, indicating a role of TCF7 as a T cell specific tumor suppressor. It was suggested that TCF7 mediates its tumor suppressive function by repression of LEF1 expression, which would propose a so far unappreciated interaction beyond T cell development (Tiemessen et al., 2012; Yu et al., 2012).

3.4.3 The role of TCF7 in immune cell function

Although TCF7 was mainly studied in the context of T cell development, TCF7 is also implicated in the function and development of immune cells outside of the thymus. During helminthic infection the innate group 2 innate lymphoid cells (ILC2) induce protective type 2 immunity. Notch-dependent induction of TCF7 is required for the development of ILC2 cells (Yang et al., 2013). TCF7 and LEF1 are both involved in NK cell development and TCF7 is required for the proper formation of Ly49 receptors on NK cells (Held et al., 2003). Upon TCR stimulation in $CD4^+$ T cells, TCF7 induces GATA3, inhibits IFNγ expression and thereby promotes T_H2 fate (Yu et al., 2009). Differentiation of *Tcf7*$^{-/-}$ $CD8^+$ T cells toward the memory phenotype and persistence of $CD8^+$ memory T cells were severely impaired probably due to reduced expression of the IL-2 receptor beta chain and reduced levels of the anti-apoptotic molecule B cell lymphoma 2 (BCL-2) (Zhou et al., 2010). In T_H17 development, TCF7 mediates repression of the IL-17 gene by epigenetic modifications. Moreover, T_H17 cells from *Tcf7*$^{-/-}$ mice express higher levels of the IL-7 receptor α-chain which might enhance their survival and expansion (Ma et al., 2011; Yu et al., 2011). Finally, previous reports also studied the role of TCF7 in the function of T_{reg} cells. Forced expression of a stable form of β-catenin resulted in enhanced survival of T_{reg} cells (Ding et al., 2008). Another report stated that T_{reg} cell suppressive function was reduced by the activation of β-catenin/TCF7 through Wnt signaling (van Loosdregt et al., 2013).

4 Aims of study

T_{reg} cells have emerged as critical control elements of the immune system, as they keep the balance between protective immune responses and tolerance.

In the past, gene expression profiles of T_{reg} cells have been intensively studied, but mRNA does not always translate into protein and so far full data sets of T_{reg} cell protein expression is missing. As a starting point of this PhD project, we aimed to characterize T_{reg} cells at the proteome level and to use this information to identify candidate proteins that are implicated in T_{reg} cell development and function. Further, we aimed to then use different *in vivo* and *in vitro* systems to analyze in detail how these candidate proteins are involved in the T_{reg} cell thymic differentiation and function.

Although T_{reg} cells have been studied for years, we still do not fully understand how these cells are generated and regulated. A better understanding of T_{reg} cells is crucial to find future treatment options that are capable of suppressing or boosting the immune response.

5 Methods

5.1 Mice

5.1.1 Keeping

Mice were 4-9 weeks old at the time of the experiments. All mice were cared for under the specific-pathogen free conditions in the animal facility of the DKFZ. All animal experiments were reviewed and approved by the governmental committee for animal experimentation in Karlsruhe, Germany.

5.1.2 Breeding

Tcf7$^{-/-}$ mice (mixed 129-C57BL/6 background) (Verbeek et al., 1995) were crossed to Foxp3-YFP (Rubtsov et al., 2008) or TEa (Grubin et al., 1997) mice in the DKFZ animal facility. Foxp3-GFP mice (Kim et al., 2007) were crossed to a CD45.1 or CD90.1 background. For experiments we used littermates as control animals unless otherwise indicated.

5.2 Cell culture techniques

5.2.1 Mammalian cell culture

Cells were cultured at 37°C, 5% (v/v) CO_2 in complete medium and treated at all times under a cell culture hood (Thermo fisher scientific). Cells were split at 1:10–1:20 depending on the level of confluence. For splitting, cells were washed with PBS and detached with trypsin-EDTA solution. Detaching reaction was stopped by adding complete medium. Cells were centrifuged and a fraction of cells was seeded in a new flask with complete medium. For the determination of cell numbers, cells were

counted using a Neubauer chamber (0.1 mm depth) and trypan blue solution. Cell count = mean number of cells per square x dilution factor x 10^4 cells/ml.

5.2.2 Bacterial cell culture

Bacteria were cultured at 37°C in LB-Medium supplemented with antibiotics in a bacterial incubator at 180 rpm. Bacteria were prepared for long-term storage at -80°C by adding 700µl of glycerol to 300 µl of bacteria. For plasmid production, bacteria were lysed and plasmids were purified according to manufacturer's instructions using a Mini or Midi preparation kit (Life technologies). Quality and concentration of the isolated DNA plasmids was analyzed using a NanoDrop 2000 (Thermo Fisher Scientific).

5.3 Proteomics

5.3.1 Protein digestion, labeling of peptides with stable isotopes and fractionation

Cell pellets of FACS-purified cells (about 6 x 10^5) were snap-frozen in liquid nitrogen. After lysis of cells in 0.1 percent RapiGest (Waters)/50 mM ammonium bicarbonate, extracted proteins were reduced/alkylated with 5 mM DTT and 10 mM iodoacetamide, then digested overnight with sequencing grade modified trypsin (Promega). Resulting peptides were dimethyl labeled on a column as previously described (Boersema et al., 2009). Briefly, peptides were labeled on SepPak C_{18} cartridges (Waters) with the labeling reagent ("light" or "intermediate" using CH_2O (Fisher) + $NaBH_3CN$ (Fluka) or CD_2O (Isotec) + $NaBH_3CN$, respectively). In the second, third and fourth biological replicate experiments, cell population reagents were swapped. The 'light' and 'intermediate' labeled samples were mixed in 1:1 ratio based on cell number. Sample complexity was reduced by fractionating the peptides with pH 3-10 IPG strips and 3100 OFFGEL fractionator (Agilent), into 12 fractions.

5.3.2 LC-ESI-MS/MS analysis

Peptides were separated by liquid chromatography (LC) using the nanoACQUITY UPLC system (Waters) fitted with a trapping column (nanoAcquity Symmetry C_{18}, 5µm particle size, 180 µm inner diameter x 20 mm length) and an analytical column (nanoAcquity BEH C_{18}, 1.7µm particle size, 75µm inner diameter x 200 mm length). Peptides were separated on a 120 min gradient and analyzed by electrospray ionization-tandem MS (ESI-MS/MS) on an LTQ Orbitrap Velos (Thermo Fisher Scientific). Full scan spectra from *m/z* 300 to 1700 at resolution 30,000 FWHM (profile mode) were acquired in the Orbitrap MS. From each full-scan spectra, the 15 ions with the highest relative intensity were selected for fragmentation in the ion trap. A lock mass correction using a background ion (m/z 445.12003) was applied.

5.3.3 Protein identification and quantification

MS raw data files were processed with MaxQuant (version 1.2.0.18) (Cox and Mann, 2008). Cysteine carbamidomethylation and methionine oxidation were selected as fixed and variable modifications, respectively. The derived peak list was searched using the built-in Andromeda search engine (version 1.2.0.18) in MaxQuant against the Uniprot mouse database (2011.06.21). Initial maximal allowed mass tolerance was set to 20 ppm for peptide masses, followed by 6 ppm in the main search, and 0.5 Dalton for fragment ion masses. A 1 percent false discovery rate (FDR) was required at both the protein level and the peptide level. In addition to the FDR threshold, proteins were considered identified if they had at least one unique peptide. The protein identification was reported as an indistinguishable “protein group” if no unique peptide sequence to a single database entry was identified.

5.3.4 Accession number

The MS proteomics data have been deposited to the ProteomeXchange Consortium (http://www.proteomexchange.org) via the PRIDE partner repository (Vizcaino et al., 2013) with the dataset identifier PXD000794.

5.4 Tissue sample preparation

5.4.1 Tissue isolation and sample preparation

For tissue isolation, spleen, thymus, and LN (axillary, brachial and inguinal) were removed and organs were processed by mashing and filtering to prepare single cell suspensions. Ammonium chloride–potassium bicarbonate (ACK) lysis buffer was used to lyse erythrocytes in spleen samples.

5.4.2 AutoMACS cell purification

Samples FACS-purified for T_{reg} protein isolation (MS experiments) were first enriched for CD25. Samples FACS-purified for T_{reg} precursors and quantitative real-time PCR (qPCR) experiments were first depleted of $CD8^+$ cells. For T cell transduction, isolation of T cells from spleen and LNs was performed by AutoMACS depletion of CD8, CD11b, CD11c, CD19, CD25 and CD49b. For enrichment and depletion, cells were labeled with biotin-conjugated antibodies and anti-biotin microbeads (Miltenyi). Magnetic cell separation was performed using an AutoMACS Pro Separator (Miltenyi).

5.5 Flow cytometry and imaging techniques

5.5.1 Flow cytometry

For surface staining cells were labeled with antibodies/streptavidin for 30 min in FACS buffer at 4°C. Intracellular staining of cells was performed after surface staining using the intracellular Foxp3 staining buffer set (eBioscience). Cells were treated with the fixation buffer for 45 min at 4°C and intracellular stained with Fix/Perm buffer and intracellular antibodies for 45 min at room temperature. CD1d tetramer staining was performed in the same manner as surface staining. Cells were filtered prior to analysis. For compensation unstained or anti-CD4 single stained (in

the colors corresponding to the staining panel) spleen cells were used. For most *in vitro* experiments OneComp compensation beads (eBioscience) were used instead. Cells were analyzed using the BD Bioscience Canto II LSR Fortessa or LSR II. For FACS-purification of cells the BD Biosciences FACSAria I, II or III instruments were used. Quality of antibodies was checked using isotype controls. Purity of cell sorts was assured through post-sort analysis. FlowJo software (Treestar) was used for the analysis of flow cytometry data.

5.5.2 Cell counting

For counting of total thymus subpopulations using beads, AccuCheck+ Counting beads (Invitrogen) were added to the sample prior to acquisition. 2 x 10^4 beads were added to 20 percent of the thymus sample. The number of cells in the total thymus was calculated according to manufacturer's instructions (total organ cell count = ((number of cells counted x number of beads added / average bead count) x dilution factor).
For *in vitro* experiment cell counts, identical numbers of cells were seeded in all wells. All cells were stained and completely acquired by flow cytometric analysis.

5.5.3 Immunofluorescence imaging

Sections (5 µm) from cryo-preserved thymi from *Tcf7*$^{+/+}$ and *Tcf7*$^{-/-}$ mice were prepared by step sectioning every 25 µm. Samples were fixed in ice-cold acetone, blocked in PBST and stained with antibody against K14 (Covance). Next, sections were stained with anti-rabbit-IgG (Jackson ImmunoResearch) and DAPI (Sigma). Imaging was performed on an Axio Imager.Z1 (Zeiss). Images were analyzed in AxioVision (Zeiss) and Adobe Photoshop (Adobe).

5.6 *In vitro* cell culture assays

5.6.1 T_{reg} precursor differentiation assay

FACS-purified late (CD4SP $CD69^+CD25^+Foxp3^-$) or early (CD4SP $CD69^+CD25^-Foxp3^-$) T_{reg} precursors were seeded at 1 x 10^5 cells per 96 round-bottom well. Late T_{reg} precursors were cultured with human IL-2 100 U/ml (Proleukin S, Novatis) and murine IL-15 100 ng/ml (Peprotech Inc.) for 1 day before analysis. Early T_{reg} precursors were cultured with human IL-2 100 U/ml, murine IL-15 100 ng/ml and anti-CD3/CD28 Dynabeads (Invitrogen) at a cell/bead ratio of 1:1 for 3 days prior to analysis.

For Wnt-activation assays, 1 x 10^5 FACS-purified early T_{reg} precursors were cultured for 3 days under the conditions described above. In addition, DMSO dissolved Wnt-activators 6-Bromoindirubin-3′-oxime (BIO) (biomol) or 6-(2-(4-(2,4-Dichlorophenyl)-5-(4-methyl-1H-imidazol-2-yl)-pyrimidin-2-ylamino)ethyl-amino)-nicotinonitrile (CHIR99021) (biomol) were added to the cultures at 1 or 2 µM. Control wells were cultured with DMSO concentrations corresponding to the highest DMSO content in the wells containing the Wnt activators.

For the *in vitro* T_{reg} cell differentiation assay with titration of anti-CD3 stimulus, 96 well flat-bottom plates were coated over-night with different concentrations (0.1, 0.25, 0.5 or 2 µg/ml) of purified anti-CD3 in PBS. Plates were washed with PBS prior to use. Purified anti-CD28 10 µg/ml was added together with 1 x 10^5 precursors, with human IL-2 100 U/ml and murine IL-15 100 ng/ml to the culture media.

5.6.2 *In vitro* iT_{reg} cell and T_H17 generation

For *in vitro* iT_{reg} and T_H17 cell generation assays, naïve T cells ($CD4^+$ $CD62L^+FOXP3^-$) were FACS-purified from spleen and LNs of Foxp3-YFP^+ mice. For the generation of iT_{reg} cells, the cells were cultured *in vitro* for 4 days in 96-well round bottom plates with human IL-2 100 U/ml (Proleukin S, Novatis), anti-CD3/CD28 Dynabeads (Invitrogen) at a cell/bead ratio of 1:1 and different concentrations of TGFβ (0.3 – 10 ng/ml) (tebu-bio). For the generation of T_H17 cells, the cells were cultured *in vitro* for 4 days in 96-well round bottom plates with human IL-2 100 U/ml,

anti-CD3/CD28 Dynabeads at a cell/bead ratio of 1:1, TGFβ 10 ng/ml and different concentrations of IL-6 (0.3 – 5 ng/ml). 5 h prior to analysis of the T_H17 assay, cells were restimulated with PMA 50 ng/ml (Biomol), Ionomycin 1 µg/ml (Biomol) and Brefeldin A 1:1000 (Biozol Diagnostica). Cells were analyzed by flow cytometry at the end of the culture period.

5.6.3 Retroviral T cell transduction

Phoenix-ECO cells were calcium-phosphate transfected either with a Murine Stem Cell Virus (MSCV)-Ctrl construct (CD90.1 expression only) or a MSCV-Foxp3 construct (CD90.1 and Foxp3 expression). For calcium-phosphate transfection Phoenix-ECO cells were seeded at a density of 4 x 10^5 cells per gelatin-coated 6-well and cultured overnight. Transfection solution (500 µl) contained per well: 3 µg MSCV-vector, 1 µg pCL-Eco, 30 µl 2 M $CaCl_2$ solution, 250 µl 2x HBS and X µl of H_2O (adds up to 500 µl). After vigorous mixing, transfection solution was rapidly added to the Phoenix-ECO cells. Medium was exchanged on the following day. Supernatants containing MSCV retroviral particles were harvested at day 3 after transfection. Phoenix-ECO transfection efficiency was controlled by flow cytometric analysis of CD90.1 expression.

24-well plates were prepared for T cell culture by coating first with goat-anti-hamster IgG (MP Biomedicals) in PBS overnight at 4°C. Secondly wells were coated with purified anti-CD3 0.1 µg/ml (BioLegend) and anti-CD28 1 µg/ml (BioLegend) in PBS for 4 h at 4°C. For T cell isolation LN and spleen cells were depleted of CD8, CD19, CD11b, CD11c, CD25 and CD49b using AutoMACS Pro Separator (Miltenyi). T cells were seeded at 2.5 x 10^6 per 24 well on the pre-coated wells. IL2 (20U/ml) was added to the T cell culture at all times. T cells were spin-transduced for 90 min at 32°C with 3 ml of fresh viral supernatants containing Polybrene 16 µg/ml 40 ± 2 hours after the start of T cell stimulation. Viral supernatants were exchanged for fresh medium. Retrovirally transduced T cells were analyzed 3 days after transduction.

5.7 PCR techniques

5.7.1 Standard PCR for genotyping

For genotyping, PCR was performed with adequate primers (listed below) on lysed mouse tissue samples according to the protocols from animal providers. Standard PCR reactions were performed using a Mastercycler Pro S (Eppendorf). After PCR quantification, loading buffer was added and samples were loaded onto ethidium bromide containing agarose gels, together with a 2-Log DNA ladder (New England Biolabs). Separation of DNA fragments was performed at 80-140 V. A UV gel documentation system (Herolab) was used to visualize DNA fragments.

5.7.2 RNA isolation and cDNA synthesis

Cells of interest were FACS-purified (1 – 5 x 10^4 cells) into 0.5 ml of TRIzol (Life technologies) and frozen at -80°C until further processing. 125 µl of chloroform was added to each sample. Samples were then vigorously shaken for 15 s, incubated for 3 min at RT and centrifuged (20 min, 4°C, max speed). Following centrifugation the clear phase was carefully transferred to a new tube, 300 µl of isopropanol were added, the mixture was incubated for 10 min at RT and stored at -80°C overnight. After thawing 1µl of GlycoBlue was added to the samples and samples were incubated for 3 min at RT. Following centrifugation (20 min, 4°C, max speed), supernatants were carefully removed and the blue RNA pellet was washed 75 % ethanol (v/v). After centrifugation (15 min, 4°C, max speed) the supernatant was completely removed and the pellet was air-dried at RT. Next, the RNA pellet was dissolved in 10 µl nuclease free H_2O. For cDNA synthesis, the SuperScript reverse transcriptase (Invitrogen) and oligo(dT) primers were used according to manufacturer's instructions.

5.7.3 Sybr green quantitative real-time PCR

cDNA samples were analyzed by quantitative real-time PCR using the Power SYBR Green master mix (Life technologies) and the ViiA7 instrument (Life technologies). Appropriate primers for *Hprt* and *Tcf7* were used. Primer sequences are listed below. mRNA (gene X) abundance was quantified as percent relative to the expression of *Hprt* by the change-in-threshold method (100*(relative expression = 2^(CT(gene X) − CT(*Hprt*)))). Prior to use all qPCR primers were tested by serial dilutions, efficiency testing and melting curve analysis.

5.8 Bioinformatic and statistical analysis

5.8.1 Proteomics and RNA microarray

Statistical analysis was performed for the proteins quantified in at least two replicates using the Limma package in R/Bioconductor (Gentleman et al., 2004; Smyth, 2004). Proteins with an adjusted p-value lower than 0.05 were considered to be differentially expressed between T_{reg} and T_{conv} cells. Network analysis was done using STRING (Jensen et al., 2009) and visualization was performed in Cytoscape v2.8 (Shannon et al., 2003).

T_{reg} specific genes (over- and under-represented) were identified based on RNA micro-array expression data that we published earlier (Feuerer et al., 2010; Hill et al., 2007). T_{reg} and T_{conv} cells from LN and thymus were included. Genes more than 1.5-fold differential expressed between T_{reg} and T_{conv} were considered significant different (Student's t-test, two-tailed, $p < 0.05$). Generated gene lists were cross-referenced with our proteomic data based on gene names and used for further analysis.

5.8.2 General statistical analysis

Statistical analysis of experimental data was performed using Prism software (GraphPad) or Excel (Microsoft). Employed statistical tests and corresponding parameters are mentioned in the respective figure legends. Results were considered statistically significant if p-values were less than 0.05.

6 Materials

6.1 Mice

Name	Official name	Origin
C57BL/6	C57BL/6 Jackson number: 664	Charles River Breeding Laboratories, Wilmington MA, USA or Jackson Laboratory, Bar Harbor ME, USA
CD45.1	B6.SJL-Ptprc^{a}Pepc^{b}/BoyJ Jackson number 002014	DKFZ Animal Facility, Heidelberg, Germany
CD90.1	B6.PL-Thy1^{a}/CyJ Jackson number: 000406	Jackson Laboratory, Bar Harbor ME, USA
Foxp3-YFP	B6.129(Cg)-Foxp3$^{tm4(YFP/cre)Ayr}$/J Jackson number 016959	A. Rudensky, Memorial Sloan Kettering Cancer Center, New York, USA
Foxp3-GFP	B6.129(Cg)-Foxp3$^{tm3(DTR/GFP)Ayr}$/J Jackson number: 016958	A. Rudensky, Memorial Sloan Kettering Cancer Center, New York, USA
Foxp3-GFP CD45.1		DKFZ Animal Facility, Heidelberg, Germany
Foxp3-GFP CD90.1		DKFZ Animal Facility, Heidelberg, Germany
Tcf7$^{-/-}$	Tcf7^{tm1Cle}, ΔVII	H. Clevers, Hubrecht Institute

		Utrecht, Netherlands
Tcf7$^{-/-}$ Foxp3-YFP		DKFZ Animal Facility, Heidelberg, Germany
Tcf7$^{-/-}$ TEa		DKFZ Animal Facility, Heidelberg, Germany
TEa	B6.Cg-Tg$^{(Tcra,Tcrb)3Ayr}$/J Jackson number: 005655	J. Marie, Cancer Research Center, Lyon, France

6.2 Mammalian and bacterial cell lines

Cell line	**Origin**
Phoenix-ECO Human kidney cells	I. Grummt, DKFZ, Heidelberg, Germany
DH5α Bacterial cells	P. Frappart, DKFZ, Heidelberg, Germany

6.3 DNA plasmids

Insert	**Vector**	**Origin**
Human *Foxp3*	MSCV Thy1.1	V. Heissmeyer, Helmholtz Zentrum München, Germany
Ctrl (no insert)	MSCV Thy1.1	V. Heissmeyer, Helmholtz Zentrum München, Germany
pCL-ECO (contains viral proteins)	Helper packaging construct for retroviral transduction	V. Heissmeyer, Helmholtz Zentrum München,

			Germany

6.4 Antibodies, streptavidin and dyes

Antigen	Clone	Isotype	Company
Bcl-2	BCL/10C4	Mouse IgG1 κ	BioLegend
Biotin		Streptavidin	BioLegend
CD103	2E7	Arm. Hamster IgG	BioLegend
CD11b	M1/70	Rat IgG2b κ	BioLegend
CD11c	N418	Arm. Hamster IgG	BioLegend
CD122	5H4	Rat IgG2a κ	BioLegend
CD19	6D5	Rat IgG2a κ	BioLegend
CD25	PC61	Rat IgG1 λ	BioLegend
CD28	37.51	Syr. Hamster IgG	BioLegend
CD304 (Nrp-1)	N43-7	Rat IgG2a κ	BioLegend
CD304 (Nrp-1)	N43-7	Rat IgG2a κ	BioLegend
CD357 (GITR)	DTA-1	Rat IgG2b λ	BioLegend
CD357 (GITR)	DTA-1	Rat IgG2b λ	BioLegend
CD39	5F2	Mouse IgG1 κ	BioLegend
CD3ε	145-2C11	Arm. Hamster IgG	BioLegend
CD4	RM4-5	Rat IgG2a κ	BioLegend
CD4	GK1.5	Rat IgG2b κ	BioLegend
CD44	IM7	Rat IgG2b κ	BioLegend
CD49b	DX5	Rat IgMκ	BioLegend
CD5	53-7.3	Rat IgG2a κ	BioLegend
CD61	2C9.G2 (HMb3-1)	Arm. Hamster IgG	BioLegend

CD69	H1.2F3	Arm. Hamster IgG	BioLegend
CD86	GL-1	Rat IgG2a κ	BioLegend
CD86	GL-1	Rat IgG2a κ	BioLegend
CD8a	53-6.7	Rat IgG2a κ	BioLegend
CD90.1	OX-7	Mouse IgG1 κ	BioLegend
CTLA-4	UC10-4B9	Arm. Hamster IgG	BioLegend
Fixable Viability Dye			eBioscience
FoxP3	FJK-16s	Rat IgG2a κ	eBioscience
GARP	YGIC86	Rat IgG2a κ	BioLegend
Hamster-IgG	Lot#06008	Goat IgG	MP Biomedicals
Helios	22F6	Arm. Hamster IgG	BioLegend
I-E (MHC II)	14-4-4S	Mouse IgG2a κ	BioLegend
IL-17A	TC11-18H10.1	Rat IgG1 κ	BioLegend
K14	polyclonal	Rabbit IgG	Covance
Ki-67	B56	Mouse IgG1 κ	Cell Signaling
KLRG1	2F1	Syr. Hamster IgG2κ	BioLegend
LEF1	C12A5	Rabbit IgG	Cell signaling
mCD1d		tetramer PBS-57	NIH tetramer core facility
Rabbit-IgG		Goat IgG	Cell signaling
Rabbit-IgG		Goat IgG	Jackson ImmunoResearch
TCF1	C63D9	Rabbit IgG	Cell signaling
TCR Vα2	B20.1	Rat IgG2a, λ	BioLegend
TCR Vβ6	RR4-7	Rat IgG2b, λ	BioLegend
TCR γ/δ	GL3	Hamster IgG	BioLegend
TCR-β-chain	H57-597	Arm. Hamster IgG	BioLegend

6.5 Cytokines

Cytokine	Company
IL-6 recombinant murine	tebu-bio
IL-15 recombinant murine	PeproTech
Proleukin S (recombinant human IL-2)	Novartis Pharma
TGFβ1 recombinant human	tebu-bio

6.6 Enzymes

Enzyme	Company
Super Script II Reverse Transcriptase	Life Technologies
Taq DNA Polymerase (Vektor: pTTQ18)	Amersham Biosciences and K. Lobbes, DKFZ, Heidelberg, Germany
Trypsin-EDTA	Sigma-Aldrich

6.7 Quantitative real-time PCR primer

Gene name	Forward primer sequence 5'-3'	Reverse primer sequence 5'-3'
Hprt	CTTTGCTGACCTGCTGGATT	TATGTCCCCCGTTGACTGAT
Tcf7	CGAGAAGAGCAGGCCAAGTA	CCTGTGGTGGATTCTTGATG

6.8 PCR primer for tail typing

Gene name	Forward primer sequence 5'-3'	Reverse primer sequence 5'-3'
YFP-Cre	AGGATGTGAGGGACTACCTCCTG TA	TCCTTCACTCTGATTCTGGCAATT T
DTR	GGTGGTGCTGAAGCTCTTTC	CCCATGACACCTCTCTCCAT
TEa	CCAGAAAGGGTGAAGTTGAGAGC TG	AAAGAAACTCGAGCCAAACTATG AACAAGTGG
Tcf7	ACCTTTTCACCCCAGCTTTC and CTAAAGCGCATGCTCCAGACT	ATTCCCCTTCCTGTGTTGAG
IEκ	CTAGCCCACTGCAAAAGGAG	CCCAGGAATGAAACTGGTTG

6.9 Reagents and Kits

Reagent/Kit	Company
2-Log DNA ladder	New England Biolabs
4',6-Di-Amidino-2-Phenylindole (DAPI)	Sigma-Aldrich
6-Bromoindirubin-3'-oxime (BIO)	Biomol
ACK lysis buffer	Lonza

Ampicillin	Carl Roth
Anti-Biotin Micro-Beads	Miltenyi Biotec
Brefeldin A	Biozol Diagnostica
CHIR99021	Biomol
Chloroform	Carl Roth
Deoxyribonucleotide Triphosphates (dNTPs)	Life Technologies
DMEM, High Glucose, with or without Phenol Red	Life Technologies
DMSO	Genaxxon Bioscience
Dulbecco's Phosphate Buffered Saline (PBS)	Sigma-Aldrich
Dynabeads mouse T-activator CD3/CD28	Life Technologies
Ethidium bromide 1 % solution	Sigma-Aldrich
Fetal Calf Serum (FCS) (Cat. No. A15-101, Lot No. A10109-2802)	PAA Laboratories
Foxp3 / Transcription Factor Staining Buffer Set	eBioscience
Gelatine Solution	Pan Biotech
GlycoBlue	Life Technologies
HEPES Solution	PAA Laboratories
Ionomycin	Biomol
Mounting medium aqueous	Dako
Nuclease free sterile water	Biomol
Oligo(dT) primers	Life Technologies
OneComp compensation beads	eBioscience
Phorbol 12-Myristate 13-Acetate (PMA)	Biomol
Polybrene (hexadimethrine bromide)	Sigma-Aldrich

Purelink Hipure Plasmid Midiprep Kit	Life Technologies
Purelink Quick Plasmid Miniprep Kit	Life Technologies
Retronectin	Axxora
RNAse Inhibitor	Genaxxon Bioscience
Sodium Pyruvate Solution	PAA Laboratories
Sybr Green Power Master Mix	Life Technologies
Thioglycollate Broth	Sigma-Aldrich
TRIzol	Life Technologies
Trypan Blue	Biochrom
Tween-20	MP Biomedicals

6.10 Plasticware and consumables

Product	**Company**
96-well reaction plate MicroAmp	Life Technologies
Cell culture plates flat bottom 6, 24, 96 well	PAA
Cell culture plates round bottom 96 well	PAA
Cell strainer 40µm	BD Falcon
Conical tubes 15 ml	Nerbe Plus
Conical tubes 50 ml	Greiner GBO
Cryo tubes 1 ml	Greiner GBO
Nitex nylon filter	SEFAR
Penicillin-Streptomycin solution	Sigma-Aldrich
Pipette filter tips 1-200, 100-1000 µl	StarLab

Pipette tips 0.1-10, 1-200, 100-1000 µl	StarLab
Reaction tubes 1.5 ml	Steinbrenner Laborsysteme
Reaction tube safe-lock	Eppendorf
Round bottom 5ml tubes	BD Falcon
Round bottom 5ml tubes with lid	BD Falcon
Serological pipettes 5, 10, 25 ml	Corning
Syringe Luer-Lok 3 ml	BD
Tissue culture flask 75cm^2	Greiner

6.11 Buffers and solutions

Buffer/Solution	**Composition**
ACK Lysis Buffer	PBS, 0.15 M NH_4Cl, 10 mM $KHCO_3$, 0.1 mM Na_2-EDTA *stored at RT, pH 7.3, sterile filtrated*
Complete Medium	DMEM, 10% (v/v) FCS, 10 mM HEPES,100 U/ml Penicillin, 100 µg/ml Streptomycin, 1 mM Pyruvate *stored at 4°C*
FACS buffer	PBS, 0.1% (w/v) NaN_3, 1% (v/v) FCS *stored at 4°C, pH 7.4*
LB-Medium	Water, 0.5% (w/v) yeast extract, 1.0% (w/v) tryptone, 0.5% (w/v) NaCl *stored at 4°C, pH 7.0, autoclaved*

Loading dye (6x)	0.2% (w/v) bromphenol blue, 0.2% (w/v) xylene cyanol, 60% (v/v) glycerol, 60 mM EDTA *stored at 4°C*
Magnesium Chloride Solution	Water, 50 mM $MgCl_2$ *stored at 4°C, autoclaved*
PBS	Water, 0.27 mM KCl, 13.7 mM NaCl, 10 mM Na_2HPO_4, 0.2 mM KH_2PO_4 *stored at RT, pH 7.4, autoclaved*
PBST	PBS, 0.1% (v/v) Tween 20, 5% (v/v) FCS and 1% (w/v) BSA
PCR buffer (10x)	Water, 500 mM KCl, 200 mM Tris-HCl (pH 8.8) *stored at 4°C*
HBS (2x)	Water, 50 mM HEPES (pH 7.05), 10 mM KCl, 12 mM Dextrose, 280 mM NaCl, 1.5 mM Na_2HPO_4 *stored at -20°C, pH 7.05, sterile filtrated*
$CaCl_2$ Solution	Water, 2 M $CaCl_2$ *stored at -20°C, sterile filtrated*

6.12 Equipment

Equipment	**Manufacturer**
AutoMACS Pro Separator	Miltenyi Biotec
Axio Imager.Z1	Carl Zeiss

Bacterial Incubators	GFL and Infors
Betain	Sigma Aldrich
Cell Culture Hood Safe 2020	Thermo fisher scientific
Cell Culture Incubator, Galaxy 170 S	Eppendorf
Centrifuge 5415 R, 5424 and 5810 R	Eppendorf
Electrophoresis system	Neolab
FACSAria I, II and III	BD Biosciences
FACSCanto II, LSR II, LSRFortessa	BD Biosciences
Freezer (-20°C, -80°C)	Liebherr and Thermo Fisher Scientific
Fridge (4°C)	Liebherr
Mastercycler Pro S	Eppendorf
Nanodrop 2000	Thermo Fisher Scientific
Neubauer Counting Chamber	Karl Hecht
pH Meter	Sartorius
Precision Balances	Sartorius and Mettler
Thermoblock Neoblock 1	Neolab
UV gel documentation system	Herolab
ViiA 7 Real-Time PCR System	Life Technologies

6.13 Software

Software	**Company**
Adobe Illustrator	Adobe System
Adobe Photoshop	Adobe System
ApE	M. Wayne Davis
AxioVision Software	Carl Zeiss
EndNote	Thomson Reuters

E.A.S.Y. Win32	Herolab
FACS DIVA	BD Biosciences
FlowJo	Treestar
Microsoft Office	Microsoft
Prism	GraphPad
ViiA 7 Software	Applied Biosystems

7 Results

7.1 Differential quantitative mass spectrometry of the T_{reg} cell proteome

Gene expression profiles of T_{reg} cells from different tissues, subphenotypes and under various conditions have been studied in the past (Feuerer et al., 2010; Feuerer et al., 2009; Heng and Painter, 2008; Hill et al., 2007). Those revealed important information about differences on the mRNA level, however precise knowledge of the complete T_{reg} proteome and its correlation with mRNA expression is currently unavailable. We decided to use a mass spectrometry (MS) based quantitative differential approach to compare the proteomes of murine T_{conv} and T_{reg} cells. Both T_{conv} and T_{reg} cells are part of the T cell lineage, but their function and attributes are quite distinct from one another. Comparison of these two groups therefore results in a data set that highlights the differences between their proteomes.

To enrich for murine T_{reg} and T_{conv} cells from LNs and spleens, we performed fluorescence-activated cell sorting (FACS). T_{conv} cells were identified by the expression of the surface markers CD4 and the absence of CD25. T_{reg} cells were distinguished from T_{conv} cells through the high surface expression of the IL-2 receptor CD25 (Figure 3A, left panel). After the purification, quality was checked by flow cytometric reacquisition of the sorted populations and by post-sort staining for FOXP3. Post sort reacquisition control showed that the reacquired populations lay almost exclusively within their sort gates (Figure 3A, middle panel). Since activated T_{conv} cells also show elevated surface expression of CD25 we stained for the major T_{reg} cell transcription factor FOXP3. FACS enriched T_{conv} cells were almost completely negative for FOXP3 and more than 90 percent of the enriched T_{reg} cells were positive for FOXP3 expression (Figure 3A, right panel). Hence, both methods confirmed that the FACS enrichment resulted in highly pure T_{conv} and T_{reg} cell populations.

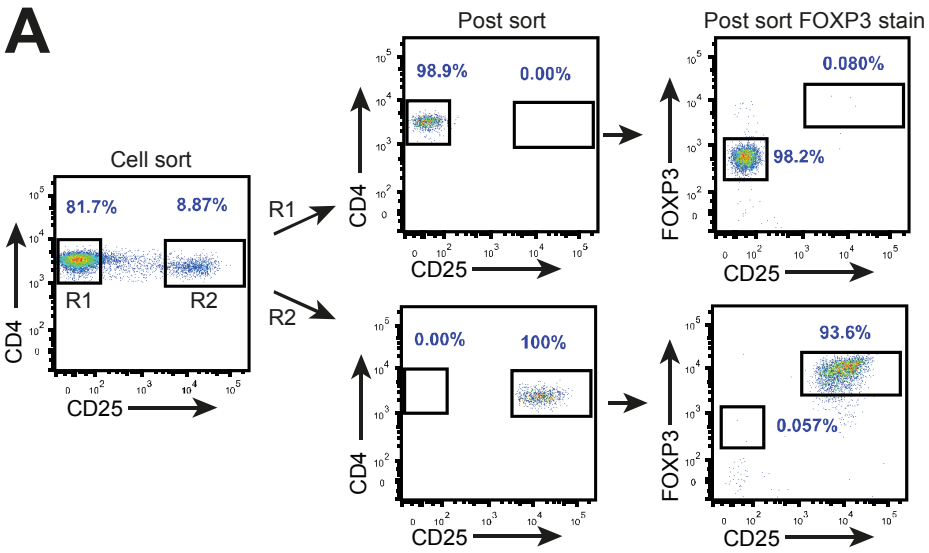

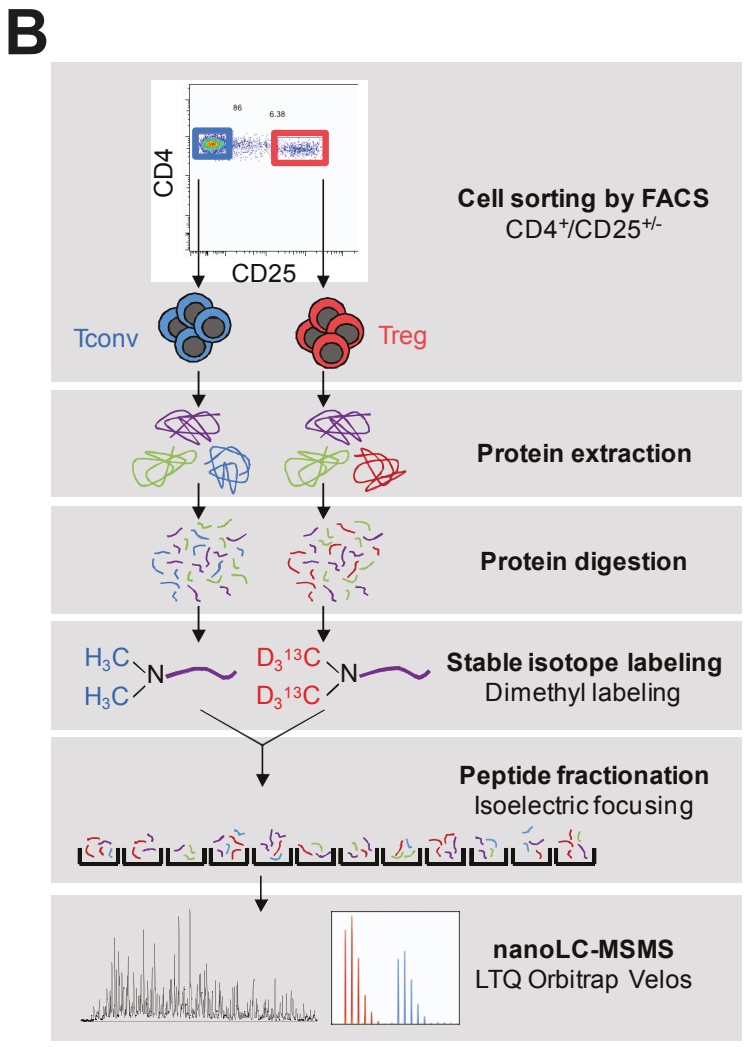

Figure 3: FACS purification and Proteomics work flow. (A) Sort gates for T_{reg} (R2; $CD4^{+}CD25^{high}$) and T_{conv} (R1; $CD4^{+}CD25^{-}$) cells. Post sort control of R1 and R2 cell populations and post sort FOXP3 staining. (B) Differential Quantitative Proteomics work flow.

After FACS purification, proteins from T_{reg} and T_{conv} cells were extracted, digested and differentially labeled with stable isotopes (Boersema et al., 2009) (Figure 3B). Peptide fractions were then analyzed by high-resolution nano liquid chromatography-tandem MS (LC-MS/MS) and relative protein abundance was determined based on relative MS signal intensities (Figure 3B). All MS experiments were performed in collaboration with Dr. Jeroen Krijgsveld and Dr. Jenny Hansson from the EMBL in Heidelberg.

Analysis of the four MS replicate identified in total of 5225 proteins, 4859 proteins were detected in at least two and 3756 were detected in all four replicates (Figure 4A). Various protein classes and cell compartments, from the nucleus to the cell surface were covered by the identified proteins (Figure 4B).

Comparison of the differentially expressed proteins identified 164 proteins which were significantly ($p < 0.05$) differentially expressed between T_{reg} cells and T_{conv} cells. Among these, we identified 51 proteins as under-represented (Appendix Table 1) and 113 proteins as over-represented in T_{reg} cells (Appendix Table 2). To better visualize differences, quantified proteins were plotted as fold change of T_{reg} versus T_{conv} against p-value (Figure 5). As expected, classic T_{reg} cell markers like FOXP3, IL-2Rβ, GITR and NRP1 were detected as highly over-represented in T_{reg} cells compared to T_{conv} cells. SATB1 and PDE3b were both previously described as directly repressed by FOXP3 (Beyer et al., 2011; Gavin et al., 2007) and were here detected as under-represented in T_{reg} cells, further confirming our results.

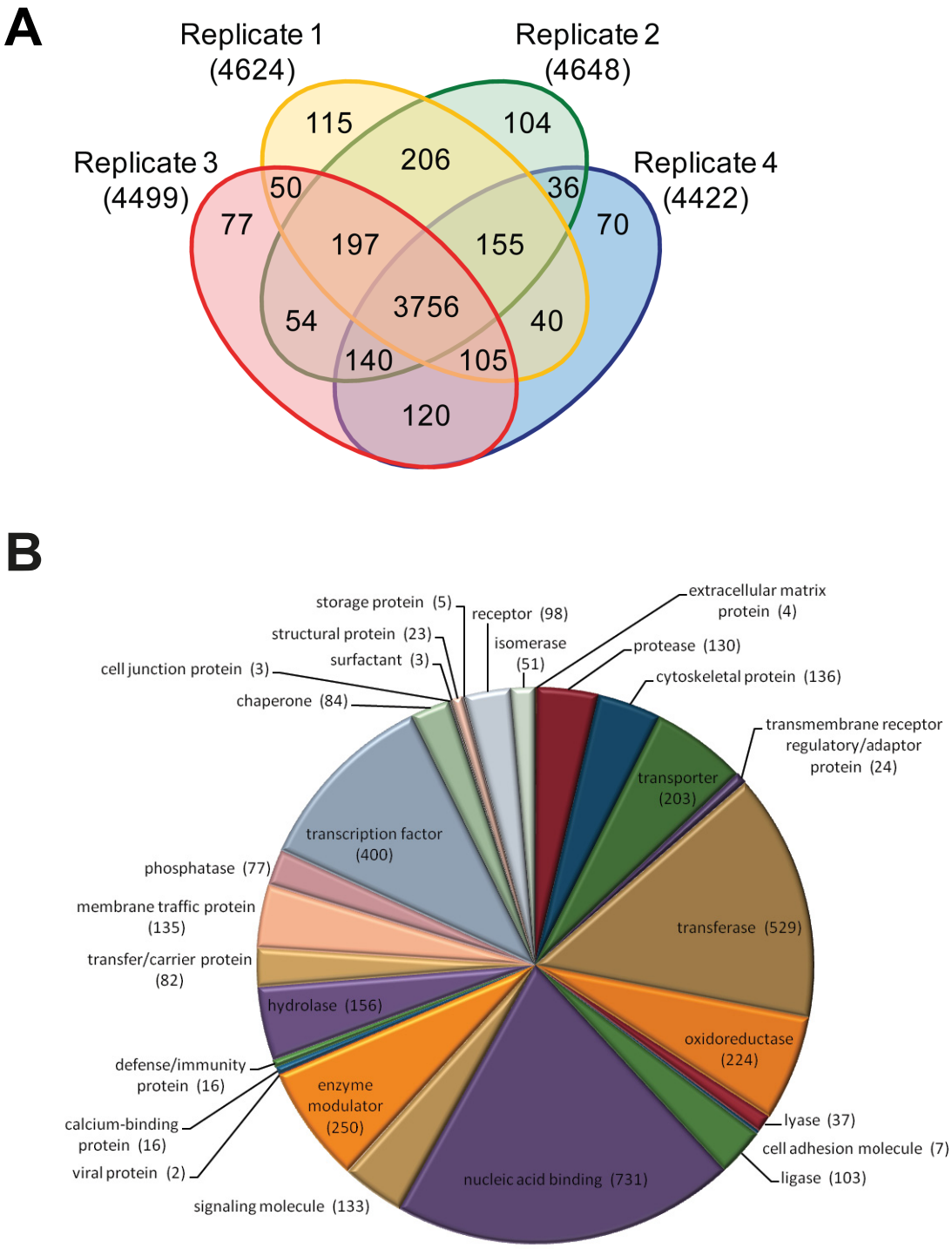

Figure 4: MS replicates and protein classes. (A) Venn diagram of the quantified proteins in four replicates. (B) Pie chart of protein classes among the identified proteins.

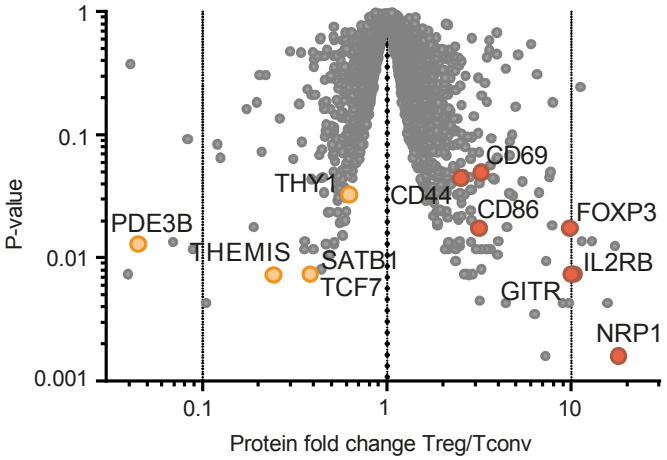

Figure 5: MS data volcano plot. Proteins were extracted from FACS-purified T_{reg} and T_{conv} cells and peptides were analyzed by LC-ESI-MS/MS (n=4). 4859 proteins were identified in at least 2 of 4 replicates and were plotted as average T_{reg}/T_{conv} fold change vs. p-value. Selected significantly over- or under-represented proteins are depicted in red or orange, respectively.

For further validation of the acquired MS data, we assembled a panel of surface markers that were detected as differentially expressed by MS and performed flow cytometry to compare expression on T_{reg} versus T_{conv} cells. Representative histograms, and quantification, are shown (Figure 6A and 6B). All obtained flow cytometric data confirmed the differences in expression detected by the MS. In addition, comparison of fold changes between T_{reg} and T_{conv} cells, detected by MS and flow cytometry showed high correlation ($R^2 = 0.8017$, $P < 0.0001$) (Figure 6C).

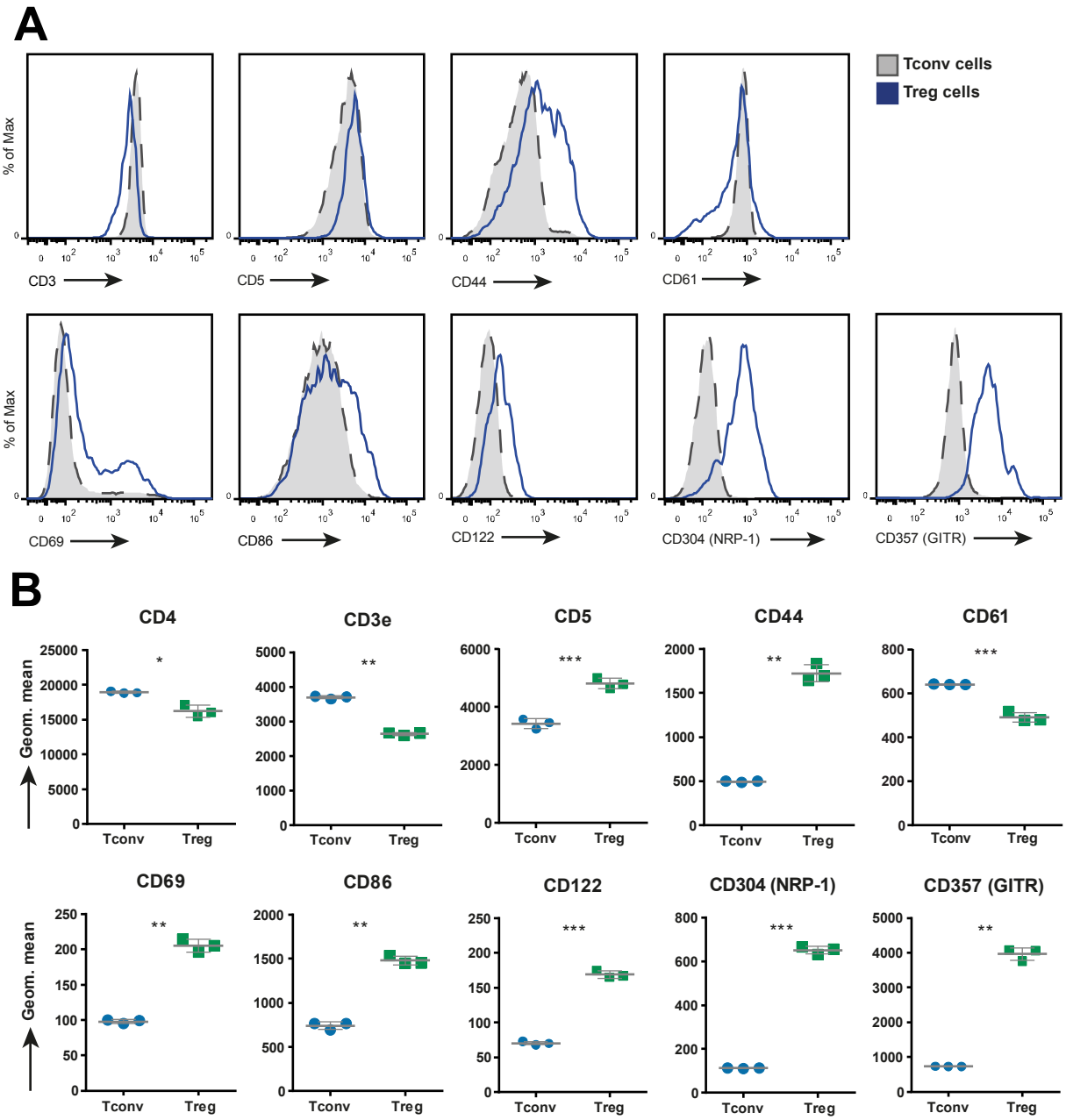
A
Tconv cells
Treg cells
% of Max
CD3
CD5
CD44
CD61
CD69
CD86
CD122
CD304 (NRP-1)
CD357 (GITR)
B
CD4
CD3e
CD5
CD44
CD61
CD69
CD86
CD122
CD304 (NRP-1)
CD357 (GITR)
Geom. mean
Tconv
Treg
C
R^2 = 0.8017
Fold change Treg/Tconv (Antibody geom. mean)
Fold change Treg/Tconv (Mass spectrometry)

Figure 6: MS confirmation by flow cytometry. (A) Flow cytometric analysis of surface molecule expression on LN T_{reg} and T_{conv} cells identified as differentially regulated by MS. Representative histograms show surface molecule expression. (B) Quantification of geometric means from 6A (n=3). Data points represent individual animals. Mean + SD is shown. (C) Correlation of T_{reg}/T_{conv} cell protein fold changes detected by MS and flow cytometry.
* P < 0.05, ** P < 0.01, *** P < 0.001 (unpaired t test).

Gene expression data of T_{reg} and T_{conv} cells was previously published (Feuerer et al., 2010; Hill et al., 2007) and gives us the opportunity to correlate mRNA and protein expression data. To learn more about possible post transcriptional gene regulation we mapped the protein data onto the mRNA expression data set. Comparison of the significantly over- or under-represented proteins to gene expression data showed an overall strong correlation (p<0.0001) (Figure 7A). In the same manner, we next correlated significantly over- and under-represented genes to the protein data and likewise detected a good correlation (p<0.0001) (Figure 7B), indicating that in most cases protein expression follows mRNA expression.

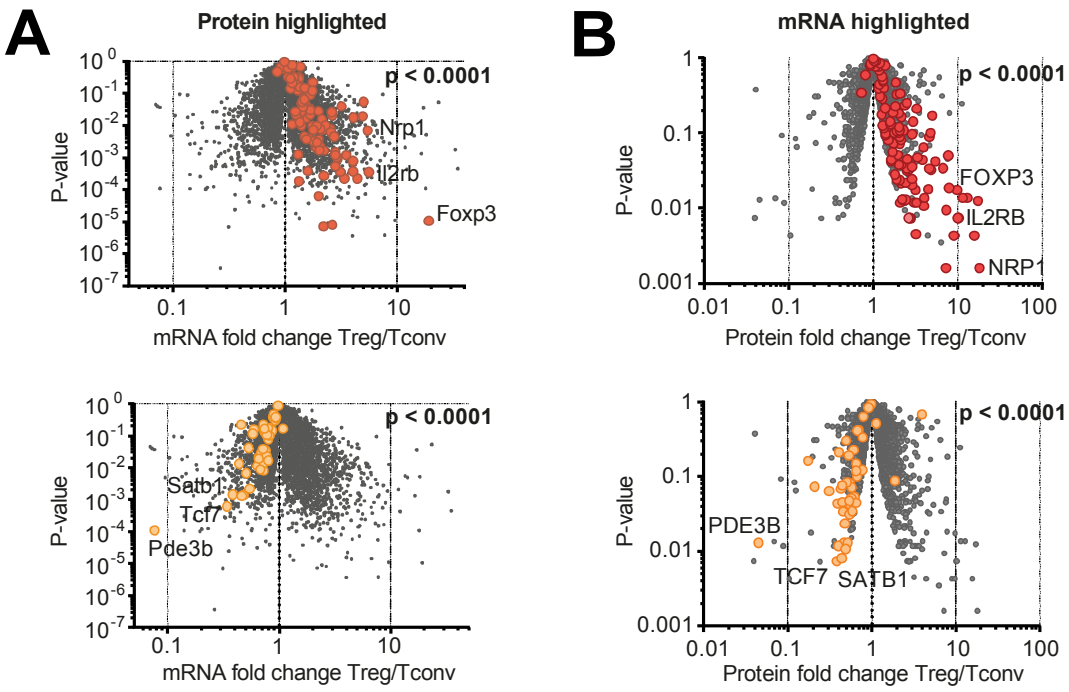

Figure 7: Correlation between mRNA and protein expression data sets. (A-B) Proteins from FACS-purified T_{reg} and T_{conv} cells. Peptides were analyzed by LC-ESI-MS/MS (n=4). Over- or under-represented targets are depicted in red or orange, respectively. P-values were calculated using the chi-square test. (A) Significantly differentially expressed proteins are highlighted onto gene expression data set from LN. (B) Significantly differentially expressed mRNA highlighted onto proteomics data.

To further analyze the similarities and difference between the protein and the gene expression data, we decided to directly compare fold changes detected by the two methods. To this end, we first selected significantly over- or under-represented proteins and then correlated the fold changes detected on the protein level to the ones detected on the mRNA level (Figure 8A, top and bottom). Next, fold change to fold change comparison was repeated in the same manner but this time significantly over- or under-represented mRNA was selected (Figure 8B, top and bottom).

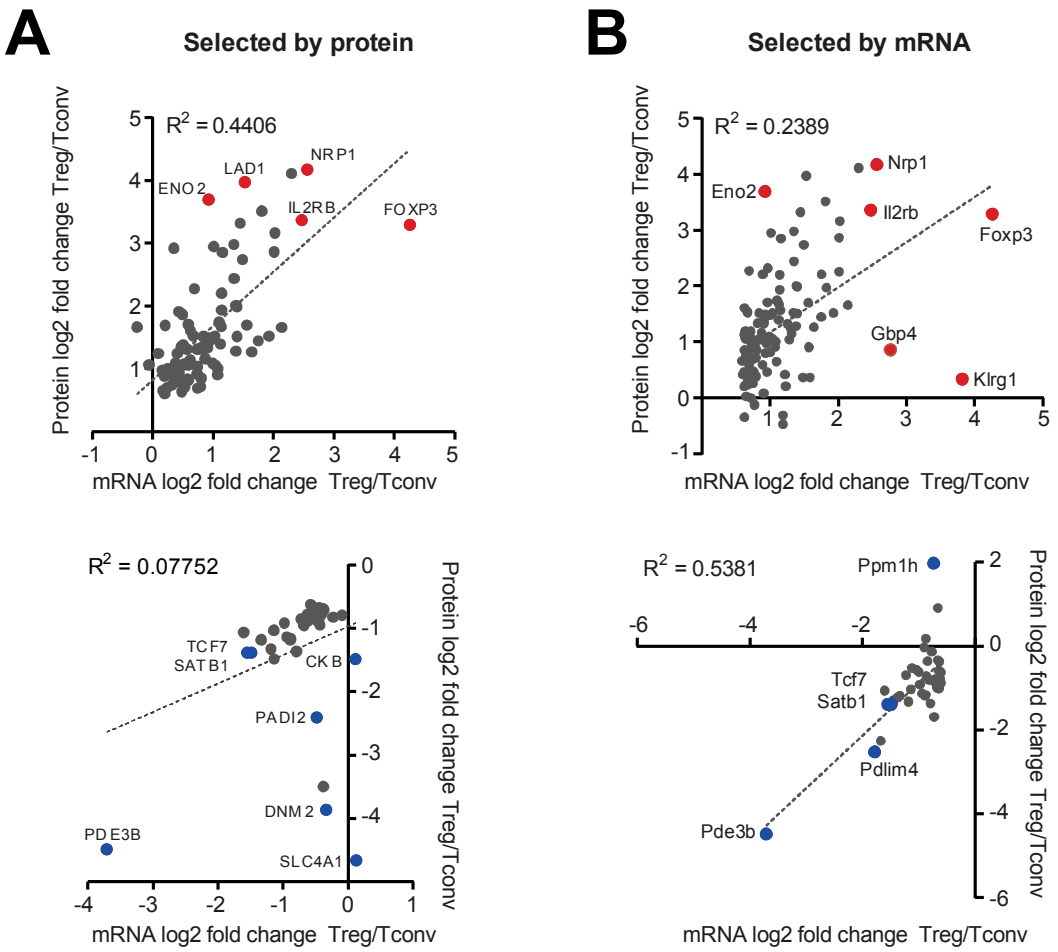

Figure 8: MS replicates and protein classes. (A-B) Protein from FACS-purified T_{reg} and T_{conv} cells. Peptides were analyzed by LC-ESI-MS/MS (n=4). Correlation of gene expression (mRNA) and proteomics data. Comparison of mRNA and protein fold changes. (A) Selected by significantly changed protein. (B) Selected by significantly changed mRNA. Selected over- or under-represented targets are depicted in red or blue, respectively.

Overall, comparisons of significantly differentially expressed proteins and mRNAs showed a reasonably good correlation for most of the candidates. However, we were also able to identify targets with differential expression selectively at the mRNA or protein level. For example SLC4A1 and DNM2 were both detected as strongly under-represented in T_{reg} cells on the protein level yet this change was not detected on the mRNA level, pointing towards possible post transcriptional regulation.

Based on their function and location, we subdivided the 164 differentially expressed proteins. Among the proteins associated with the plasma membrane or the cell surface, we identified already known but also unappreciated candidates, which might be interesting for antibody-mediated targeting of T_{reg} cells. For example, P2RX7, SLC2A3, SLAMF1, ITGA6 or CLEC2D might be attractive T_{reg} cell surface targets (Figure 9, left panel).

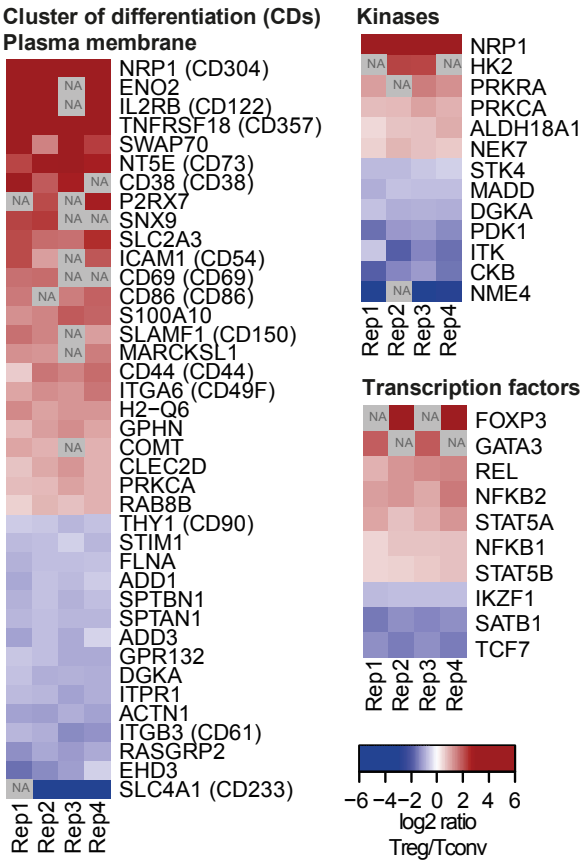

Figure 9: MS replicates and protein classes. Proteins from FACS-purified T_{reg} and T_{conv} cells. Peptides were analyzed by LC-ESI-MS/MS (n=4). Protein expression heat map of groups: CD-listed and plasma membrane, kinases and transcription factors of significantly differentially expressed proteins identified in 2 or more replicates. Not available (NA).

The kinases CKB and NME4, for which protein levels were significantly under-represented in T_{reg} cells, were previously not detected by analysis of gene expression profiles (Figure 9, upper right). The transcription factors GATA3, REL, NFKB2, STAT5A, NFKB1, STAT5B and of course FOXP3 were detected as over-represented in T_{reg} cells. IKZF1, SATB1 and TCF7 were detected as under-represented in T_{reg} cells by our MS analysis (Figure 9, lower right).

Thus, we used quantitative mass spectrometry to delineate the proteome of T_{reg} cells in comparison to the T_{conv} cell proteome and, thereby, identified 164 differentially regulated proteins. While in most cases protein follows mRNA, comparative analysis of the two data sets revealed some relevant differences between protein and mRNA expression and identified unappreciated differences on the protein level.

7.2 Expression of the transcription factor TCF7 in T_{reg} cells

Our MS analysis identified 51 significantly under-represented proteins in T_{reg} cells. We were especially interested in these under-represented proteins, since repression of gene expression is often essential for proper function and differentiation of cells. We cross-compared our set of 51 proteins with mRNA expression data from LN and thymus to screen for interesting candidates (Feuerer et al., 2010; Hill et al., 2007). 43 of the proteins were mapped to the gene expression data and a gene cluster that was prominently under-represented in tT_{reg} cells was identified through hierarchical clustering. The fact that this cluster included 3 genes that were previously described in the context of T_{reg} cells (Figure 10), *Pde3b*, *Satb1* and *Itk* (Beyer et al., 2011; Gavin et al., 2007; Gomez-Rodriguez et al., 2014), made it particularly interesting. The transcription factor *Tcf7,* which was also one of the strongest under-represented proteins in T_{reg} cells (Appendix table 1), was also found within this cluster. The role of TCF7 during thymocyte differentiation has been well established (Verbeek et al., 1995), but its function in the context of tT_{reg} cell generation has not been analyzed.

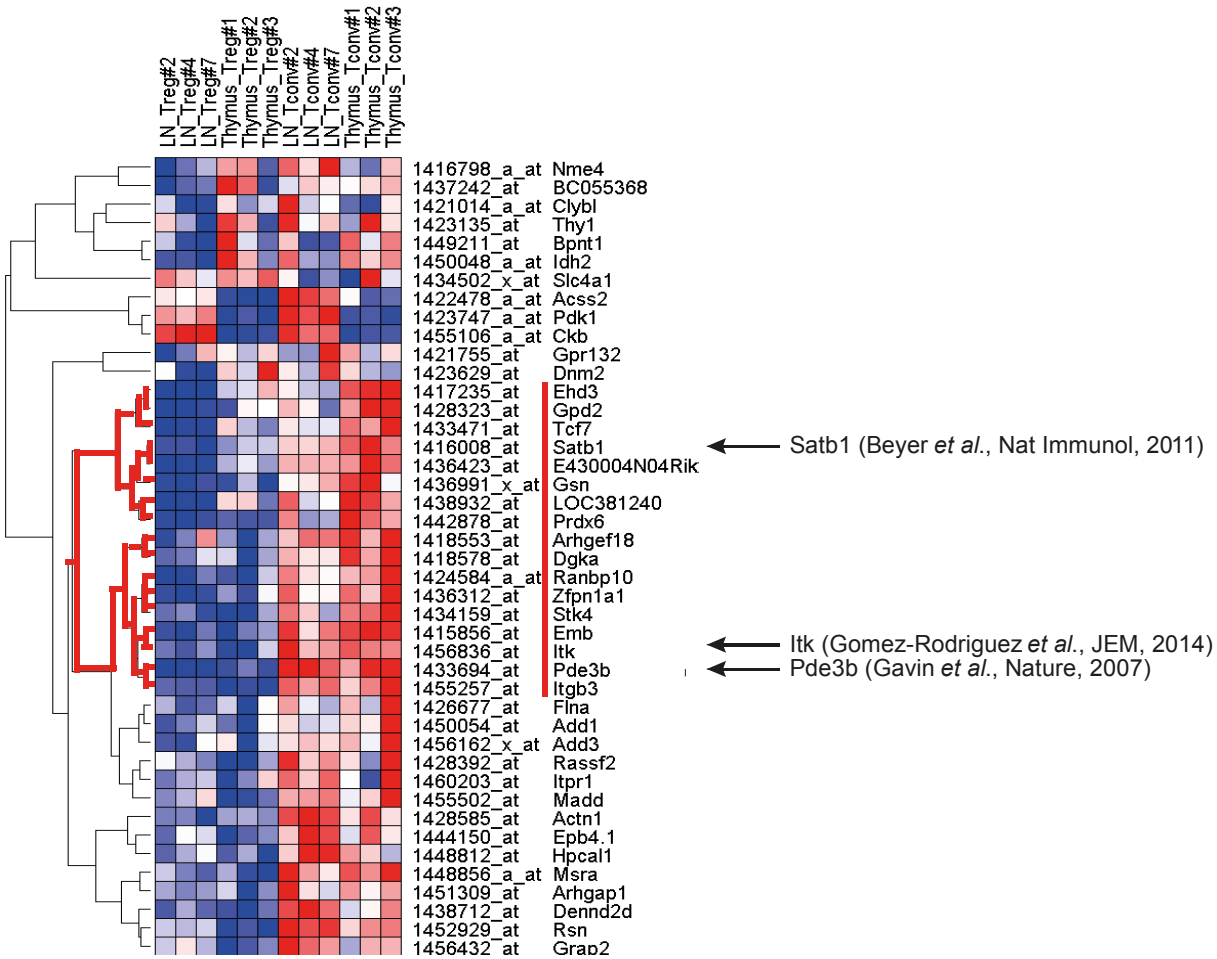

Figure 10: mRNA expression cluster. Gene expression heat map of T_{reg} and T_{conv} cells isolated from LN or thymus with greatest (red) and least (blue) gene expression. Genes selected from the 43 significantly under-represented proteins (T_{reg} compared to T_{conv} cells) identified by differential MS. Hierarchical clustering using Pearson's correlation (row normalized). Red line marks cluster.

The ImmGen consortium recently described a *Tcf7-Lef1* co-regulated cluster of genes in developing thymocytes (Mingueneau et al., 2013). We matched our proteomics data to the *Tcf7-Lef1* co-regulated cluster and thereby identified 19 members in our data set (Figure 11A). Among those were TCF7 and LEF1, THEMIS, ITK and multiple CD3 family members. Interestingly, the whole cluster was significantly ($p = 0.00015$) under-represented in T_{reg} cells in our proteome data set (Figure 11A and 11B).

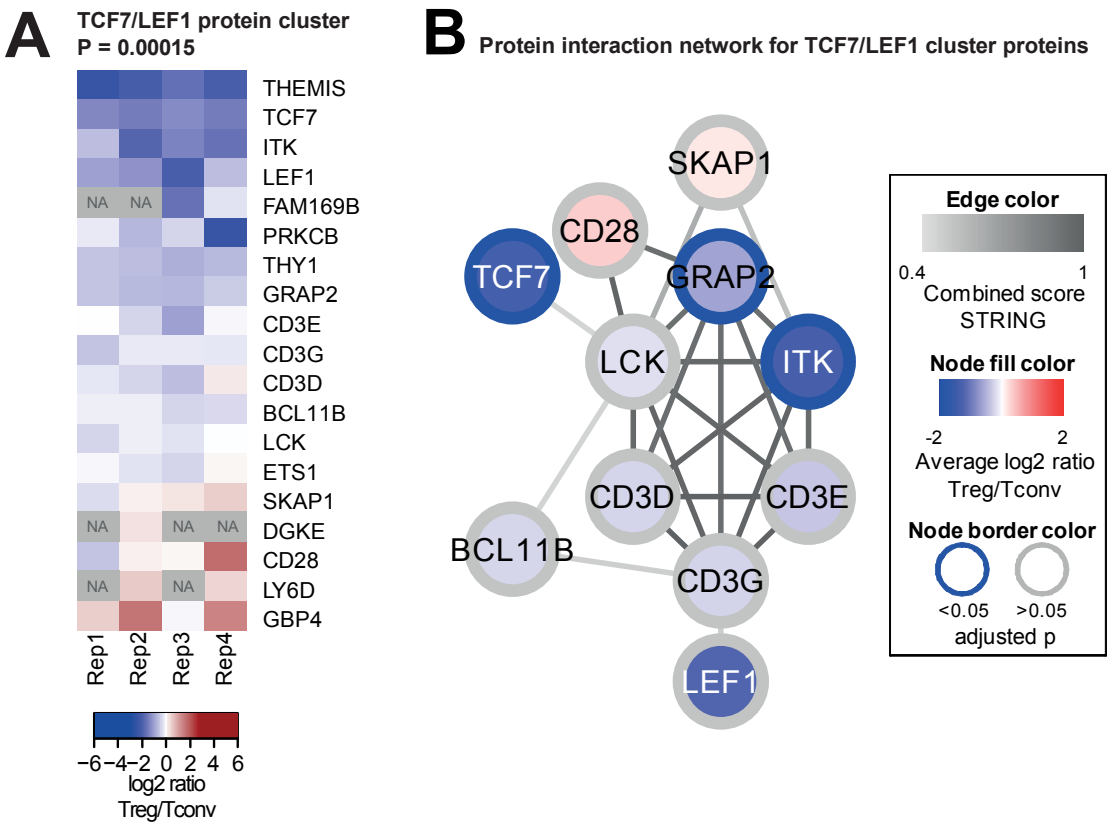

Figure 11: TCF7/LEF1 protein cluster. (A) Heat map of TCF7/LEF1 co-regulated cluster related proteins. (B) Force directed STRING network of interacting proteins from the TCF7/LEF1 cluster.

Our quantitative proteomics analysis identified TCF7 as one of the significantly under-represented proteins in T_{reg} cells. To confirm these findings, we performed intracellular flow cytometric staining for TCF7 in the thymus, LN and spleen (Figure 12A). We included staining for the transcription factor LEF1, as it was part of the *Tcf7-Lef1* co-regulated cluster and can partly compensate for TCF7 function (Okamura et al., 1998). In line with our MS data, we detected reduced TCF7 levels in T_{reg} compared to T_{conv} cells in thymus, LN and spleen. Similarly, LEF1 expression was lower in T_{reg} compared to T_{conv} cells from all 3 organs (Figure 12B). TCF7 and LEF1 staining of B cells was included as negative control. For the thymus, staining of DN cells was included since previous reports stated that TCF7 expression is highest at this developmental stage, which was confirmed by our analysis.

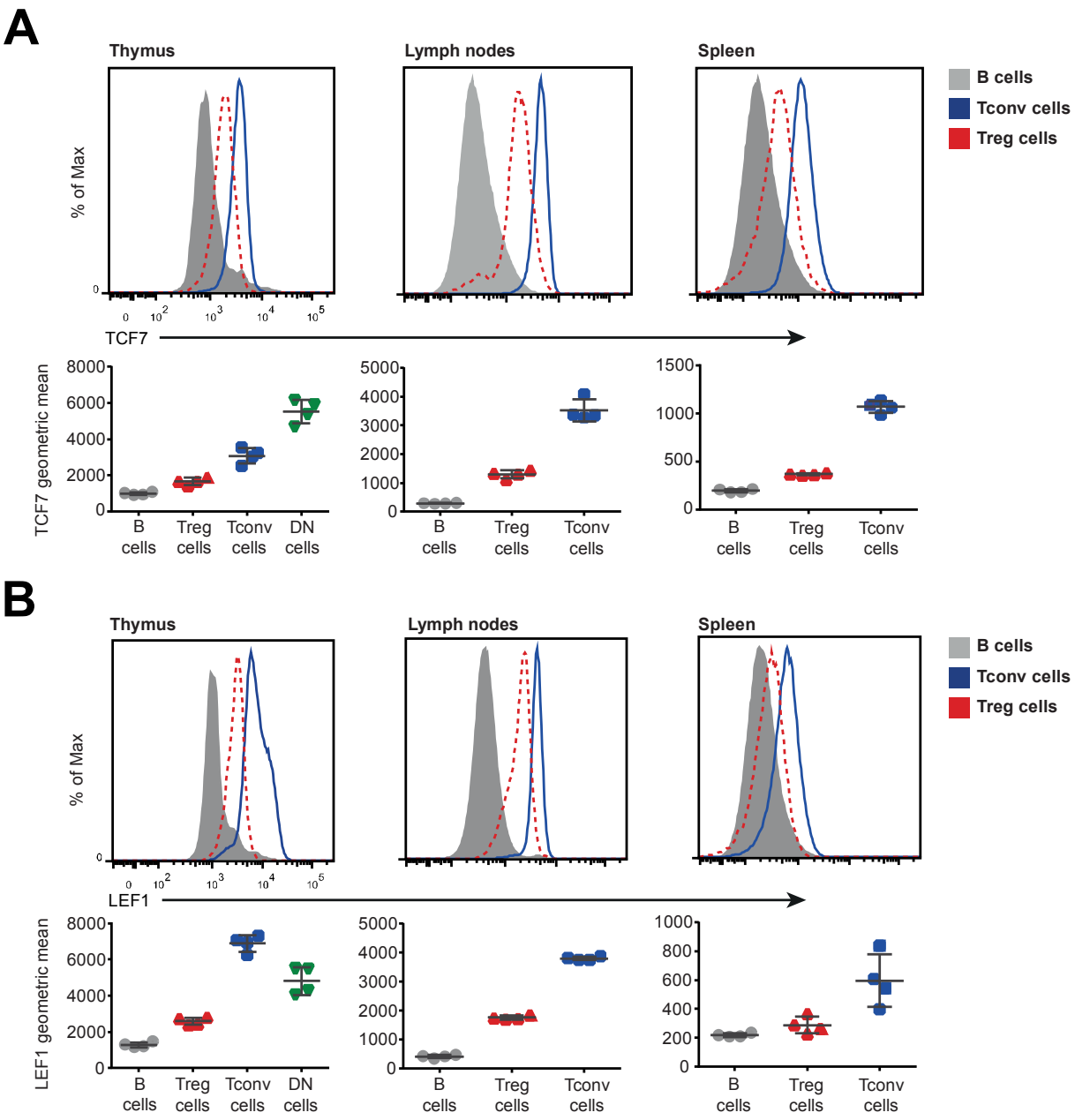

Figure 12: EndogeniousTCF7 and LEF1 expression. (A-B) Flow cytometric analysis of TCF7 and LEF1 expression in T_{reg}, T_{conv} cells, B cells and DN cells from thymus, LN and spleen of *Tcf7*$^{+/+}$ mice. B cells served as a negative control. (A) Representative histograms of intracellular TCF7 staining from individual animals and TCF7 geometric mean with mean and standard deviation (SD) (n=4). (B) Representative histograms of intracellular LEF1 staining from individual animals and LEF1 geometric mean with mean and SD (n=4).

Through our comparative proteomics data and detailed analysis, we identified the transcription factor TCF7 as a promising candidate for further investigations in the context of tT_{reg} cell generation.

7.3 TCF7 deficiency results in an increased fraction of T_{reg} cells in the CD4SP and DP populations

To study the role of TCF7 in tT_{reg} cell differentiation, we made use of the *Tcf7*$^{-/-}$ mouse model (Verbeek et al., 1995). A short deletion was introduced into exon 7 of the *Tcf7* gene which encodes for the DNA binding HMG-box region. As a result of the deletion, the thymus of *Tcf7*-deficient mice is greatly reduced in size and cellularity. Previous studies of the *Tcf7*$^{-/-}$ mouse showed that the T cell maturation is impaired with several developmental defects at the DN and DP stages of thymocyte development (Kovalovsky et al., 2009; Schilham et al., 1998; Verbeek et al., 1995). As a starting point for further investigations of the *Tcf7*$^{-/-}$ mouse, we first wanted to study the thymus in more detail through flow cytometric analysis and cell counting of the DN, DP, CD4SP and CD8SP populations (Figure 13A-C).

Comparison of DN, DP CD4SP and CD8SP thymocytes from *Tcf7*-deficient (*Tcf7*$^{-/-}$), heterozygous (*Tcf7*$^{+/-}$) and wild-type (*Tcf7*$^{+/+}$) littermate controls showed that the fractions of DN and CD8SP cells were increased while the fraction of DP cells was significantly decreased in *Tcf7*$^{-/-}$ compared to *Tcf7*$^{+/-}$ and *Tcf7*$^{+/+}$ mice. The percentage of CD4SP cells was not changed in *Tcf7*$^{-/-}$ compared to the other two groups. No differences were detected between *Tcf7*$^{+/-}$ and *Tcf7*$^{+/+}$ thymic populations (Figure 13A-B). As previously described, we found that the total cell numbers of DN, DP, CD4SP and CD8SP thymocytes were reduced in *Tcf7*$^{-/-}$ compared to the *Tcf7*$^{+/-}$ and *Tcf7*$^{+/+}$ littermate controls (Figure 13C). The greatest difference in cell numbers was detected at the DP stage. Here we found that the difference between *Tcf7*$^{+/+}$ and *Tcf7*$^{-/-}$ was 14-fold, while the detected difference at the DN stage was only about 4-fold (Figure 13C, right panel). Between the *Tcf7*$^{+/+}$ and the *Tcf7*$^{+/-}$ mice only minor differences in the cell numbers were detected.

Morphologically a healthy thymus is organized into a central medulla and a peripheral cortex region. To control for thymic organization we performed immunohistological staining of *Tcf7*$^{-/-}$ and *Tcf7*$^{+/+}$ thymi with keratin 14 (K14), a marker for thymic medullary epithelial cells. Tcf7$^{-/-}$ thymi showed an overall reduced size, but a relatively normal organization of the thymus into medullary and cortical regions (Figure 14A-B).

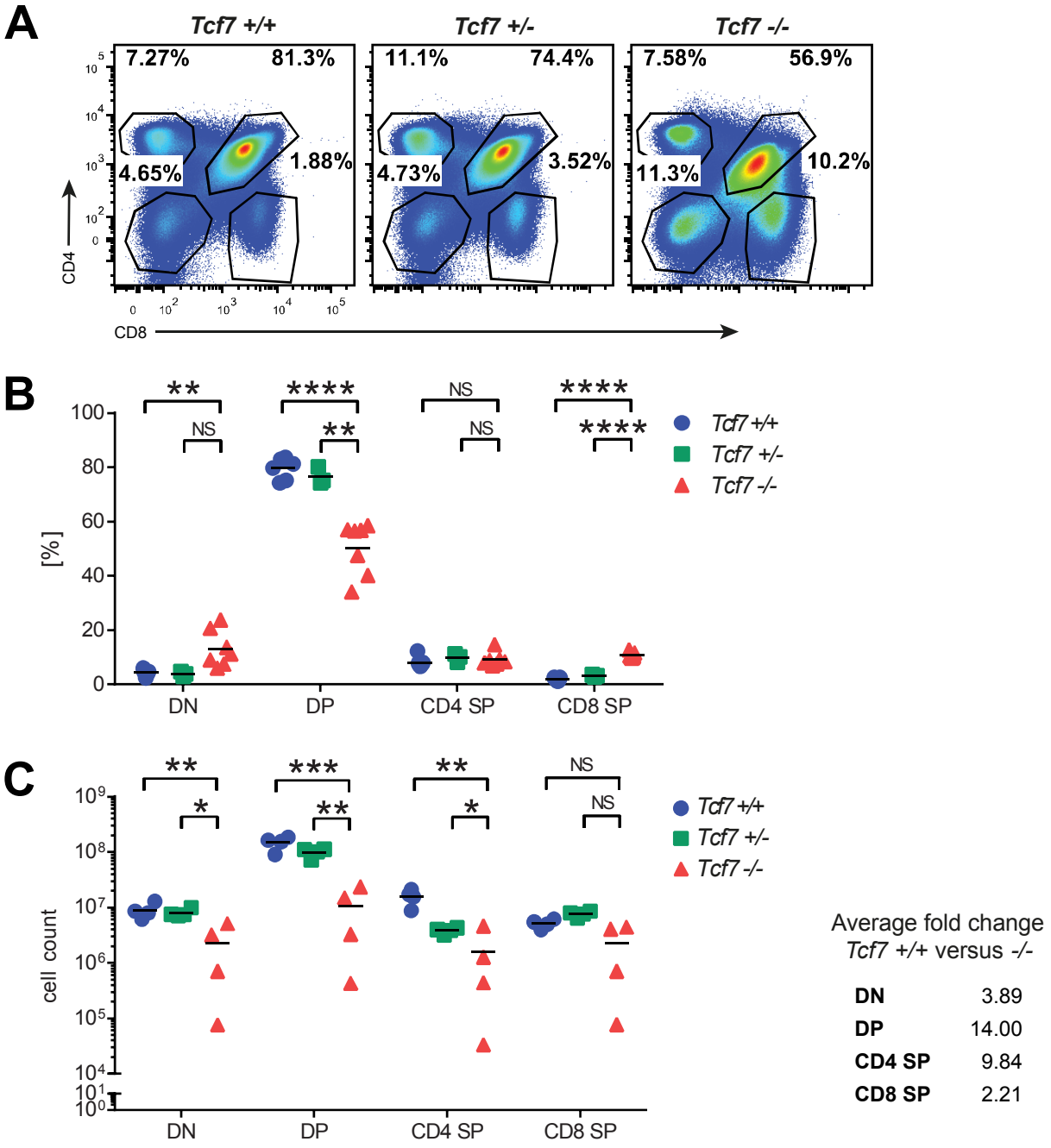

Figure 13: Analysis of the *Tcf7*$^{+/+}$, *Tcf7*$^{+/-}$ and *Tcf7*$^{-/-}$ thymi (A-C) Flow cytometric analysis of thymic populations from *Tcf7*$^{+/+}$, *Tcf7*$^{+/-}$ and *Tcf7*$^{-/-}$ mice. (A) Representative dot plots of thymic CD4 and CD8 populations. (B) Quantified percentages with mean of DN, DP, CD4SP and CD8SP populations pregated on CD11b^{-}CD11c^{-}CD19^{-} thymocytes. (C) Quantified cell counts of DN, DP, CD4SP and CD8SP populations from total thymus. Cell counts were performed using counting beads. Table shows fold change of the average cell count between *Tcf7*$^{+/+}$ and *Tcf7*$^{-/-}$ from DN, DP, CD4SP and CD8SP populations.

NS P > 0.05, * P < 0.05, ** P < 0.01, *** P < 0.001, **** P < 0.0001 (unpaired t-test or ordinary one-way ANOVA).

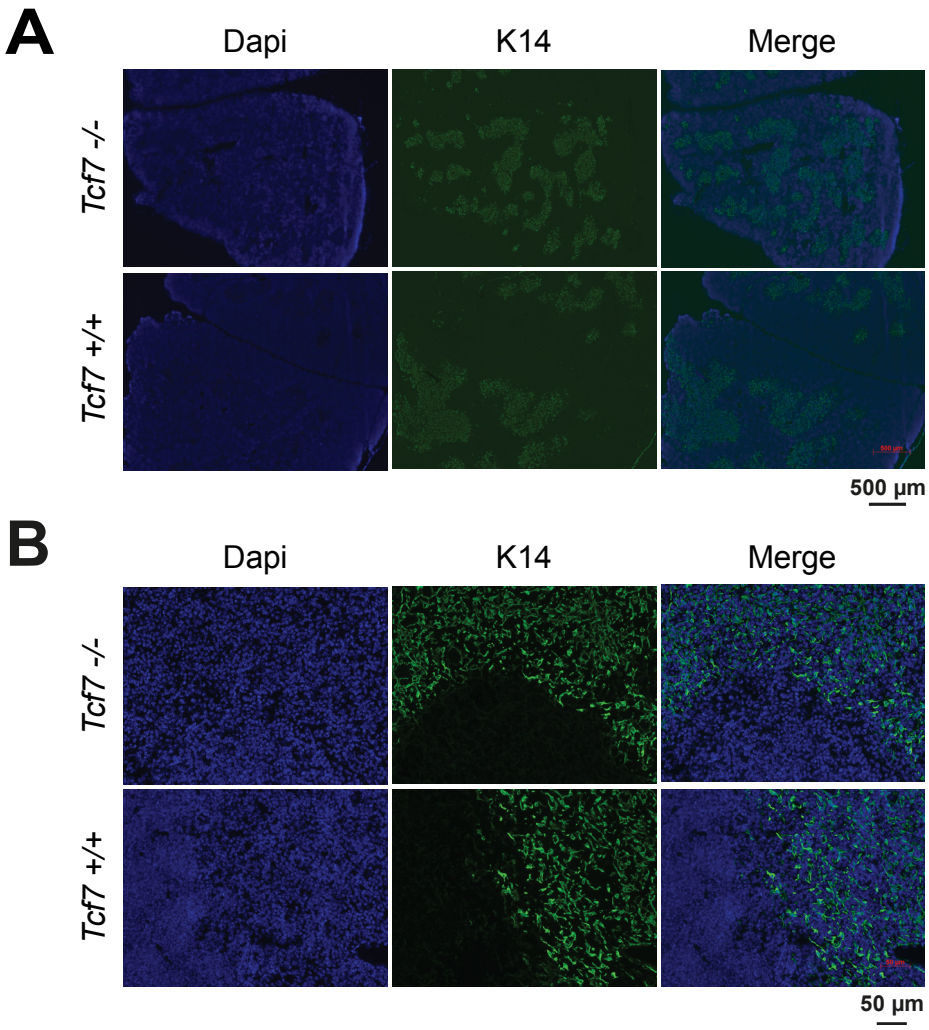

Figure 14: Thymus immunofluorescence. (A-B) Immunofluorescence imaging of $K14^+$ medullary epithelial cells from *Tcf7*$^{+/+}$ and *Tcf7*$^{-/-}$ thymi. Representative data for 2 to 3 individual thymi is shown (A) 2.5-fold magnification and 500 µm scale bar. (B) 20-fold magnification and 50 µm scale bar.

So far, studies of CD4 T cell development in the absence TCF7 focused on the development of CD4 T cells without discrimination between T_{conv} and T_{reg} cells. We now aimed to characterize the development of tT_{reg} cells more closely with the help of the *Tcf7*$^{-/-}$ model. Analysis of the $Foxp3^+$ T_{reg} cell frequency among the CD4SP population revealed that the fraction of T_{reg} cells in *Tcf7*$^{-/-}$ mice was about three times larger than in *Tcf7*$^{+/+}$ mice (5 versus 15 percent) (Figure 15A). However, the T_{reg} cell count was not elevated due to the massive reduction of total thymocytes in the *Tcf7*$^{-/-}$ thymus (data not shown).

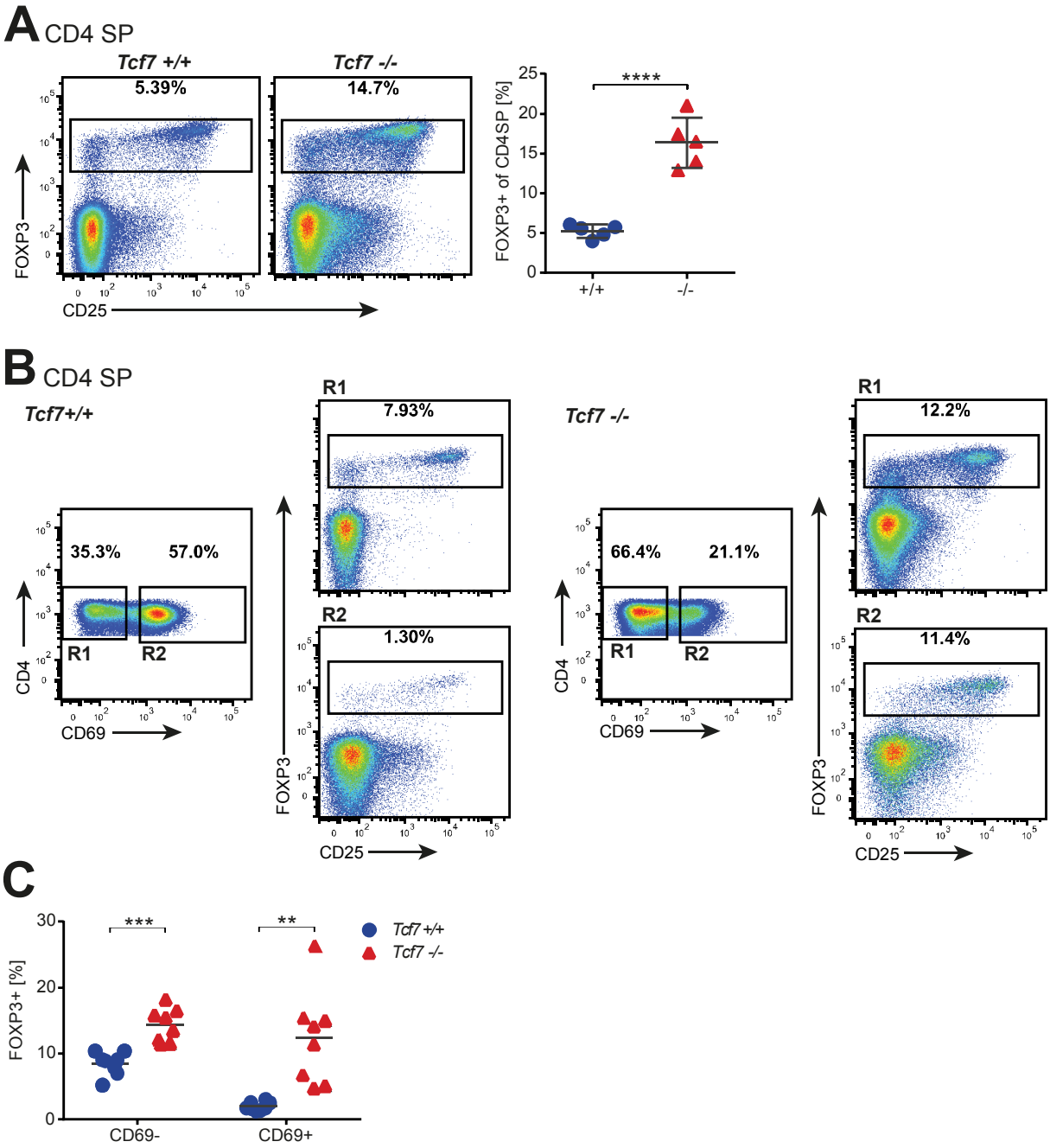

Figure 15: Influence of TCF7 on the FOXP3 expression at the CD4SP stage. (A-C) Flow cytometric analysis in CD4SP thymocytes from *Tcf7*$^{+/+}$ and *Tcf7*$^{-/-}$ mice. Numbers show percentages of cells within the indicated box. (A) Representative plots of FOXP3 and CD25 expression in CD4SP cells and quantification with mean + SD from individual mice (n=5). (B) Representative plots of CD69^{+} (R2) and CD69^{-} (R1) T_{reg} cells among CD4SP cells. (C) Quantification and mean of B for individual mice (n=8).

** P < 0.01, *** P < 0.001, **** P < 0.0001 (unpaired t-test).

CD69, a C-type lectin-like signaling receptor, is transiently expressed on DP thymocytes that undergo positive and negative selection. Expression of CD69 is lost at the CD4SP/CD8SP stage before emigration to the periphery (Feng et al., 2002; Nakayama et al., 2002). We subdivided the CD4SP population based on CD69 expression into mature ($CD69^-$) and more immature ($CD69^+$) CD4SP thymocytes and looked at FOXP3 expression in these cells. In line with this, we observed that in *Tcf7*$^{+/+}$ mice, differentiated $FOXP3^+$ tT_{reg} cells were mainly located within the mature $CD69^-$ compartment (Figure 15B, left). Interestingly, *Tcf7*$^{-/-}$ mice showed an almost equal distribution of $FOXP3^+$ T_{reg} cells between the $CD69^+$ and $CD69^-$ compartment. And both populations were present at significantly higher frequencies of CD4SP cells compared to *Tcf7*$^{+/+}$ mice (Figure 15B-C).

FOXP3 expression depends on TCR/MHC interaction and $FOXP3^+$ cells are therefore first detectable at the DP stage (Fontenot et al., 2005b). We looked at FOXP3 expression in DP cells of *Tcf7*$^{+/+}$ and *Tcf7*$^{-/-}$ mice and observed a 6 times higher frequency of $FOXP3^+$ cells in the *Tcf7*$^{-/-}$ mice (Figure 16).

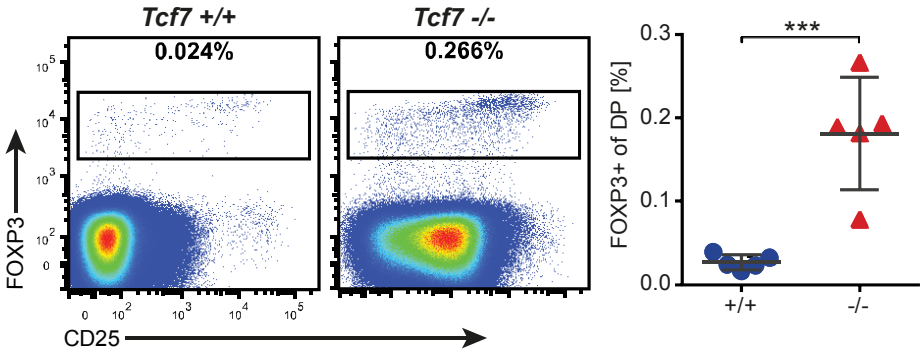

Figure 16: Influence of TCF7 on the FOXP3 expression at the DP stage. Flow cytometric analysis of FOXP3 expression in DP thymocytes from *Tcf7*$^{+/+}$ and *Tcf7*$^{-/-}$ mice. Numbers show percentages of cells within the indicated box. Representative plots of FOXP3 and CD25 expression in DP cells and quantification with mean + SD for individual mice are shown (n=5).

*** $P < 0.001$ (unpaired t-test).

In summary, analysis of the *Tcf7*$^{-/-}$ thymus compared to *Tcf7*$^{+/-}$ and *Tcf7*$^{+/+}$ confirmed previous reports of reduced cellularity, changed frequencies of DN, DP, CD4SP and CD8SP cells and a normal organization into medullar and cortex regions. In addition, our observations demonstrate that the frequency of T_{reg} cells in the CD4SP and DP stages is elevated in the absence of TCF7.

7.4 TCR-independent expression of FOXP3 in thymic DN cells

It is currently believed that the expression of FOXP3 is induced in a TCR-dependent fashion at the DP or CD4SP stage of thymocyte development (Fontenot et al., 2005b). Nevertheless, we examined the DN cells for the presence of FOXP3. Surprisingly, we detected that between 0.5 and 3 percent of the total DN cells from *Tcf7*$^{-/-}$ mice expressed FOXP3 (Figure 17A).

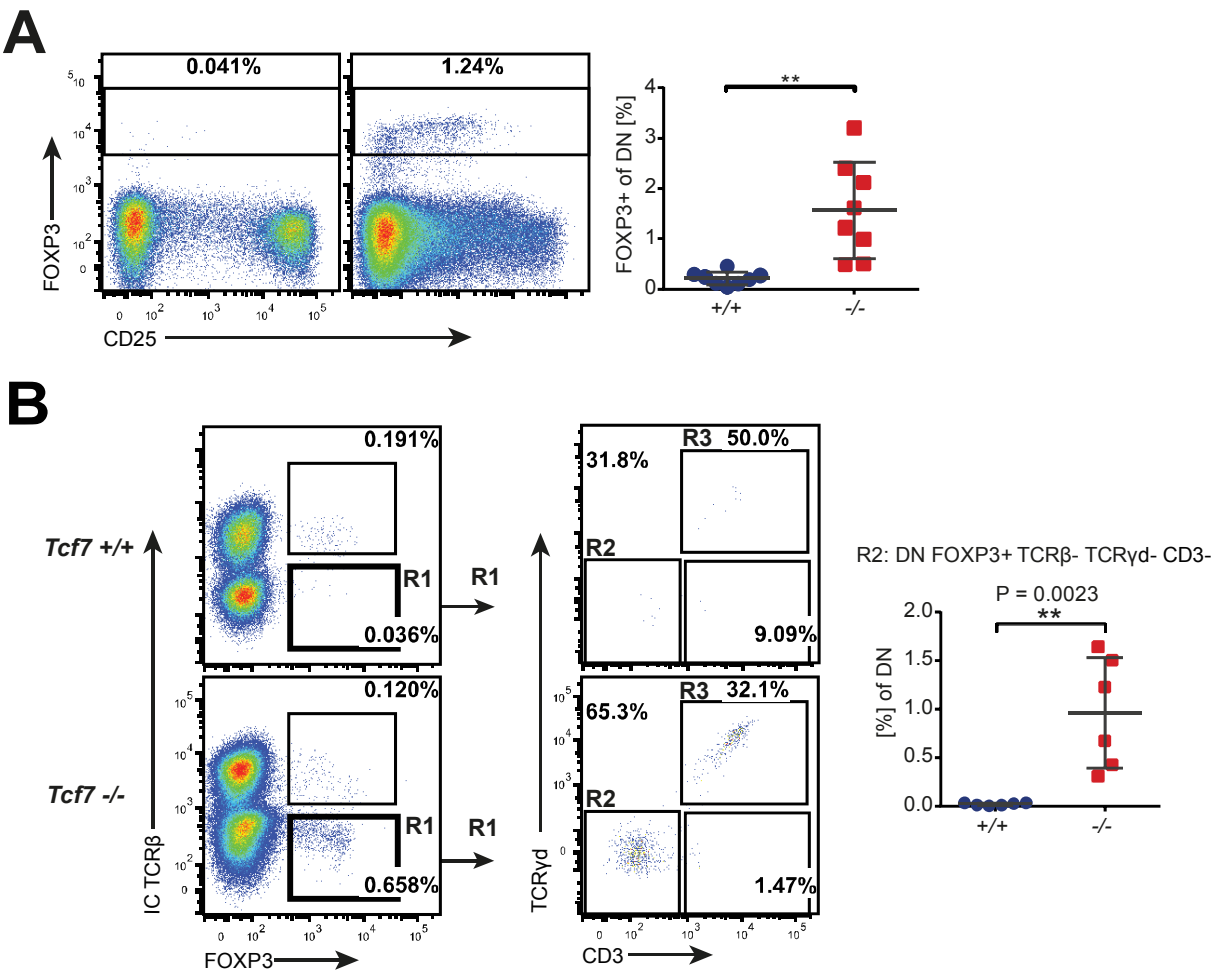

Figure 17: FOXP3 expression at the DN cell stage in *Tcf7*-deficient mice. (A-B) Flow cytometric analysis of DN cells from *Tcf7*$^{+/+}$ and *Tcf7*$^{-/-}$ mice. Mean + SD are shown for all quantified data. Numbers show percentages of cells within the indicated box. (A) Representative plots of FOXP3 staining in DN cells and quantification for individual mice (n=8). (B) Representative plots of the identification of DN FOXP3^{+}, CD3^{-}, IC TCRβ^{-}, and TCRγδ^{-} cells (R2 gate) and quantification of R2 depicted as percentage of total DN cells (n=6). TCRβ was intracellular (IC) stained. ** P < 0.01 (unpaired t-test).

Given the current dogma that *Foxp3* gene induction only occurs after TCR engagement, and that cells at the DN stage should not yet express a TCR, we decided to further study this unique cell population. For a closer analysis of the DN population we stained for CD3, TCRβ and TCRγδ (for γδ T cells), to exclude mature T cells that abrogated the expression of CD4 or CD8. Intracellular (IC) TCRβ staining was applied to detect cells that were just about to express or that had internalized their TCR. When we excluded all $CD3^+$, $TCR\beta^+$ or $TCR\gamma\delta^+$ DN cells we were left with a population of TCR^- $FOXP3^+$ DN cells that was present in the *Tcf7*$^{-/-}$ but not in the *Tcf7*$^{+/+}$ mice (Figure 17B, R2). This population represented between 0.2 and 1.5 percent of the total DN cells.

The stable expression of the trans-membrane glycoprotein CD5 occurs only after the positive selection step and the CD5 surface expression level on thymocytes and mature T cells was directly correlated to the overall avidity of the MHC-TCR interaction strength during positive selection (Azzam et al., 1998). The CD5 expression level can therefore be used as an indicator for previous TCR engagement and positive selection. We examined CD5 surface expression of $FOXP3^+$ DN cells from *Tcf7*$^{-/-}$ mice and found that they, just like the classical DN cells, did not show CD5 expression (Figure 18). This is in contrast to the DP and CD4SP $FOXP3^+$ or $FOXP3^-$ T cell populations in the thymus (Figure 18A-B).

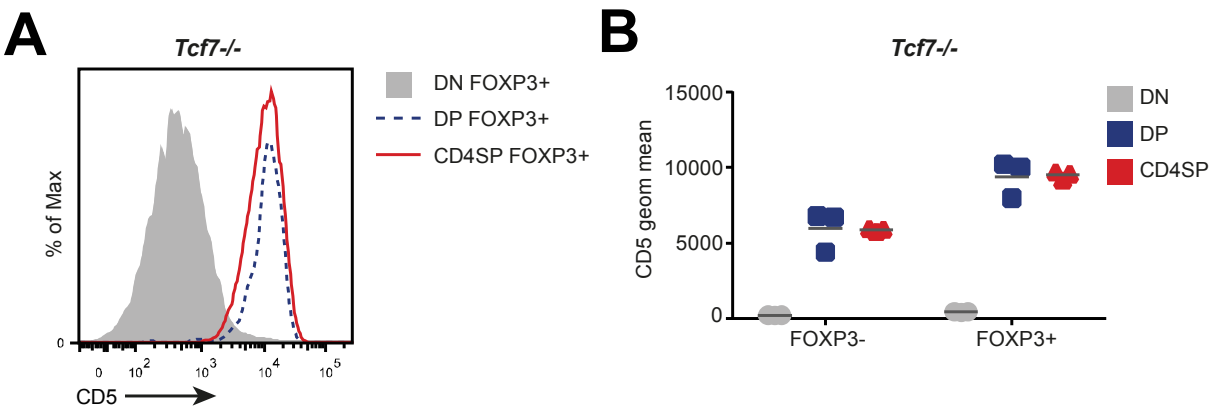

Figure 18: Expression of CD5 in $FOXP3^-$ and $FOXP3^+$ cells from *Tcf7*$^{-/-}$ mice. (A-B) Flow cytometric analysis of CD5 expression in DN, DP and CD4SP cells from *Tcf7*$^{-/-}$ mice. (A) Representative histogram of CD5 staining on $Foxp3^+$ DN, DP, and CD4SP cells from *Tcf7*$^{-/-}$ mice. (B) Quantification of CD5 geometric mean from DN, DP, and CD4SP $FOXP3^+$ or $FOXP3^-$ populations. Mean is shown for quantified data. Each symbol represents an individual animal (n=3).

Notably, the CD5 expression of the FOXP3+ populations was in general higher than the surface expression of the FOXP3- populations. The obtained results indicate that FOXP3+ DN cells had no previous TCR engagement which distinguishes them from other FOXP3$^+$ T_{reg} cells.

The DN population can be sub-divided into the DN1-DN4 developmental stages depending on the expression of the markers CD44 and CD25 (Figure 19A) (Godfrey et al., 1993). Staining of CD44 and CD25 was performed to further characterize the FOXP3$^+$CD3$^-$TCR$^-$ DN population. We thereby identified the FOXP3$^+$ TCRβ$^-$ population (R1) as a transition state between DN1 and DN2, with high CD44 and low CD25 expression (Figure 19B, R1). In *Tcf7*$^{-/-}$ mice we also detected this transition population among the FOXP3$^-$ DN cells, while the population was barely present in *Tcf7*$^{+/+}$ mice (Figure 19B, R2 and R3).

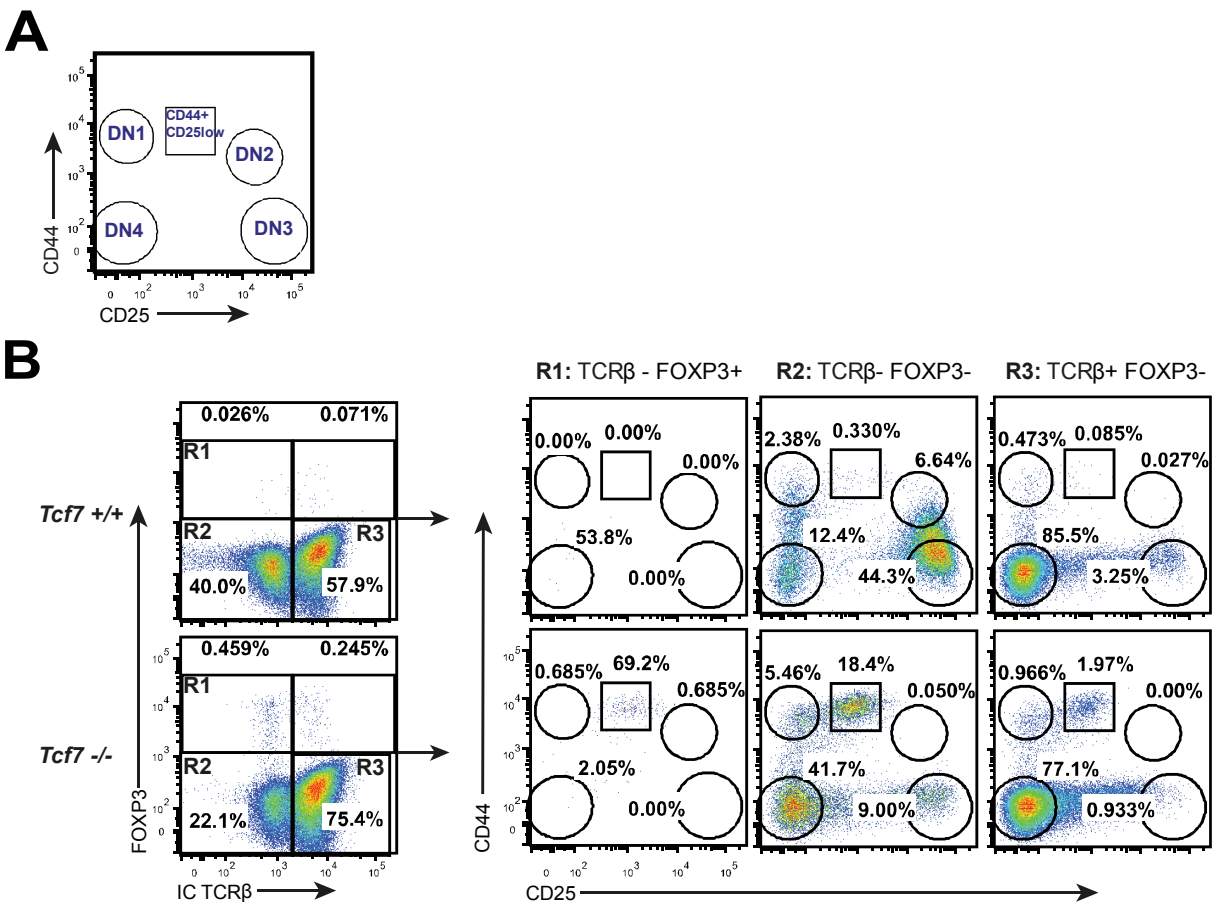

Figure 19: Expression of FOXP3 at thymic DN1-4 stages. (A) Thymus gating scheme for the identification of DN1-4 stages, based on the expression of CD44 and CD25. (B) Flow cytometric analysis of DN cells from *Tcf7*$^{+/+}$ and *Tcf7*$^{-/-}$ mice. Numbers show percentages of cells within the indicated box. TCRβ was intracellular (IC) stained. Representative plots for the gating of DN1-4 stages based on CD44 and CD25 staining of indicated populations (R1-R3).

Examination of the DN population in *Tcf7*-deficient mice indicates that TCF7 inhibits premature FOXP3 expression that can arise independently of TCR expression.

7.5 FOXP3-expressing DN cells do not respond to TCR stimulation *in vivo*

For a better functional characterization of the unique FOXP3-expressing DN cells in *Tcf7*$^{-/-}$ mice we induced the expression of a transgenic (TG) TCR in the *Tcf7*$^{-/-}$ mice and analyzed their ability to respond to antigen stimulation. The cognate antigen of our transgenic TCR is expressed on all thymic MHC class II positive APCs, including mTECs, cTECs and DCs. The generated mouse line expressed the “TEa” transgenic TCR with specificity for a peptide “Eα” derived from the MHC class II I-E molecule (Grubin et al., 1997). The Eα peptide from the MHC class II I-E molecule is presented by the MHC class II I-A. C57BL/6 mice express the restricting MHC (I-A) but not the donor MHC of the peptide (I-E). Since our *Tcf7*$^{-/-}$ mouse line was bred on a mixed C57BL/6-129 background and the 129 mouse strain expresses both, the restricting MHC and the donor MHC, the cognate antigen is present in a fraction of the mice. Since the transgenic TCRαβ chains are already expressed at the DN stage, we were able to study the influence of the antigen presence on FOXP3^{+} DN cells in our transgenic mice. We identified the mice that were positive for the donor peptide (Eα) either by PCR or antibody staining (Figure 20A-B).

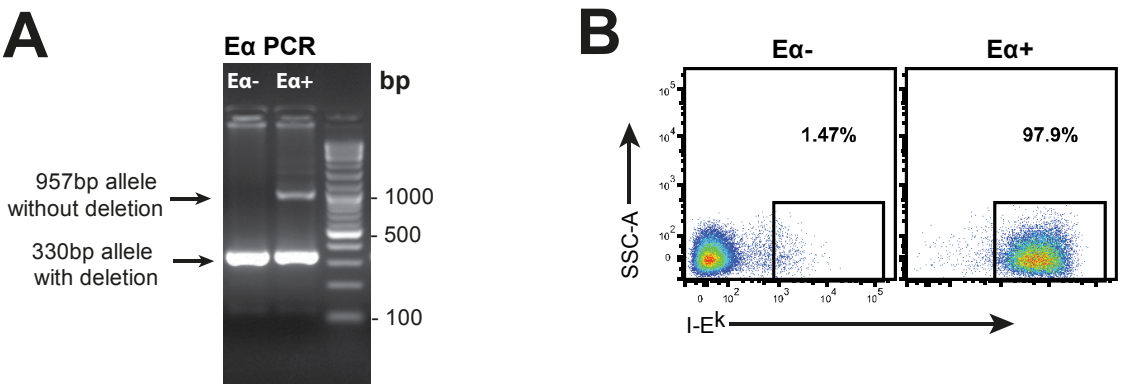

Figure 20: Identification of I-E^{k} antigen positive mice. (A) PCR from digested tail tissue identified mice with the I-E^{k} deletion (only 330bp fragment, Eα peptide^{-}, left lane) and partially without the deletion (957bp + 330bp fragment, Eα peptide^{+}, right lane). (B) Representative plots for the identification of I-E^{k} antigen expression in splenic CD19^{+} B cells by flow cytometry using anti-I-E^{k} antibody.

We were able to detect the two chains of the TEa-transgenic TCR, Vα2 and Vβ6, by flow cytometry. As expected, a significantly lower percentage of TCR-transgenic T cells was observed among the CD4SP cells from I-E^{k} antigen positive mice, indicating that a large part of the T cells carrying the transgenic TCR were deleted in antigen expressing mice (Figure 21A-B). In this respect, we did not detect differences between the *Tcf7*$^{+/+}$ and *Tcf7*$^{-/-}$ mice (Figure 21A-B).

We separated the transgenic T cells into TCR^{low} and TCR^{high} TG populations for a more in-depth analysis of the CD4SP $FOXP3^{-}$ T cells (Figure 21A). Our analysis demonstrated that the TCR^{high} TG fraction of the CD4SP $FOXP3^{-}$ cells was significantly reduced in the presence of the antigen (Figure 21C). For the CD4SP $FOXP3^{+}$ population similar observations were made (Figure 21D-E).

The data collected for the CD4SP cells demonstrated that we had established a robust model with strong negative selection pressure. Antigen exposure was even so strong that T_{reg} cells only partially survived negative selection. We next started to analyze the DN compartment and, in line with our previous findings, FOXP3 expressing DN cells were again only found in the *Tcf7*$^{-/-}$ mice (Figure 22A-B). TCR expression levels of TCR TG $FOXP3^{+}$ DN were analyzed and we observed that $FOXP3^{+}$ DN cells were mainly found in the TCR^{high} compartment (Figure 22C-D). In contrast to the $FOXP3^{+}$ CD4SP T cells, there was no influence of the cognate antigen presence on the $FOXP3^{+}$ DN cells. The frequencies of TG TCR expressing $FOXP3^{+}$ DN cells, as well as the expression levels of the TG TCR were not changed, indicating that there was no TCR engagement at the level of $FOXP3^{+}$ DN cells (Figure 22C-D).

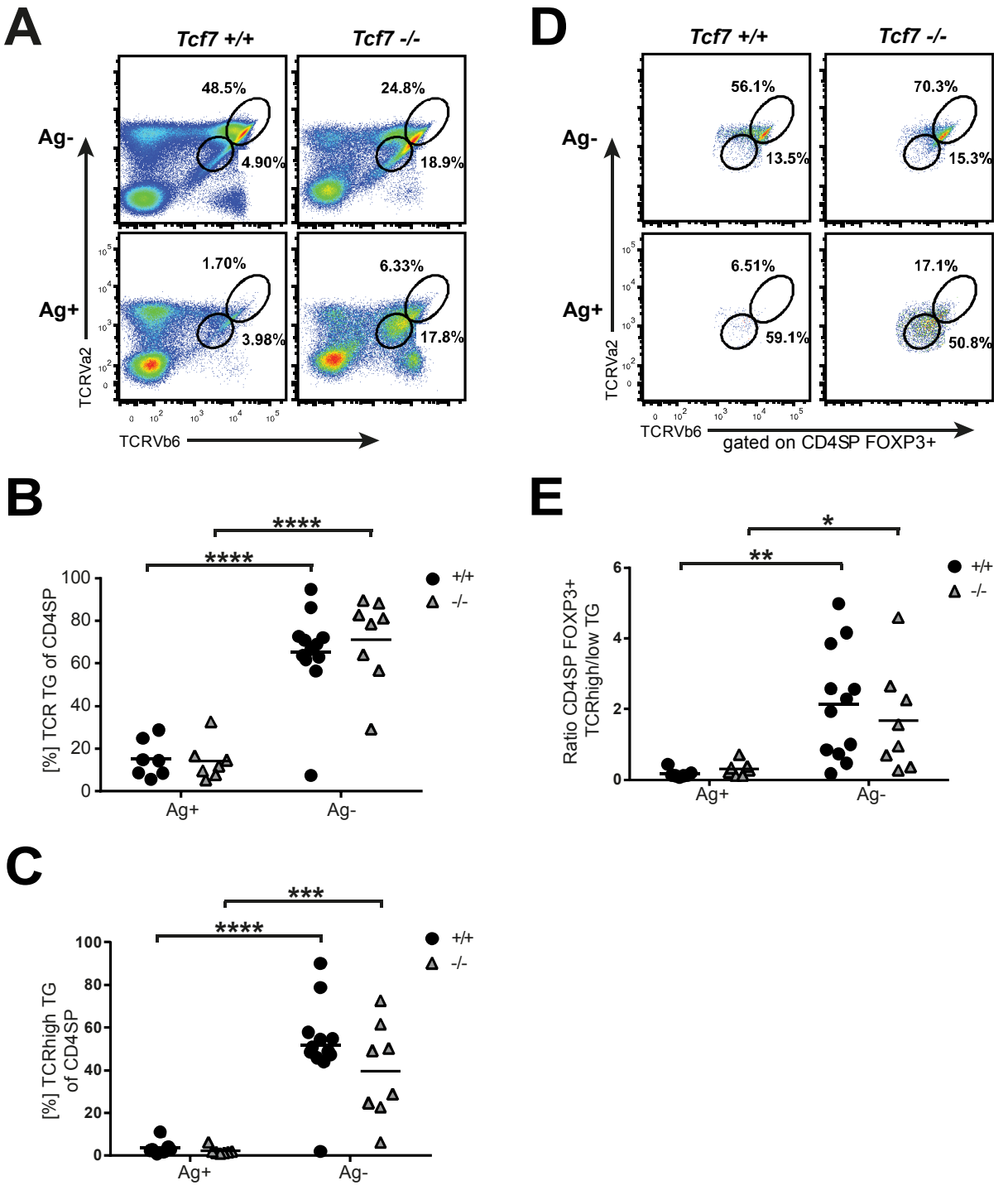

Figure 21: Analysis of CD4SP cells from TEa Tcf7$^{-/-}$ mice. (A-E) Flow cytometric analysis of CD4SP cells from TEa *Tcf7*$^{+/+}$ and *Tcf7*$^{-/-}$ mice. Mean is shown for all quantified data. Numbers show percentages of cells within the indicated box. Ag+: cognate antigen is present. For quantified data: each dot represents one individual animal. Data pooled from 5 independent experiments. (A) Representative plots of the TG TCR expression identified by TCRVβ6 and TCRVα2 co-expression on CD4SP cells. TCR TG population divided into TCR^{high} and TCR^{low} populations. (B) Quantified percentage of TCR TG among CD4SP cells in *Tcf7*$^{+/+}$ and *Tcf7*$^{-/-}$ mice and in the presence or absence of the antigen. (C) Quantified percentage of TCR^{high} TG population among CD4SP cells as depicted in A. (D) Representative plots of the TG TCR expression identified by TCRVβ6 and TCRVα2 co-

expression among CD4SP FOXP3^{+} cells. TCR TG population divided into TCR^{high} TG and TCR^{low} TG populations. (E) Quantified ratio of TCR^{high} versus TCR^{low} TG cells from CD4SP Foxp3+ cells as depicted in D.

* P < 0.05, ** P < 0.01, *** P < 0.001, **** P < 0.0001 (unpaired t test).

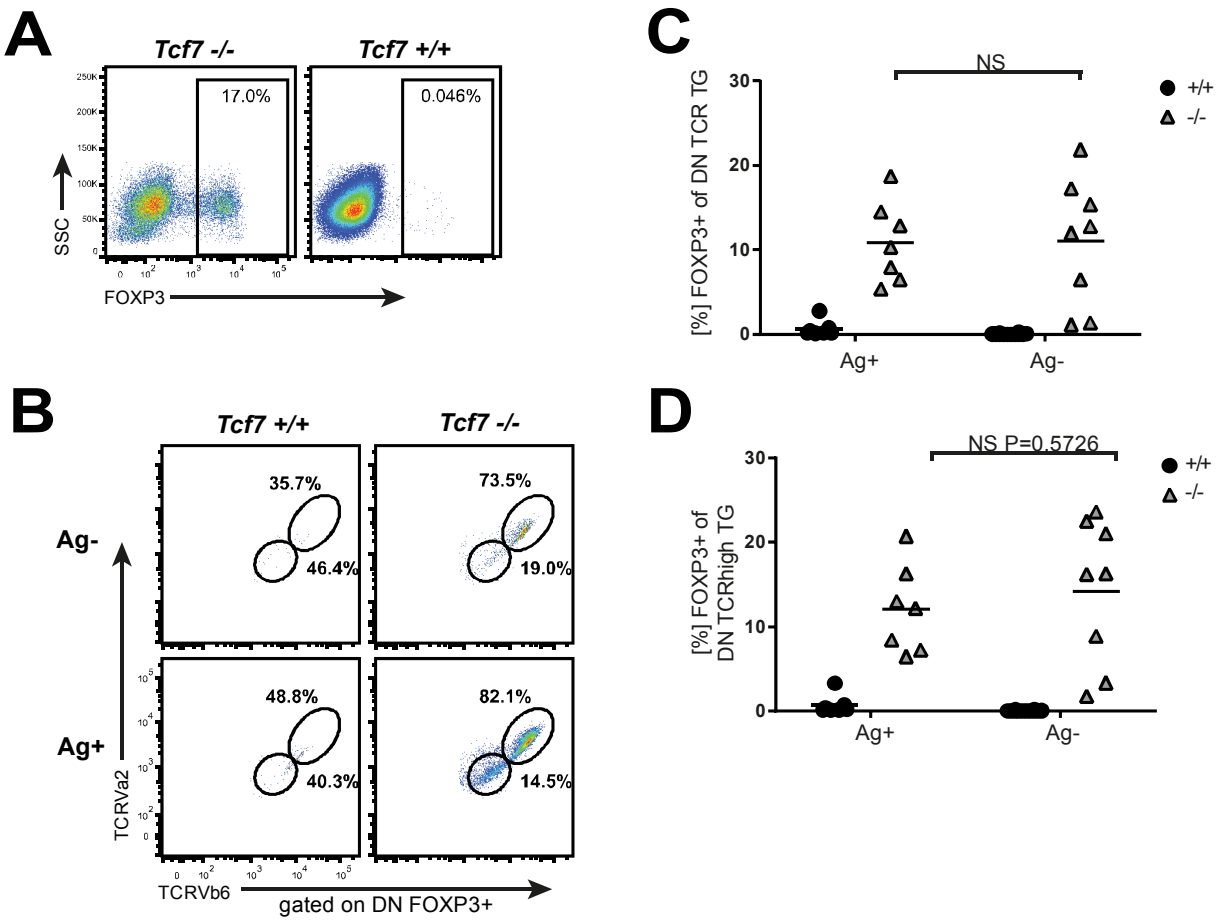

Figure 22: Analysis of DN cells from TEa *Tcf7*$^{-/-}$ mice. (A-D) Flow cytometric analysis of DN cells from TEa *Tcf7*$^{+/+}$ and *Tcf7*$^{-/-}$ mice. Mean is shown for all quantified data. Numbers show percentages of cells within the indicated box. Ag^{+}: cognate antigen is present. For quantified data: each symbol represents one individual animal. Data pooled from 5 independent experiments. (A) Representative dot plot of FOXP3 expression in antigen negative, *Tcf7*$^{+/+}$ and *Tcf7*$^{-/-}$ DN cells among on TCR TG cells. (B) Representative plots of the TG TCR expression identified by TCRVβ6 and TCRVα2 co-expression among DN FOXP3^{+} cells. TCR TG population divided into TCR^{high} TG and TCR^{low} TG populations. (C) Quantified percentage of FOXP3^{+} cells among TCR TG DN cells. (D) Quantified percentage of FOXP3^{+} cells among TCR^{high} TG DN cells as depicted in B. NS P > 0.05 (unpaired t test).

In summary, we generated a *Tcf7*-deficient TCR-transgenic mouse model in which the cognate antigen was present and the FOXP3^{+} DN cells were forced to express the transgenic TCR. Even under these conditions, we did not see any evidence of

TCR usage, further supporting the TCR-independent origin of the FOXP3$^+$ DN cells and their functional immaturity.

7.6 Dosage effect: reduction of TCF7 protein level results in higher T_{reg} cell generation capacity

Tcf7 deficiency during early T cell development was associated with several complications. To avoid difficulties we decided to study T_{reg} cell differentiation in an environment with reduced levels of *Tcf7* but otherwise normal T cell development. The heterozygous *Tcf7*$^{+/-}$ mice fulfilled our criteria. We first compared the TCF7 expression levels in the thymus, LN and spleen from *Tcf7*$^{+/+}$, *Tcf7*$^{+/-}$ and *Tcf7*$^{-/-}$ mice (Figure 23A). As expected, we were not able to detect expression of TCF7 in the *Tcf7*$^{-/-}$ littermate mice. Expression of TCF7 in B cells was examined as an additional negative control. Comparison of TCF7 expression between *Tcf7*$^{+/-}$ and *Tcf7*$^{+/+}$ littermate mice showed a significant decrease of TCF7 levels in *Tcf7*$^{+/-}$ T_{reg} and T_{conv} cells from spleen, LN and thymus.

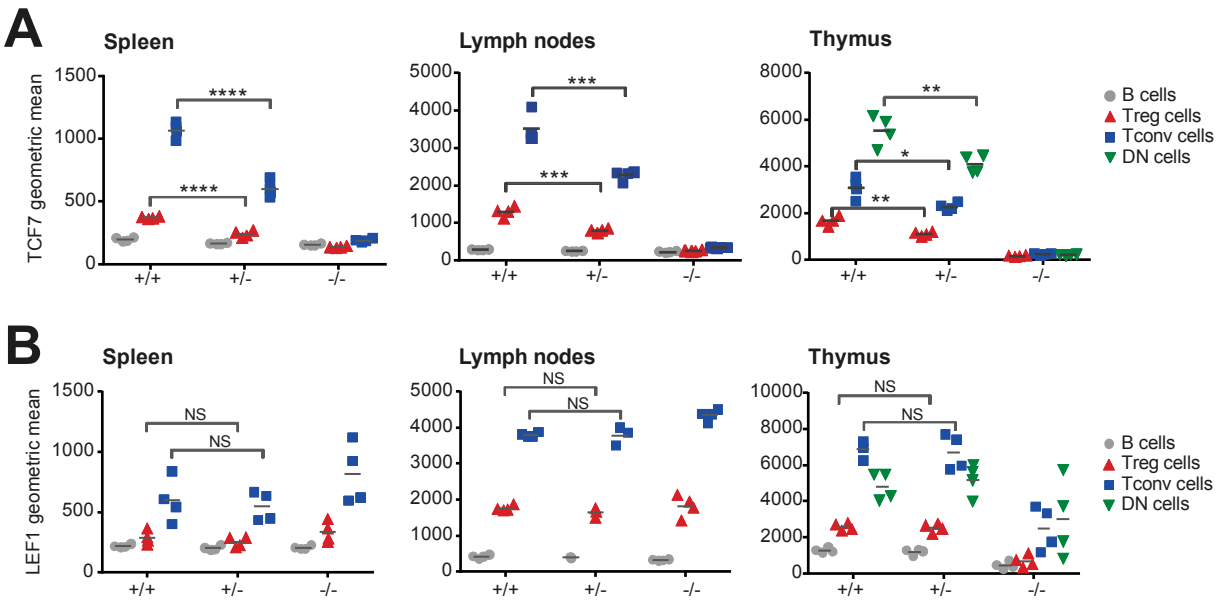

Figure 23: TCF7 and LEF1 expression in different thymic population from *Tcf7*$^{+/+}$, *Tcf7*$^{+/-}$ and *Tcf7*$^{-/-}$ mice. Flow cytometric analysis T_{reg}, T_{conv}, B cells and DN cells from thymus, LN and spleen of *Tcf7*$^{+/+}$, *Tcf7*$^{+/-}$ and *Tcf7*$^{-/-}$ mice. Mean is shown for all quantified data. Each symbol represents an individual animal (n=4). *Tcf7*$^{+/+}$ data was shared with Figure 12. (A) Quantified geometric mean of TCF7 expression. (B) Quantified geometric mean of LEF1 expression.
* P < 0.05, ** P < 0.01, *** P < 0.001, **** P < 0.0001 (unpaired t test).

Since the loss of TCF7 can be partially compensated by the cognate transcription factor LEF1 (Okamura et al., 1998), we also examined the expression of LEF1 in these cells (Figure 23B). For LEF1, no expression differences were observed between *Tcf7*$^{+/+}$ and *Tcf7*$^{+/-}$ littermate mice in any of the organs. In T_{conv} and T_{reg} cells from spleen and LN of the *Tcf7*$^{-/-}$ mice, expression of LEF1 was slightly elevated compare to *Tcf7*$^{+/+}$ and *Tcf7*$^{+/-}$ mice. Surprisingly, we even observed decreased LEF1 expression in all thymic cell populations of the *Tcf7*$^{-/-}$ compared to the *Tcf7*$^{+/+}$ and *Tcf7*$^{+/-}$ mice.
The obtained results confirmed that the *Tcf7*$^{+/-}$ mouse was the ideal model to study the dosage effect of *Tcf7* expression.

Since our main point of interest was the differentiation of T_{reg} cells in the thymus, we examined the T_{reg} precursors in the thymus. The TCR-dependent early T_{reg} precursor is characterized by the expression of CD4SP CD69^{+}CD25^{-}FOXP3^{-}, while the late TCR-independent, but common-γ-chain signaling-dependent, precursor is defined by the expression of CD4SP CD69^{+}CD25^{+}FOXP3^{-} (Lio and Hsieh, 2008; Wirnsberger et al., 2009). Early and late T_{reg} precursors were FACS-purified (Figure 26) and then analyzed by *Tcf7*-specific real-time PCR. The results obtained by real-time PCR revealed that gene expression levels of *Tcf7* in both precursor populations isolated from the *Tcf7*$^{+/-}$ mice were about half that of *Tcf7*$^{+/+}$ mice (Figure 24).

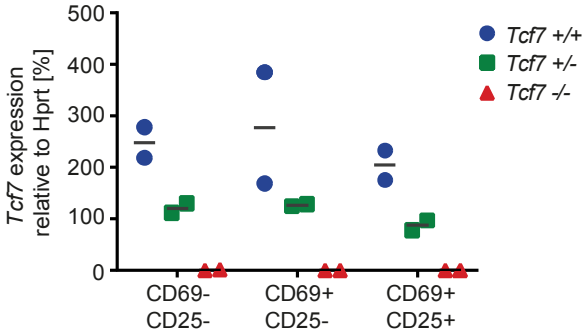

Figure 24: *Tcf7* qPCR in thymic T_{reg} cell precursors. Analysis of *Tcf7* mRNA expression in FACS-purified FOXP3^{-} T_{reg} precursors from CD4SP cells of *Tcf7*$^{+/+}$, *Tcf7*$^{+/-}$ and *Tcf7*$^{-/-}$ thymi via qPCR. Data are presented as percentage relative to Hprt expression.

We continued by flow cytometric analysis of the T_{reg} cell and T_{reg} precursor populations in the *Tcf7*$^{+/-}$ thymus. Analysis of the CD4SP FOXP3^{+} population showed that the frequency of these cells was significantly elevated in the *Tcf7*$^{+/-}$ mice compared to the *Tcf7*$^{+/+}$ (Figure 25B). Likewise, the frequency of the TCR committed

CD4SP CD69^{+}CD25^{+}FOXP3^{-} late T_{reg} precursor was significantly increased in the *Tcf7* thymus (Figure 25A).

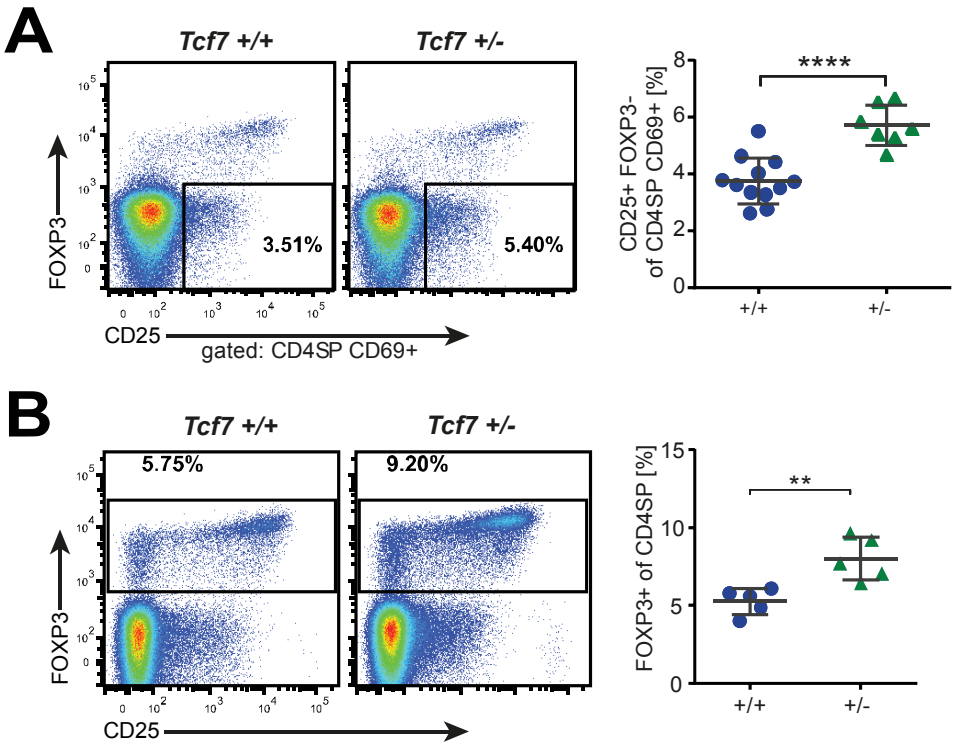

Figure 25: T_{reg} cells and T_{reg} precursors in the *Tcf7*$^{+/+}$ and *Tcf7*$^{+/-}$ thymus. (A-B) Flow cytometric analysis of *Tcf7*$^{+/+}$ and *Tcf7*$^{+/-}$ mice. Numbers show percentages of cells within the indicated box. Symbols represent individual mice. (A) Representative dot plots and quantification with mean + SD of the CD4SP CD69^{+}CD25^{+}Foxp3^{-} late T_{reg} precursor (n=7-12). (B) Representative dot plots and quantification with mean + SD of CD4SP FOXP3^{+} T_{reg} cells (n=5). ** P < 0.01, **** P < 0.0001 (unpaired t test).

To compare the differentiation potential of the *Tcf7*$^{+/-}$ and *Tcf7*$^{+/+}$ late T_{reg} precursors we FACS-purified the late precursors (see gating scheme, Figure 26, R4) and incubated them *in vitro* in a cytokine stimulation assay. Cells were cultured with the cytokines IL-2 and IL-15, but without TCR stimulus, since development into T_{reg} cells is TCR-independent at this stage. After one day in culture we measured the expression of FOXP3 and CD25. Under these conditions precursors from both *Tcf7*$^{+/-}$ and *Tcf7*$^{+/+}$ mice differentiated into CD4^{+} CD25^{+}FOXP3^{+} T_{reg} cells, but *Tcf7*$^{+/-}$ cells did at a significantly higher level (Figure 27).

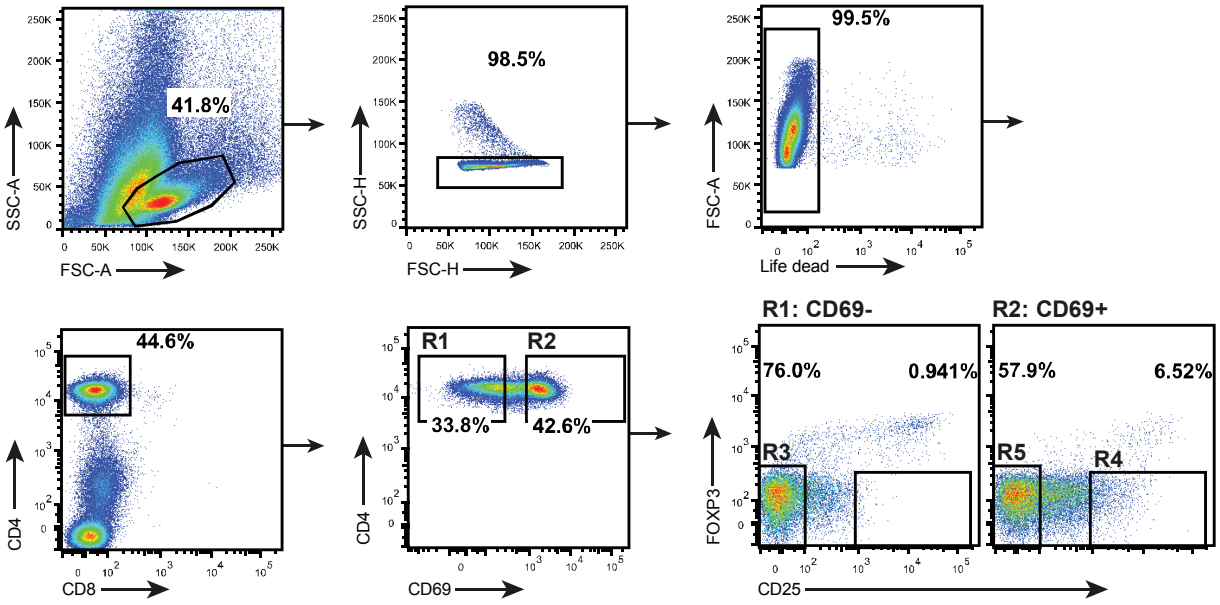

Figure 26: FACS layout for T_{reg} precursor purification. Representative FACS layout for a *Tcf7*$^{+/+}$ Foxp3-YFP^{+} thymus after AutoMACS depletion of CD8^{+} cells. R1: CD4SP CD69^{-}; R2: CD4SP CD69^{+}; R3: CD4SP CD69^{-}CD25^{-}Foxp3^{-} (CD69^{-} control population); R4: CD4SP CD69^{+}CD25^{+}Foxp3^{-} (late T_{reg} precursor); R5: CD4SP CD69^{+}CD25^{-}Foxp3^{-} (early T_{reg} precursor).

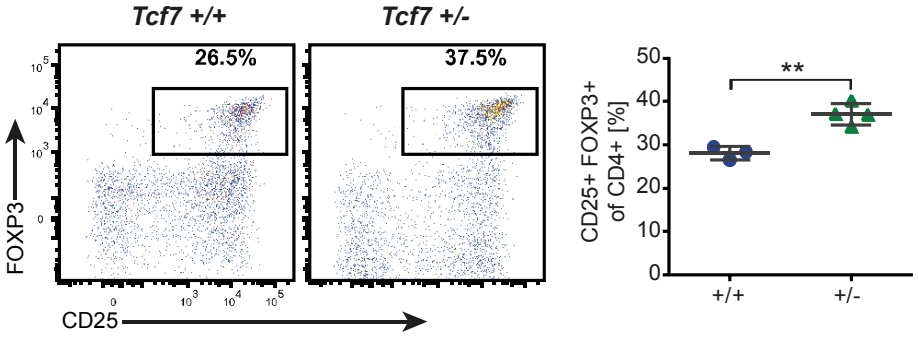

Figure 27: 1 day culture of the late T_{reg} precursor. The late T_{reg} precursor (CD4SP CD69^{+}CD25^{+}FOXP3^{-}) was FACS-purified from Foxp3-YFP^{+} *Tcf7*$^{+/+}$and *Tcf7*$^{+/-}$ mice. Cells were cultured for 1 day *in vitro* with IL-2 and IL-15 (n=3-4). Percentages of CD25^{+}FOXP3^{+} cells among CD4^{+} cells were subsequently analyzed by flow cytometry. Numbers show percentages of cells within the indicated box. Representative dot plots and quantification with mean + SD are shown (n=3-4). Each symbol represents an individual mouse. ** $P < 0.01$ (unpaired t test).

To analyze the differentiation potential of the early TCR-dependent T_{reg} precursors, we tested different culture conditions using the differentiation assay (Figure 28A-B). The CD4SP CD69^{+}CD25^{-}FOXP3^{-} early T_{reg} precursors were FACS-purified and subsequently cultured for 3 days *in vitro*. To avoid influence from APCs, we chose a system that used an anti-CD3/CD28 bead-based stimulus instead. The highest

output in total cell number and frequency of $CD4^+$ $CD25^+FOXP3^+$ T_{reg} cells was generated with a combination of an IL-2, IL-15 and anti-CD3/CD28 stimulus (Figure 28A-B). Under these conditions sixty to eighty percent of the cells differentiated into T_{reg} cells. The combination of an IL-2 and anti-CD3/CD28 stimulus resulted in the lowest output of T_{reg} cells at the end of the culture period, while culture with an IL-15 and anti-CD3/CD28 stimulus gave an intermediate result (Figure 28B). $CD69^-$ mature CD4SP thymocytes served as a negative control, since they got strongly activated ($CD25^{high}$) but had lost the ability to differentiate into T_{reg} cells under these conditions (Figure 28A-B and data not shown).

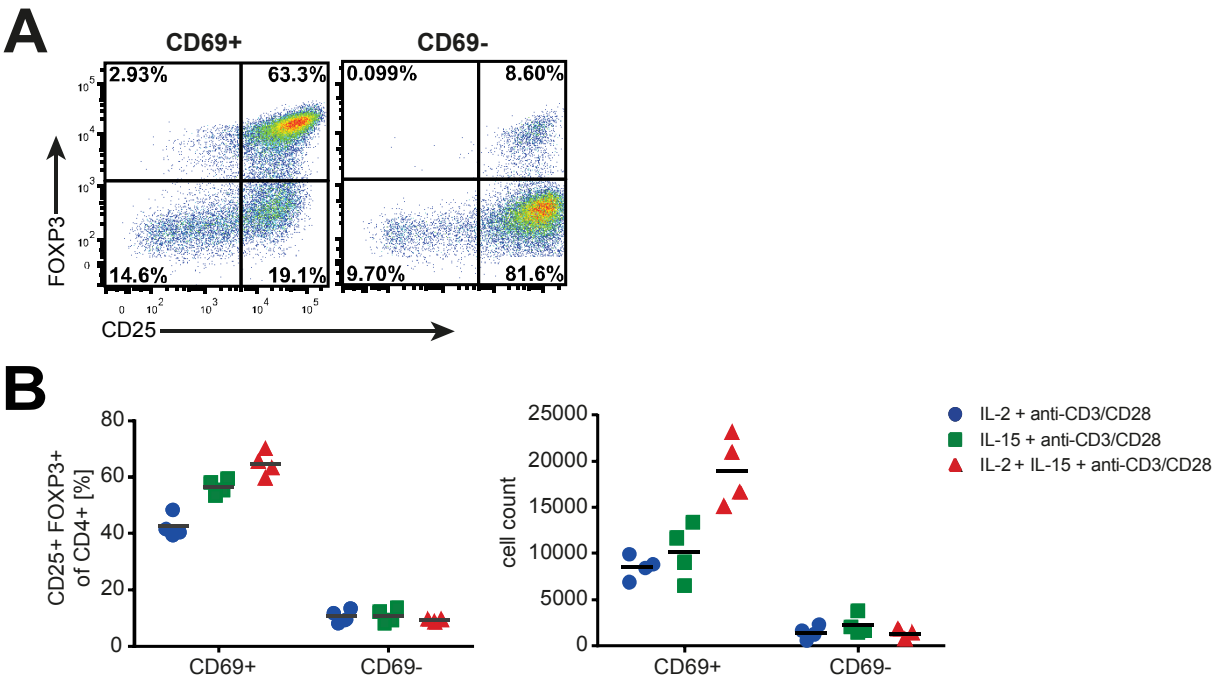

Figure 28: 3 day culture of the early T_{reg} precursor under different conditions. (A-B) The early T_{reg} precursor (CD4SP $CD69^+CD25^-FOXP3^-$) and the $CD69^-$ control population (CD4SP $CD69^-CD25^-FOXP3^-$) were FACS-purified from Foxp3-GFP^+ mice. Cells were cultured for 3 days *in vitro*. Percentages of $CD25^+FOXP3^+$ cells among $CD4^+$ cells were subsequently analyzed by flow cytometry. (A) Representative dot plots for the T_{reg} precursors and $CD69^-$ control population cultured with IL-2, IL15 and anti-CD3/CD28 beads. Numbers show percentages of cells within the indicated box. (B) Quantified percentages and cell counts of $CD4^+$ $CD25^+FOXP3^+$ cells with mean + SD (n=3-4). Cells were cultured under different stimulating conditions (as depicted) with anti-CD3/CD28 beads, IL-2 and/or IL-15. Each symbol represents an individual mouse. Cell counts were determined by flow cytometry.

Next, the differentiation assay was used for a side-by-side comparison of FACS-purified early precursors from *Tcf7*$^{+/-}$ and *Tcf7*$^{+/+}$ mice. They were either incubated

with the weaker (IL-2 and anti-CD3/CD28 beads) or the full (IL-2, IL-15 and anti-CD3/CD28 beads) stimulus. The results demonstrated that significantly more T_{reg} cells, in frequency and cell count, were generated from the *Tcf7*$^{+/-}$ precursor (Figure 29A-B). This result was independent of the stimulus strength applied to the culture. The weaker stimulus generated an output of about 50 percent T_{reg} cells, while the full stimulus generated about 80 percent of T_{reg} cells from the *Tcf7*$^{+/-}$ precursor (Figure 29A-B).

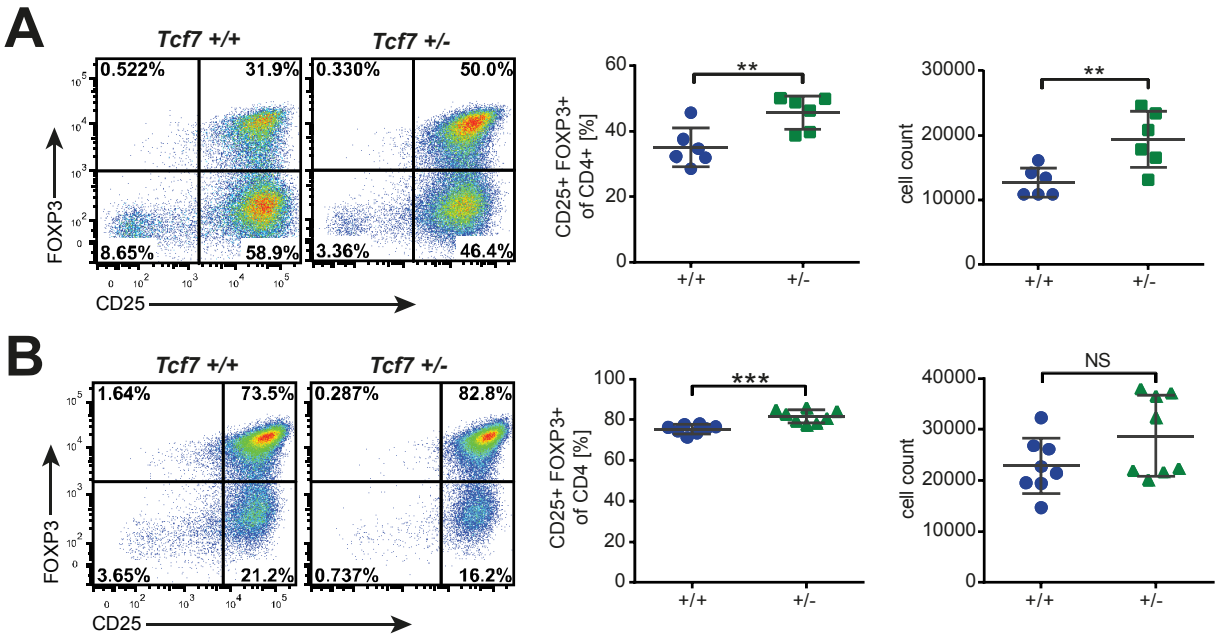

Figure 29: 3 day culture of the early T_{reg} precursor from *Tcf7*$^{+/+}$and *Tcf7*$^{+/-}$ mice. (A-B) The early T_{reg} precursor (CD4SP CD69^{+}CD25^{+}FOXP3^{-}) was FACS-purified from Foxp3-YFP^{+} *Tcf7*$^{+/+}$ and *Tcf7*$^{+/-}$ mice. Cells were cultured for 3 days *in vitro.* Percentages of CD25^{+}FOXP3^{+} cells among CD4^{+} cells were subsequently analyzed by flow cytometry. Numbers in dot plots show percentages of cells within the indicated box. Mean + SD are shown for all quantified data. Each symbol represents an individual mouse. Cell counts were determined by flow cytometry. (A) Representative dot plots, quantified percentages and cell counts of CD4^{+} CD25^{+}FOXP3^{+} cells cultured with IL-2 and anti-CD3/CD28 beads (n=6). (B) Representative dot plots, quantified percentages and cell counts of CD4^{+} CD25^{+}FOXP3^{+} cells cultured with IL-2, IL-15 and anti-CD3/CD28 beads (n=8).
NS P > 0.05, ** P < 0.01, *** P < 0.001 (unpaired t test).

Our *ex vivo* analysis and *in vitro* culture demonstrated that decreased expression of TCF7 results in an enhanced T_{reg} cell differentiation capacity.

7.7 Limiting T_{reg} precursor differentiation potential

The T_{reg} lineage decision strongly depends on the strength of the TCR signal. We modified our *in vitro* differentiation system to test a range of TCR signal strengths. We changed our strong anti-CD3/CD28 bead-based stimulus to an anti-CD3 plate bound system to allow increasing anti-CD3 concentrations that mimic different TCR affinities. To this end, we titrated the anti-CD3 antibody from 0.1 to 2 µg/ml and added a fixed concentration of anti-CD28. We then compared the T_{reg} generation capacity of *Tcf7*$^{+/+}$ and *Tcf7*$^{+/-}$ early precursors (Figure 30A-B). Across all anti-CD3 concentrations tested the *Tcf7*$^{+/-}$ precursor produced a significantly higher percentage of T_{reg} cells.

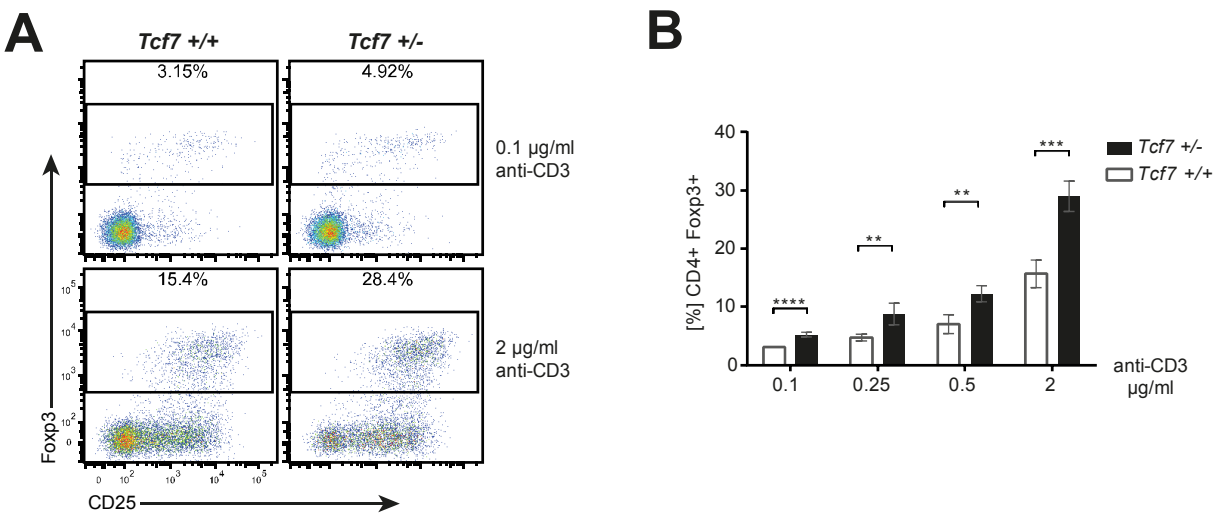

Figure 30: T_{reg} precursor culture with anti-CD3 titration. (A-B) The early T_{reg} precursor (CD4SP CD69^{+}CD25^{-}FOXP3^{-}) was FACS-purified from Foxp3-YFP^{+} *Tcf7*$^{+/+}$ and *Tcf7*$^{+/-}$ mice. The cells were cultured *in vitro* for 3 days in plates coated with 0.1, 0.25, 0.5 or 2 µg/ml of anti-CD3. IL-2, IL-15 anti-CD28 were added to the culture. Flow cytometric analysis was performed at the end of the culture period. (A) Representative dot plots for anti-CD3 0.1 and 2 µg/ml are shown. Numbers show percentages of cells within the indicated box. (B) Quantified percentages with mean + SD of CD4^{+} FOXP3^{+} cells generated from *Tcf7*$^{+/+}$ and *Tcf7*$^{+/-}$ precursors after 3 days of culture (n=4). Representative experiment is shown.
** P < 0.01, *** P < 0.001, **** P < 0.0001 (unpaired t-test).

Hence, TCR-dependent differentiation into the T_{reg} lineage is restricted by normal levels of TCF7 in T_{reg} precursors.

Since Wnt signaling can trigger the activation of TCF7 through β-catenin (Staal et al., 2008), we tested, in a gain-of-function experiment, if Wnt signaling could interfere with the development of T_{reg} cells from *Tcf7* wild-type mice. To this end, two different activators of the Wnt pathway were added to our anti-CD3/CD28 bead-based T_{reg} differentiation assay. The early T_{reg} precursor was cultured in the presence of the Wnt signaling activators 6-bromoindirubin-3'-oxime (BIO) and CHIR99021 (Figure 31A-B). Both Wnt activators are inhibitors of the Wnt negative regulator glycogen synthase kinase 3 (GSK-3). Frequencies of T_{reg} cells generated in the presence of BIO or CHIR99021 at different concentrations were significantly reduced (Figure 31A-B).

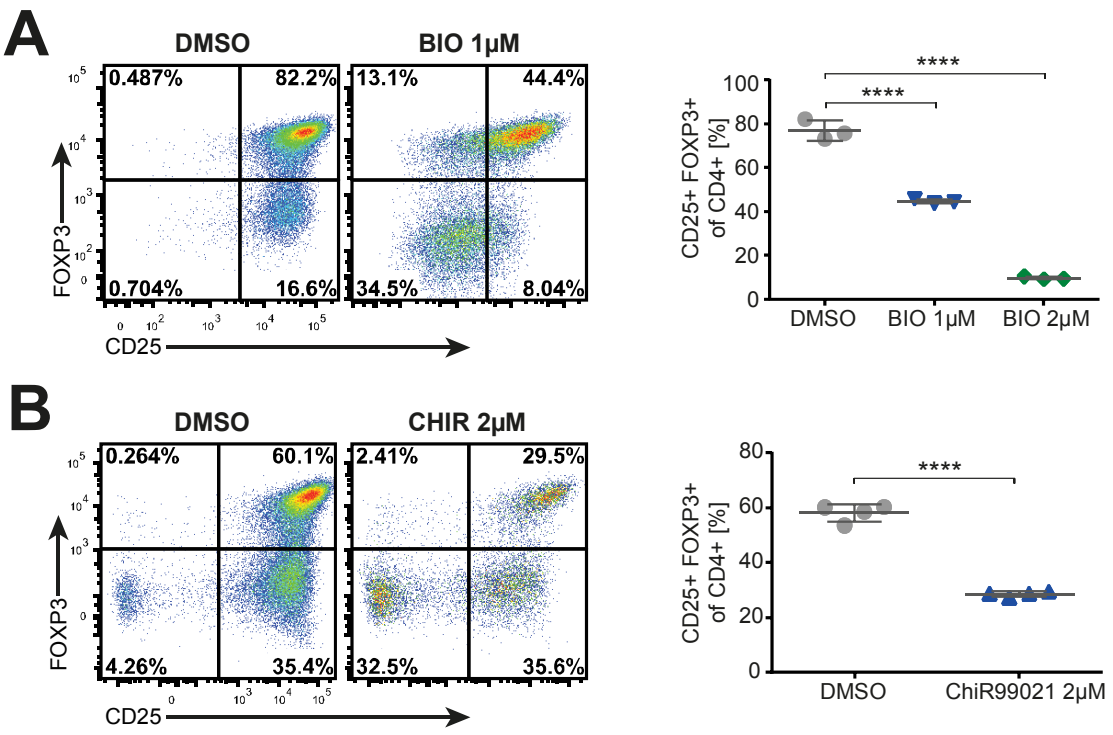

Figure 31: T_{reg} precursor culture with β-CATENIN/TCF7 activators. (A-B) The early T_{reg} precursor (CD4SP $CD69^+CD25^-FOXP3^-$) was FACS-purified from Foxp3-GFP^+ mice. The cells were cultured *in vitro* for 3 days with IL-2, IL-15, anti-CD3/CD28 and β-CATENIN/TCF7 activators. Cells cultured with DMSO served as a control. Percentages of $CD25^+FOXP3^+$ cells among $CD4^+$ cells were subsequently analyzed by flow cytometry. Numbers in dot plots show percentages of cells within the indicated box. Data points represent individual animals. Representative experiments are shown. (A) Representative dot plots of cells cultured with BIO 1 µM or DMSO and quantified percentages with mean + SD of $CD4^+$ $CD25^+FOXP3^+$ cells cultured with BIO 1µM, BIO 2 µM or DMSO are shown (n=3). (B) Representative dot plots and quantified percentages with mean + SD of CD4+ CD25+FOXP3+ cells cultured with CHIR99021 2µM or DMSO are shown (n=4). **** $P < 0.0001$ (unpaired t-test).

For a closer look at the role of TCF7 in the development of T_{reg} cells, we examined the TCF7 expression levels at the different developmental stages. TCF7 expression stayed roughly at the same level in DP cells as well as, early and late T_{reg} precursors. In mature FOXP3$^+$ T_{reg} cells we saw a massive drop in TCF7 levels (Figure 32). We previously described that the TCF7 expression was decreased in thymic T_{reg} compared to T_{conv} cells (Figure 12A). This analysis revealed the decrease in TCF7 expression levels occurred after both, the early and the late T_{reg} precursor stage and in coincidence with the first expression of FOXP3 in these cells.

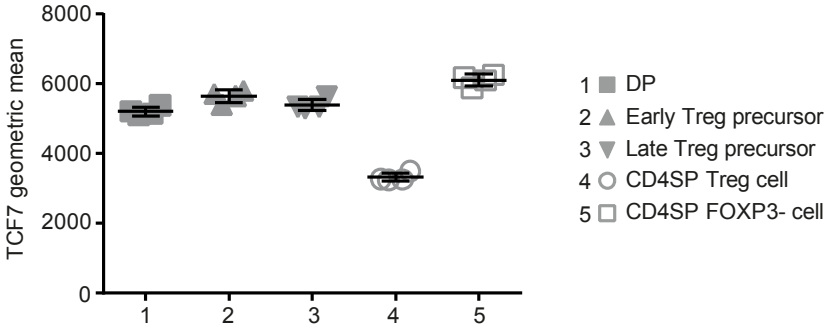

Figure 32: TCF7 expression in different thymic populations. Flow cytometric analysis of TCF7 expression in different cell populations of the thymus from C57BL/6 wild-type mice (as indicated). Quantification with mean + SD of the TCF7 geometric means are plotted. Data points represent individual animals (n=4).

Based on our findings that decrease of TCF7 expression coincided with the first expression of FOXP3 in thymic T_{reg} cells, we decided to analyze if FOXP3 can influence the TCF7 expression level. To this end, we retrovirally over-expressed FOXP3 in isolated peripheral T cells *in vitro* (Figure 33). T cells transduced with the control vector construct expressed CD90.1 only. T cell transduced with the *Foxp3* vector over-expressed both CD90.1 and FOXP3. Indeed, we observed that *Foxp3* over-expressing T cells showed significantly decreased levels of TCF7, while T cells transduced with the control vector did not (Figure 33). These results demonstrated that FOXP3 induces a decrease of TCF7 on the protein level.

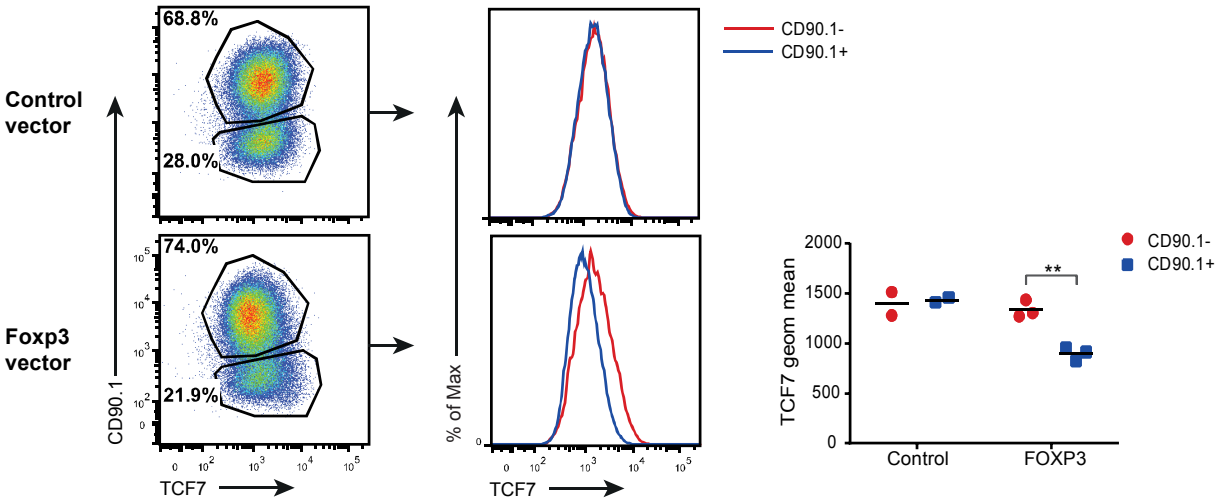

Figure 33: Relationship between FOXP3 and TCF7. Flow cytometric analysis of retroviral over expression of control- (CD90.1$^+$) or FOXP3-vector (CD90.1$^+$ and FOXP3$^+$) in T cells 3 days after transduction. Left panel: Representative dot plots of the CD90.1 and TCF7 expression in transduced T cells analyzed. Numbers in dot plots show percentages of cells within the indicated box. Middle panel: histograms of TCF7 expression in CD90.1$^-$ and CD90.1$^+$ T cells. Right panel: Quantification of the TCF7 geometric mean in CD90.1$^-$ and CD90.1$^+$ cells (n=2-3). Representative data from two independent experiments is shown. ** P < 0.01 (unpaired t test).

Forced expression of the anti-apoptotic factor B cell lymphoma 2 (BCL-2) was able to rescue T cells from negative selection (Strasser, 2005). TCF7 was reported to reduce the level of BCL-2 in post-selected DP thymocytes (Kovalovsky et al., 2009). Hence, we examined the expression levels of BCL-2 in the early and late T_{reg} precursors and found the BCL-2 expression was significantly elevated in both precursor populations from the *Tcf7*$^{-/-}$ compared to the *Tcf7*$^{+/+}$ mouse, indicating that TCF7 reduces BCL-2 expression (Figure 34A-B).

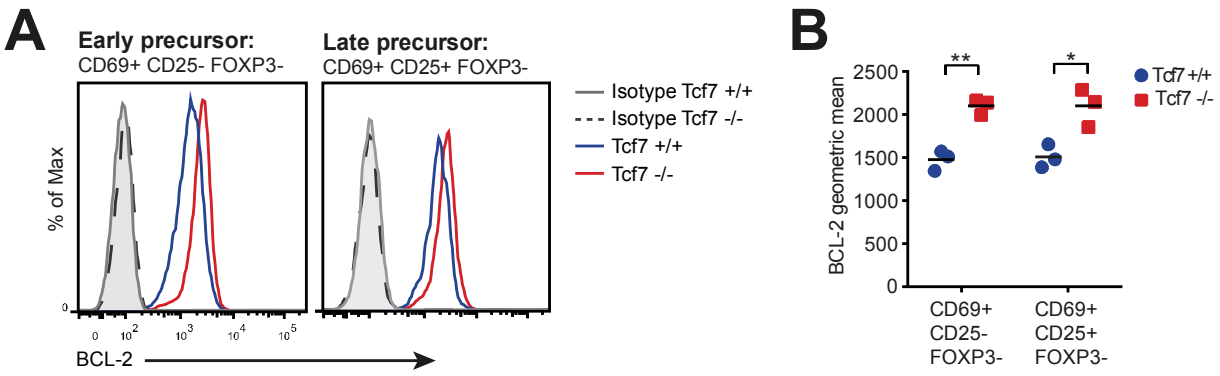

Figure 34: Expression of the anti-apoptotic marker BCL-2 T_{reg} precursors. (A-B) Intracellular staining for the anti-apoptotic marker BCL-2 in thymic cells from *Tcf7*$^{+/+}$ or *Tcf7*$^{-/-}$ mice was analyzed using flow cytometry. (A) Representative histograms of BCL-2 expression in the early and late T_{reg} precursors, including isotype, controls are shown. (B) Quantification of the BCL-2 geometric mean with mean value is shown. Symbols represent individual mice (n=3).
* P < 0.05, ** P < 0.01 (unpaired t test).

The overall avidity of the MHC-TCR interaction during positive selection was previously described to correlate with the surface expression of CD5 (Azzam et al., 1998). CD5 surface expression levels are usually higher on T_{reg} cells compared to the T_{conv} cells. This is presumably due to the higher affinity of their TCRs towards self-peptide (Figure 18). We analyzed the CD5 surface expression in the early and late T_{reg} precursors and the mature tT_{reg} cells from *Tcf7*$^{-/-}$ and *Tcf7*$^{+/+}$ mice (Figure 35A-B). In the *Tcf7*$^{+/+}$ mice, we observed a progressing decrease in the frequency of CD5^{low} cells from the early to the late precursor and to the mature tT_{reg} cell, indicating that the CD5^{low} cells were not selected into the T_{reg} cell lineage during the developmental process. In the absence of TCF7 on the other hand, the TCR committed late precursor and the differentiated tT_{reg} cells did not show a decrease of CD5^{low} cells compared to the early T_{reg} precursor (Figure 35A-B). These findings indicate that the pool of *Tcf7*-deficient tT_{reg} cells includes a higher fraction of T_{reg} cells with low TCR affinity.

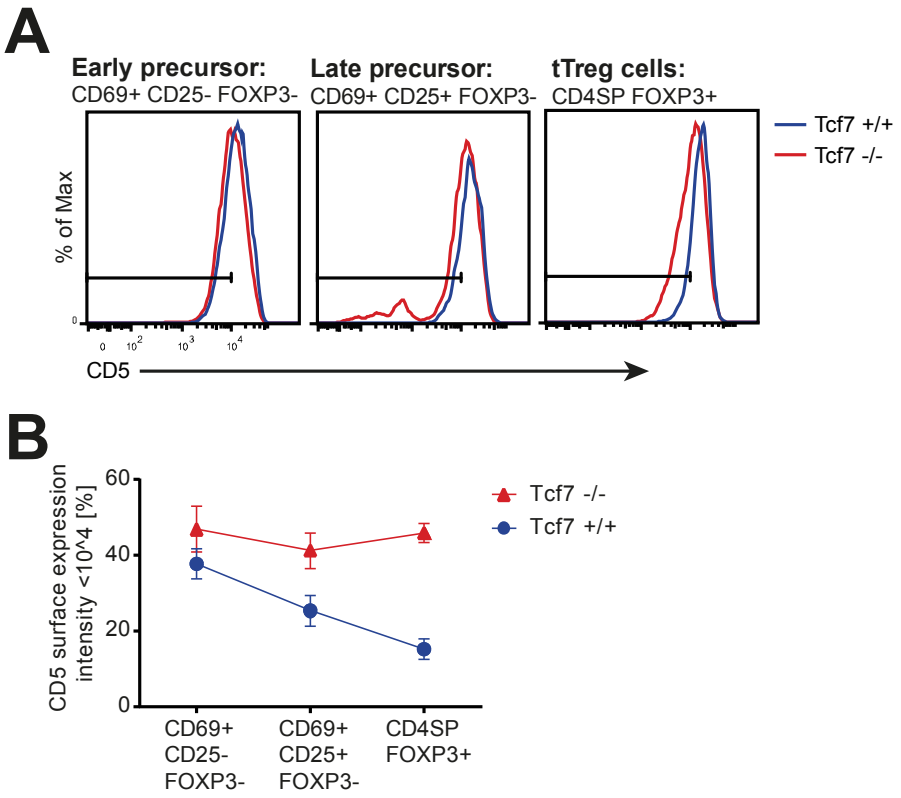

Figure 35: CD5 surface expression of T_{reg} precursors. CD5 surface expression on early and late T_{reg} precursors and tT_{reg} cells from *Tcf7*$^{+/+}$ and *Tcf7*$^{-/-}$ mice. Data was analyzed via flow cytometry. (A) Representative histograms are shown. The gate marks cells with a CD5 surface expression intensity < 10^4. (B) Quantified percentages with mean + SD of cells with a CD5 surface expression intensity < 10^4 are shown (n=3).

In summary, the results obtained demonstrated that the endogenous level of TCF7 limits the efficiency of differentiation from T_{reg} precursors into mature T_{reg} cells, over a wide range of TCR signaling strengths. In addition activation of β-catenin/TCF7 through Wnt signaling resulted in decreased T_{reg} precursor differentiation capacity. Examination of the TCF7 levels in the thymic T_{reg} cell development showed that the decrease in TCF7 expression coincided with the first expression of FOXP3. In line with these findings we showed that the forced over expression of *Foxp3 in vitro* also led to reduced TCF7 levels. Finally, we detected elevated levels of the anti-apoptotic factor BCL-2 in *Tcf7*$^{-/-}$ T_{reg} precursors and demonstrated that *Tcf7*$^{-/-}$ tT_{reg} cells had a higher frequency CD5low cells.

7.8 TGFβ triggered iT_{reg} cell generation is not influenced by TCF7 deficiency.

After close analysis of thymic T_{reg} development, we aimed to characterize the influence of TCF7 deficiency on the T cells in the peripheral lymphoid organs in more detail. Our analysis of the thymus revealed that development into the T_{reg} cell lineage was facilitated in the absence of TCF7. We therefore hypothesized that after induction with TGFβ peripheral naïve T cells from *Tcf7*$^{-/-}$ mice would turn into iT_{reg} cells at a higher rate than naïve T cells from *Tcf7*$^{+/+}$ mice. The *in vitro* induction of iT_{reg} cells through TGFβ was previously described (Chen et al., 2003).

To test our hypothesis, we cultured naïve T cells from *Tcf7*$^{-/-}$ and *Tcf7*$^{+/+}$ mice with rising concentrations of TGFβ. Since naïve T cells from *Tcf7*$^{-/-}$ mice were difficult to keep alive under normal culture conditions (IL-2 20 U/ml), higher concentrations of IL-2 were added to the culture system (IL-2 100 U/ml) which resulted in better viability of the *Tcf7*$^{-/-}$ cells (data not shown). Analysis of the frequencies of $CD4^+$ $CD25^+FOXP3^+$ iT_{reg} cells generated after 3 days of culture revealed no differences between the *Tcf7*$^{-/-}$ and *Tcf7*$^{+/+}$ cells (Figure 36A-B). In both groups, frequencies of iT_{reg} cells generated increased with rising concentrations of TGFβ added to the culture. The maximum iT_{reg} cell generation capacity, with about 90 percent iT_{reg} cell output, was reached at a TGFβ concentration of 5ng/ml. The experiment was repeated but the expected advantage of naïve T cells from *Tcf7*$^{-/-}$ mice in iT_{reg} cell induction was not observed.

The results obtained from the iT_{reg} cell generation assays did not show an influence of TCF7 on the generation of these cells.

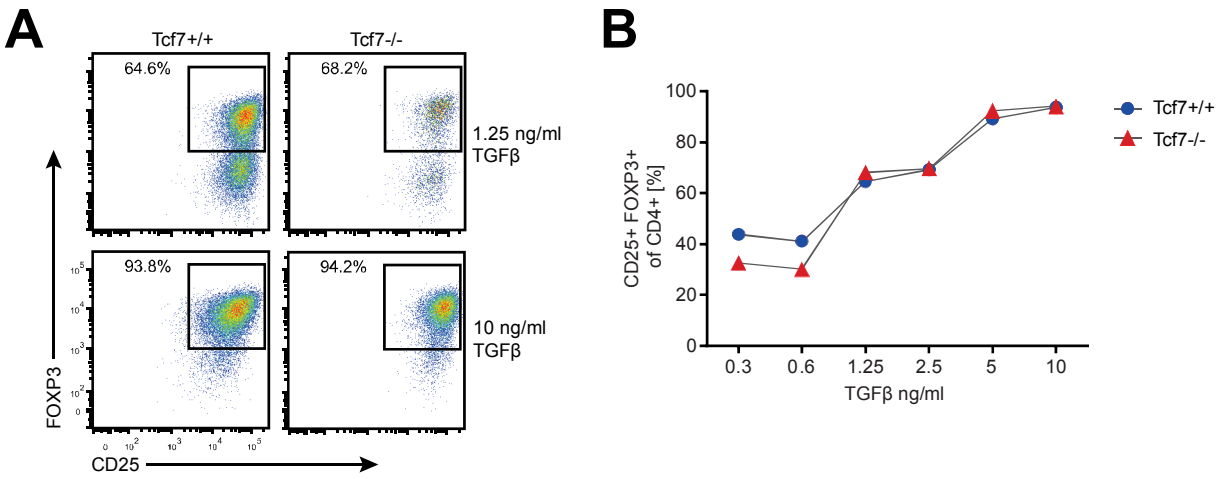

Figure 36: iT_{reg} induction with TGFβ titration. (A-B) Naïve T_{conv} cells ($CD4^+$ $CD62L^+FOXP3^-$) were FACS-purified from spleen and LNs of Foxp3-YFP$^+$ *Tcf7*$^{+/+}$ and *Tcf7*$^{-/-}$ mice. The cells were cultured *in vitro* for 4 days with IL-2, anti-CD3/CD28 and different concentrations of TGFβ. Flow cytometric analysis was performed at the end of the culture period. (A) Representative dot plots of CD25 and FOXP3 expression among $CD4^+$ cells for TGFβ 1.25 and 10 ng/ml are shown. Numbers show percentages of cells within the indicated box. (B) Quantified percentages of $CD4^+$ $CD25^+FOXP3^+$ iT_{reg} cells generated from *Tcf7*$^{+/+}$ and *Tcf7*$^{-/-}$ T_{conv} cells after 4 days of culture (n=1). Representative experiment is shown.

7.9 T_H17 induction assay produces $FOXP3^+IL\text{-}17^+$ cells under *Tcf7*-deficient conditions.

The subset of IL-17 producing T helper 17 (T_H17) cells is involved in the defense against pathogens and has a role in the induction of tissue inflammation in the context of autoimmune disease (Korn et al., 2009). *In vitro* development of T_H17 cells from naïve T cells is induced through the combination of TGFβ and IL-6 (Bettelli et al., 2006). While TGFβ alone induces the generation of iT_{reg} cells, IL-6 inhibits this process and instead drives the generation of the T_H17 lineage. Previous reports showed that TCF7 mediates the repression of the IL-17 gene locus through epigenetic modifications and that the absence of TCF7 leads to increased T_H17 differentiation (Ma et al., 2011; Yu et al., 2011).

We were interested in investigating the transition phase between iT_{reg} and T_H17 cell generation in the *Tcf7*-deficient environment. We therefore analyzed the *in vitro* generation of T_H17 cells from naïve *Tcf7*$^{+/+}$ or *Tcf7*$^{-/-}$ T cells in a culture system with

constant concentrations of TGFβ (10 ng/ml) and gradually increasing concentrations of IL-6. At the end of the culture period we analyzed the expression of both FOXP3 and IL-17 to identify the generated iT_{reg} and T_H17 cells (Figure 37A-B). As expected, we observed a gradual decrease of ($CD4^+$ $Foxp3^+IL17^-$) iT_{reg} cell generation with increasing concentrations of the cytokine IL-6. Frequencies of iT_{reg} cells generated started dropping at an IL-6 concentration of 0.3 ng/ml and the turning point was reached at 0.6 ng/ml. At 0.6 ng/ml of IL-6 iT_{reg} generation dropped to about 20 percent iT_{reg} output and stayed at this level even with higher concentrations of IL-6. We did not observe any difference between *Tcf7*$^{+/+}$ and *Tcf7*$^{-/-}$ cells in this analysis (Figure 37A and 37B, top panel). Simultaneously, with the drop in iT_{reg} cell generation, the frequency of IL-17 producing T_H17 cells ($CD4^+$ $FOXP3^-IL\text{-}17^+$) started to rise. In line with previously published results, we observed a difference between *Tcf7*$^{+/+}$ and *Tcf7*$^{-/-}$ cells at this point (Yu et al., 2011). The frequency of IL-17 producing cells generated from naïve *Tcf7*$^{-/-}$ T cells increased to about 20 percent, while the frequency generated from naïve *Tcf7*$^{+/+}$ T cells stayed below 5 percent (Figure 37A and 37B, middle panel). Quite surprisingly, we also observed $CD4^+FOXP3^+IL17^+$ cells that occurred among *Tcf7*$^{-/-}$ cells at a frequency of up to 5 percent and stayed below 0.5 percent in the *Tcf7*$^{+/+}$ cells (Figure 37A and 37B, bottom panel). These cells could not be clearly assigned to either of the subsets.

In summary, the results obtained from the *in vitro* induction of T_H17 cells confirmed that the T_H17 cell generation is enhanced by the absence of TCF7, while there is no effect on the generation of iT_{reg}. In addition, we observed the enhanced generation of $FOXP3^+IL\text{-}17^+$ cells under these conditions.

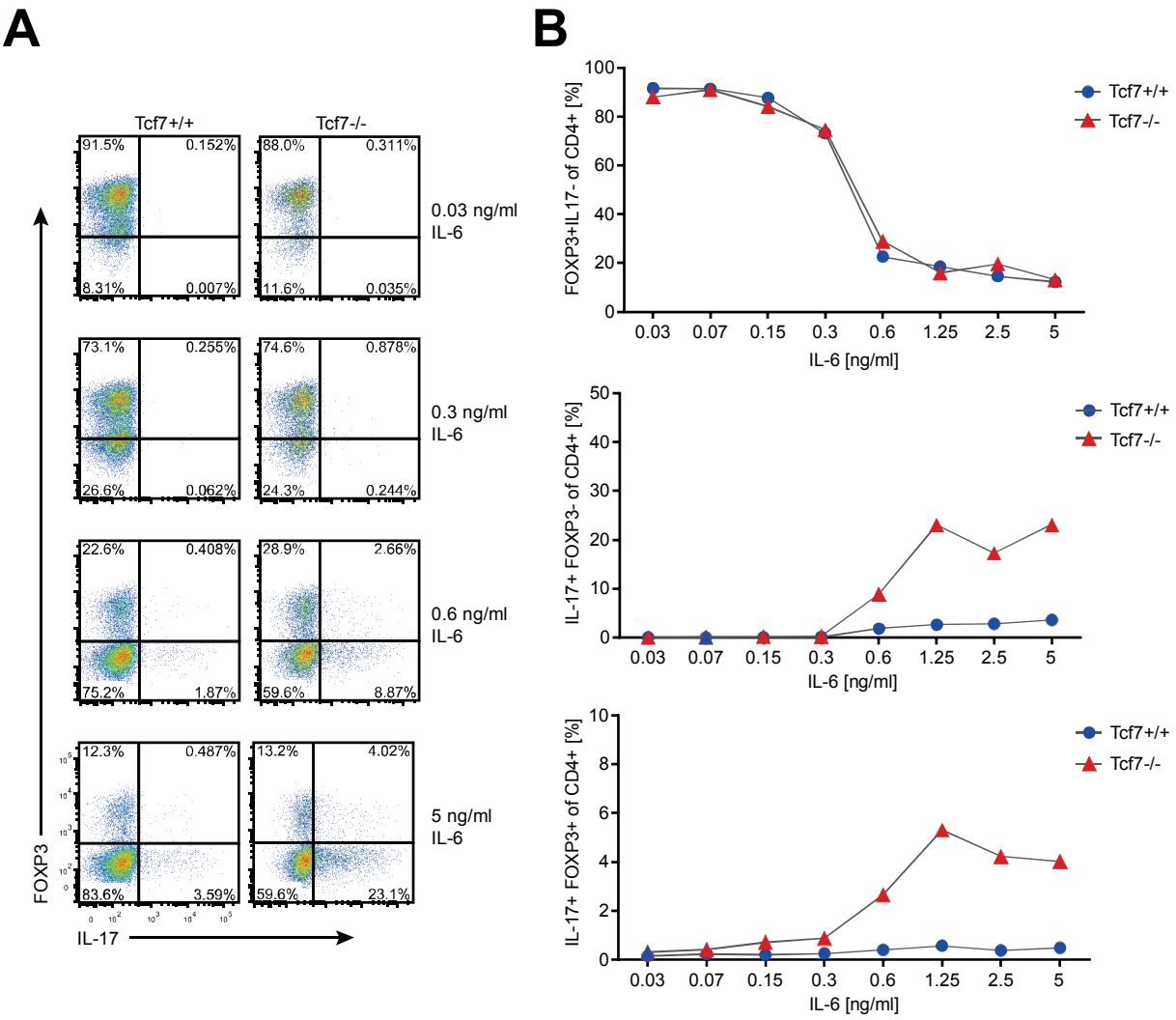

Figure 37: T_H17 induction assay with IL-6 titration. (A-B) Naïve T_{conv} cells ($CD4^+$ $CD62L^+FOXP3^-$) were FACS-purified from spleen and LNs of Foxp3-YFP$^+$ *Tcf7*$^{+/+}$ and *Tcf7*$^{-/-}$ mice. The cells were cultured *in vitro* for 4 days with IL-2, anti-CD3/CD28, TGFβ and different concentrations of IL-6. At the end of the culture period cells were treated with PMA, Ionomycin and Brefeldin A before flow cytometric analysis was performed. (A) Representative dot plots of IL17 and FOXP3 expression among $CD4^+$ for IL6 0.03, 0.3, 0.6, and 5 ng/ml are shown. Numbers show percentages of cells within the indicated box. (B) Quantified percentages of $CD4^+$ $IL17^-FOXP3^+$ (top panel), $CD4^+$ $IL17^+FOXP3^-$ (middle panel) and $CD4^+$ $IL17^+FOXP3^+$ (bottom panel) cells generated from *Tcf7*$^{+/+}$ and *Tcf7*$^{-/-}$ T_{conv} cells after 4 days of culture (n=1). A representative experiment is shown.

7.10 Marker panel analysis of peripheral T_{conv} and T_{reg} cells: TCF7 deficiency changes expression profiles.

T cells can be phenotypically characterized through the analysis of marker expression. To examine whether TCF7 deficiency has an influence on the T cells phenotype, we assembled a collection of different T_{reg} and T cell markers to stain T_{conv} and T_{reg} cells from pooled LN and spleen (Figure 38A-C and 39A-C). Surface expression of TCRβ was analyzed to control for the level TCR expression. CD44, CD69 and Ki67 are markers of T cell memory, activation or proliferation, respectively. CD39, CD103, CTLA-4, GARP, GITR, HELIOS, KLRG1 and NRP1 are discussed as potential T_{reg} cell and T_{reg} cell subset markers. This does not exclude their expression on T_{conv} cells. The co-stimulatory molecule CD86 was identified as over-represented on T_{reg} cells by our MS analysis.

Analysis of the marker expression in T_{conv} cells demonstrated that CD86, CD103 and NRP1 were significantly over-represented in *Tcf7*$^{-/-}$ T_{conv} cells compared to *Tcf7*$^{+/+}$ T_{conv} cells (Figure 38A, 40A, 40C and 41A). On the under-represented side, CD69 and HELIOS are significantly changed in *Tcf7*$^{-/-}$ compared to *Tcf7*$^{+/+}$ T_{conv} cells (Figure 38B and 40B). All other analyzed markers did not show significantly altered regulation (Figure 38C).

Analysis of the marker panel in T_{reg} cells detected that the expression of CD39, CD44, CD86 and CD103 was significantly over-represented in *Tcf7*$^{-/-}$ compared to *Tcf7*$^{+/+}$ T_{reg} cells (Figure 39A). GARP and HELIOS were significantly under-represented in T_{reg} cells from *Tcf7*$^{-/-}$ (Figure 39B). No significant changes could be detected for the other markers tested, even though KLRG-1 showed a strong tendency towards over-representation in *Tcf7*$^{-/-}$ (Figure 39C).

Regarding CD86, CD103 and HELIOS, the pattern seen in T_{conv} repeated for T_{reg} cells. CD86, the co-stimulatory molecule for activating CD28 and inhibitory CTLA-4 receptors, was over-represented on T_{reg} cells from *Tcf7*$^{-/-}$ (Figure 41A) (Carreno and Collins, 2002). The integrin CD103 binds to E-cadherin and is highly expressed on T cell and APC populations at mucosal sites (Annacker et al., 2005). CD103 was also described as a marker for a highly potent T_{reg} subset specialized for epithelial environments (Lehmann et al., 2002). Our marker panel screen detected CD103 as over-represented in T_{reg} cells of *Tcf7*$^{-/-}$ (Figure 40A).

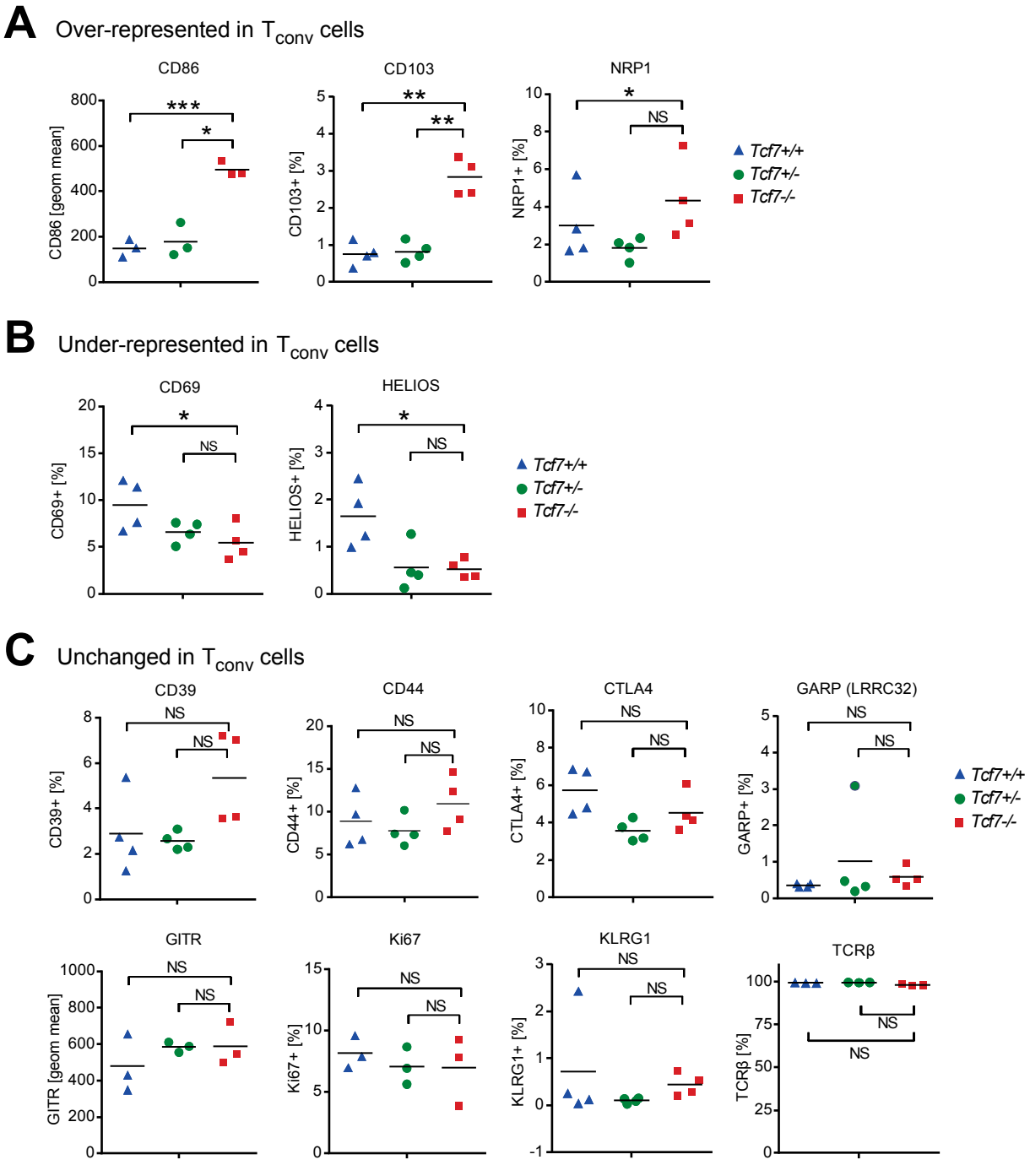

Figure 38: Marker panel analysis in T_{conv} cells. (A-C) Flow cytometric analysis of protein marker expression (as depicted) on $CD4^+$ peripheral T_{conv} cells of pooled LNs and spleen from *Tcf7*$^{+/+}$, *Tcf7*$^{+/-}$ and *Tcf7*$^{-/-}$ mice. Quantified percentages including mean values of marker expression on peripheral T_{conv} cells are shown. For CD86 and GITR the quantified geometric mean is shown instead of the percentage. Each symbol represents an individual mouse. (A) Protein markers significantly over-represented in *Tcf7*$^{-/-}$ compared to *Tcf7*$^{+/-}$ or *Tcf7*$^{+/+}$ T_{conv} cells. (B) Protein markers significantly under-represented in *Tcf7*$^{-/-}$ compared to *Tcf7*$^{+/-}$ or *Tcf7*$^{+/+}$ T_{conv} cells. (C) Protein markers unchanged in *Tcf7*$^{-/-}$ compared to *Tcf7*$^{+/-}$ or *Tcf7*$^{+/+}$ T_{conv} cells.
NS $P > 0.05$, * $P < 0.05$, ** $P < 0.01$, *** $P < 0.001$, **** $P < 0.0001$ (Ordinary one-way ANOVA).

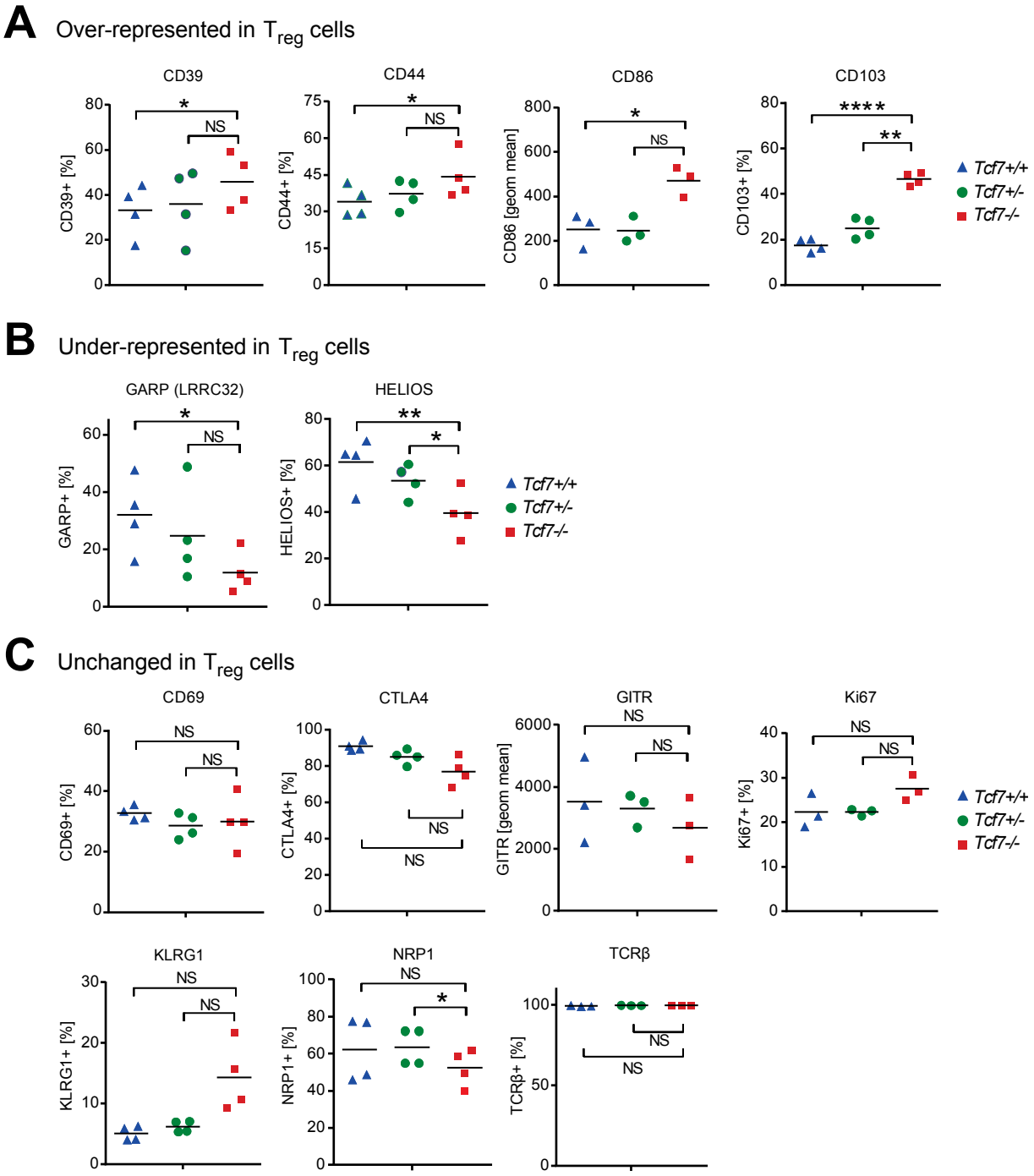

Figure 39: Marker panel analysis in T_{reg} cells. (A-C) Flow cytometric analysis of protein marker expression (as depicted) on $CD4^+$ $FOXP3^+$ peripheral T_{reg} cells of pooled LNs and spleen from *Tcf7*$^{+/+}$, *Tcf7*$^{+/-}$ and *Tcf7*$^{-/-}$ mice. Quantified percentages including mean values of marker expression on peripheral T_{reg} cells are shown. For CD86 and GITR the quantified geometric mean is shown instead of the percentage. Each symbol represents an individual mouse. (A) Protein markers significantly over-represented in *Tcf7*$^{-/-}$ compared to *Tcf7*$^{+/-}$ or *Tcf7*$^{+/+}$ T_{reg} cells. (B) Protein markers significantly under-represented in *Tcf7*$^{-/-}$ compared to *Tcf7*$^{+/-}$ or *Tcf7*$^{+/+}$ T_{reg} cells. (C) Protein markers unchanged in *Tcf7*$^{-/-}$ compared to *Tcf7*$^{+/-}$ or *Tcf7*$^{+/+}$ T_{reg} cells.
NS P > 0.05, * P < 0.05, ** P < 0.01, *** P < 0.001, **** P < 0.0001 (Ordinary one-way ANOVA).

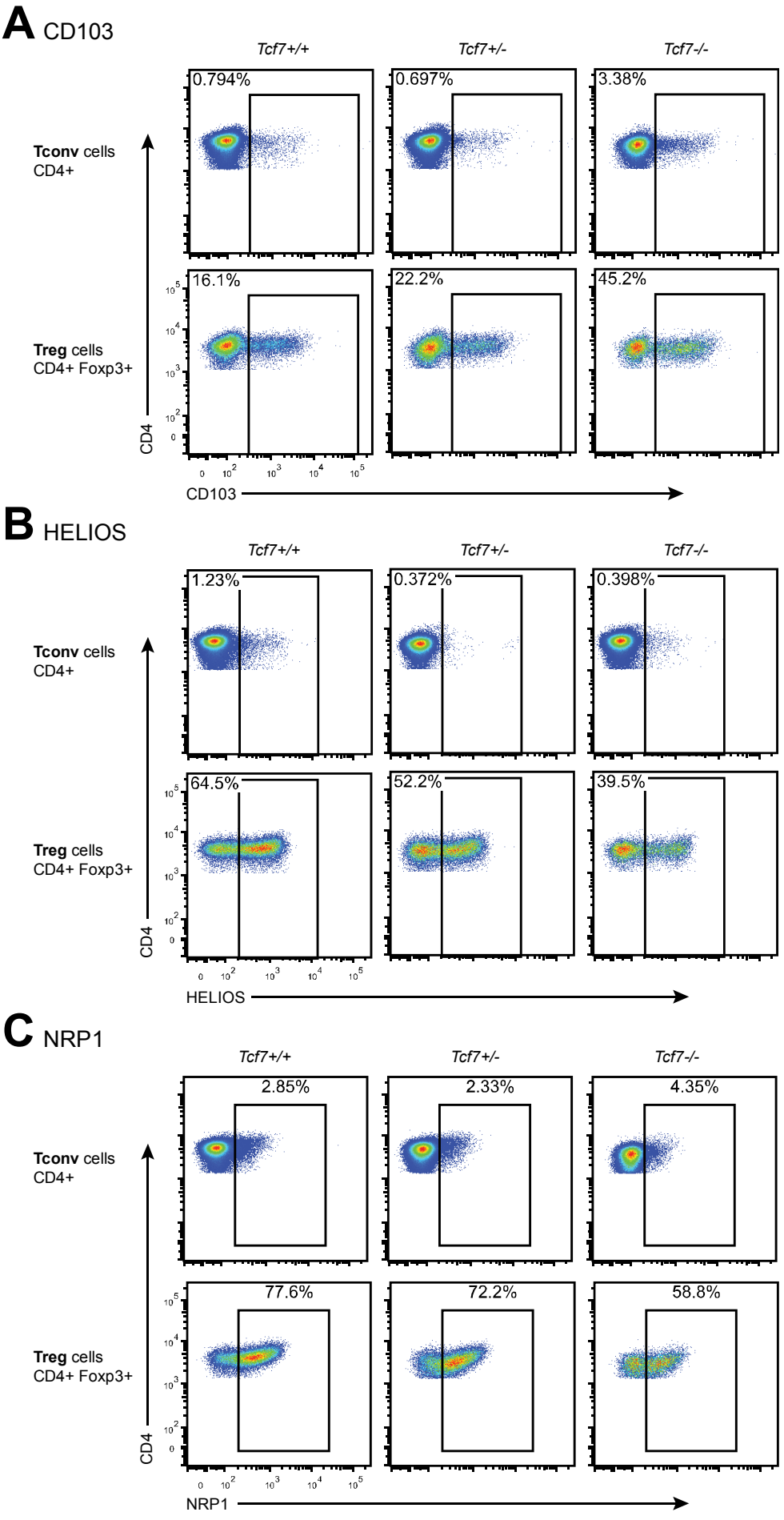
A CD103
Tcf7+/+
Tcf7+/-
Tcf7-/-
0.794%
0.697%
3.38%
Tconv cells
CD4+
16.1%
22.2%
45.2%
Treg cells
CD4+ Foxp3+
CD4
CD103
B HELIOS
Tcf7+/+
Tcf7+/-
Tcf7-/-
1.23%
0.372%
0.398%
Tconv cells
CD4+
64.5%
52.2%
39.5%
Treg cells
CD4+ Foxp3+
CD4
HELIOS
C NRP1
Tcf7+/+
Tcf7+/-
Tcf7-/-
2.85%
2.33%
4.35%
Tconv cells
CD4+
77.6%
72.2%
58.8%
Treg cells
CD4+ Foxp3+
CD4
NRP1

Figure 40: Expression of CD103, HELIOS and NRP1 in T_{conv} and T_{reg} cells. Flow cytometric analysis of protein marker expression in peripheral $CD4^+$ T_{conv} and $CD4^+$ $FOXP3^+$ T_{reg} cells from *Tcf7*$^{+/+}$, *Tcf7*$^{+/-}$ and *Tcf7*$^{-/-}$ mice. Numbers in dot plots show percentages of cells within the indicated box. (A) Representative dot plots of CD103 expression. (B) Representative dot plots of HELIOS expression. (C) Representative dot plots of NRP1 expression.

HELIOS, a member of the Ikaros transcription factor family was previously described as a marker for thymic derived tT_{reg} cells (Thornton et al., 2010). Our marker panel screen shows a significant under-representation of HELIOS in T_{reg} cells from *Tcf7*$^{-/-}$ compared to *Tcf7*$^{+/+}$ (Figure 40B). The ectoenzyme CD39, expressed on the surface of T_{reg} cells, produces adenosine from extracellular nucleotides which can than bind to adenosine receptors on activated T_{conv} cells and thereby silence them (Borsellino et al., 2007; Deaglio et al., 2007). We detected a significantly increased frequency of CD39 expression in T_{reg} cells from *Tcf7*$^{-/-}$ mice. For *Tcf7*$^{-/-}$ T_{reg} cells we detected a slight but significant over-representation of CD44 compared to *Tcf7*$^{+/+}$. CD44 is a transmembrane glycoprotein involved in T cell activation and memory (Dutton et al., 1998). Interaction between E-selectin and CD44 is involved in leukocyte rolling (Yago et al., 2010). The leucine-rich molecule GARP is expressed on the surface of a high fraction of activated T_{reg} cells and binds TGFβ in its latent form to the surface of T_{reg} cells. Even though the mechanism is not completely clear, binding of latent TGFβ to their surface is likely a way for T_{reg} cells to confer immune tolerance (Probst-Kepper and Buer, 2010). We detected a significantly reduced level of $GARP^+$ T_{reg} cells in *Tcf7*$^{-/-}$ mice compared to *Tcf7*$^{+/+}$. KLRG1, which showed a trend towards over-representation in T_{reg} cells from *Tcf7*$^{-/-}$ mice is an inhibitory lectin-like receptor that is a marker for a small but potent T_{reg} cell subpopulation (Beyersdorf et al., 2007).
The frequency of CTLA-4^+ cells among *Tcf7*$^{-/-}$ T_{reg} cells showed a trend toward reduction but was not significantly reduced (Figure 39C and 41B). The negative regulator of T cell activation CTLA-4 engages with its ligands CD80 or CD86 and thereby modifies the signals of the TCR. CTLA-4 transcription is induced by T cell activation and CTLA-4 expression is hence not found on naïve T cells (Rudd et al., 2009). CTLA-4 is also an essential molecule for T_{reg} cell suppressive function (Wing et al., 2008). Closer analysis of the $Foxp3^+$ but CTLA-4^- T_{reg} cells showed this population was significantly increased among T_{reg} cells from *Tcf7*$^{-/-}$ compared to *Tcf7*$^{+/+}$ (Figure 41C, R1).

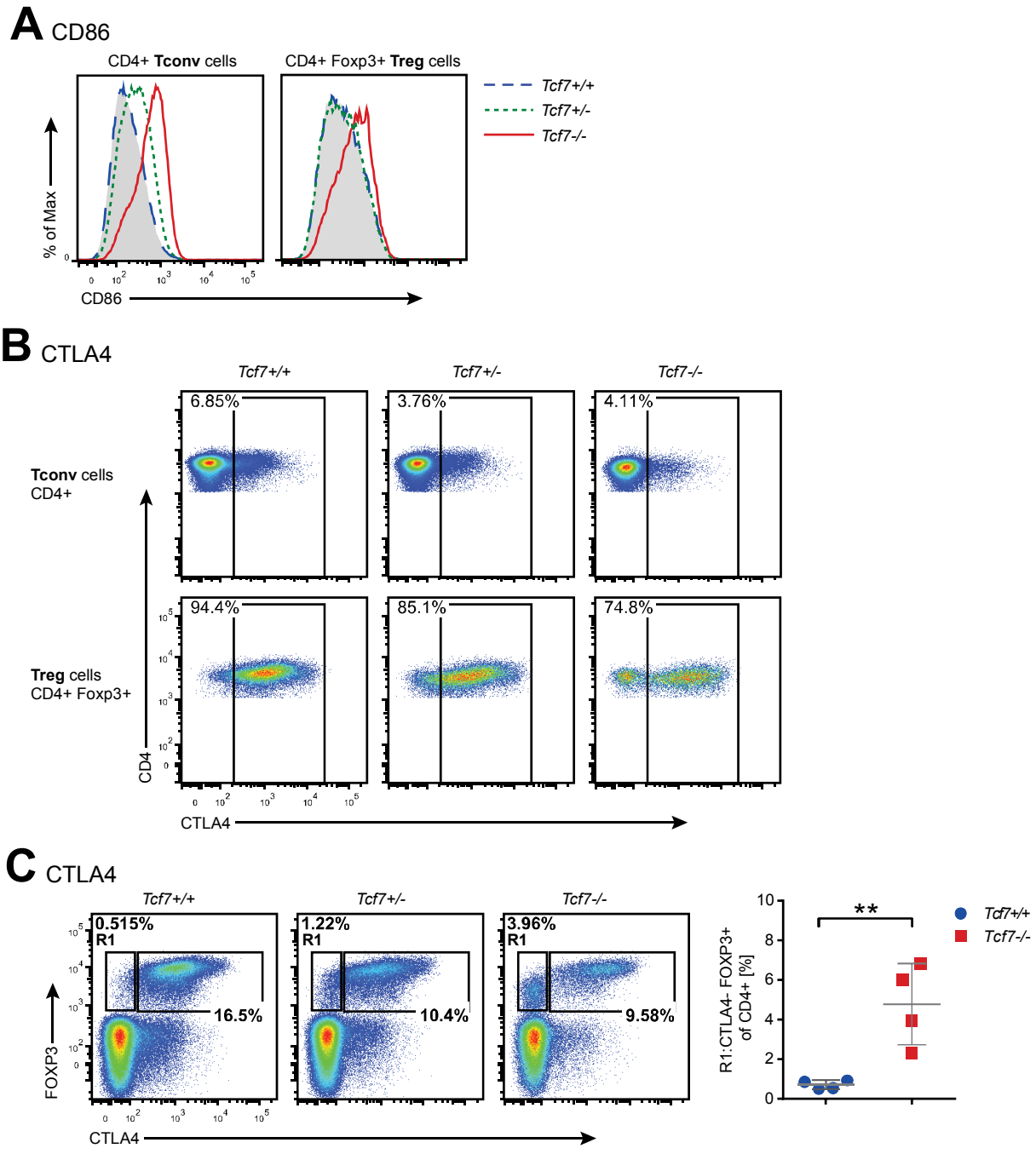

Figure 41: Expression of CD86 and CTLA-4 in T_{conv} and T_{reg} cells. Flow cytometric analysis of protein marker expression in peripheral $CD4^+$ T_{conv} and $CD4^+$ $FOXP3^+$ T_{reg} cells from *Tcf7*$^{+/+}$, *Tcf7*$^{+/-}$ and *Tcf7*$^{-/-}$ mice. (A) Representative dot plots of CD25 and FOXP3 expression. Numbers in dot plots show percentages of cells within the indicated box. (B) Quantified percentages with mean + SD of $FOXP3^+$, $CD25^-FOXP3^+$ or $CD25^+FOXP3^+$ populations as indicated in A. Each symbol represents an individual animal. ** $P < 0.01$ (unpaired t test).

In summary, CD86, CD103 and HELIOS showed a similar regulatory pattern in T_{conv} and T_{reg} cells from *Tcf7*$^{-/-}$ compared to *Tcf7*$^{+/+}$ mice, while NRP1, CD39, CD44 CD69 GARP and CTLA-4 expression was differentially influenced in T_{reg} and T_{conv} by TCF7 deficiency. KLRG1 showed a tendency towards over-representation in T_{reg} cells from *Tcf7*$^{-/-}$. We did not detect changes for Ki67, TCRβ or GITR.

7.11 *Tcf7* deficiency induces elevated frequencies of CD25^{-} FOXP3^{+} T_{reg} cells.

All murine T_{reg} cells subsets are usually phenotypically described, and are distinguished from other T cells, by a high expression of the IL-2 receptor molecule CD25 in combination with the expression of their master transcription factor FOXP3 (Fontenot et al., 2003; Hori et al., 2003; Khattri et al., 2003). For FACS purification, FOXP3 staining cannot be applied and differentiation between T_{conv} and T_{reg} cells has to rely on CD25 staining.

We stained CD4^{+} T cells from thymus, LN and spleen of *Tcf7*$^{+/+}$ *Tcf7*$^{+/-}$ and *Tcf7*$^{-/-}$ mice for CD25 and FOXP3 to look at T_{reg} cells frequencies in these different organs (Figure 3.38A-B). We first quantified the fraction of CD4^{+} FOXP3^{+} T_{reg} cells from all 3 organs (Figure 42B, left panel). As we had previously detected for Foxp3^{+} T_{reg} cells from the thymus, the frequency of CD4 FOXP3^{+} T_{reg} cells was significantly elevated in T_{reg} cells from *Tcf7*$^{-/-}$ compared to *Tcf7*$^{+/-}$ or *Tcf7*$^{+/+}$ mice. In contrast to the thymus, where we could see a dosage effect between *Tcf7*$^{+/-}$ and *Tcf7*$^{+/+}$, this effect was not detectable in the peripheral lymphoid organs. Although the *Tcf7*$^{+/-}$ plots and quantified data are shown, we will in the following focus on the comparison between *Tcf7*$^{-/-}$ and *Tcf7*$^{+/+}$ conditions. Next, we looked at the population of CD4^{+} CD25^{+}FOXP3^{+} T_{reg} cells (Figure 42B, middle panel). We noticed that while the frequencies of these cells were significantly elevated in *Tcf7*$^{-/-}$ compared to the *Tcf7*$^{+/+}$ mice, we could not detect a difference in the frequencies from LN and spleen. Last we analyzed the population of CD4^{+} CD25^{-}Foxp3^{+} T_{reg} cells (Figure 42B, right panel). Surprisingly, this population, which stayed below 2 percent under *Tcf7*$^{+/+}$ conditions, rose up to about 3 times the average frequency in *Tcf7*$^{-/-}$ mice for all 3 organs.

In summary, in the absence of TCF7 we detected a significant increase of the CD4^{+} CD25^{-}Foxp3^{+} T_{reg} cell population from thymus, LN and spleen.

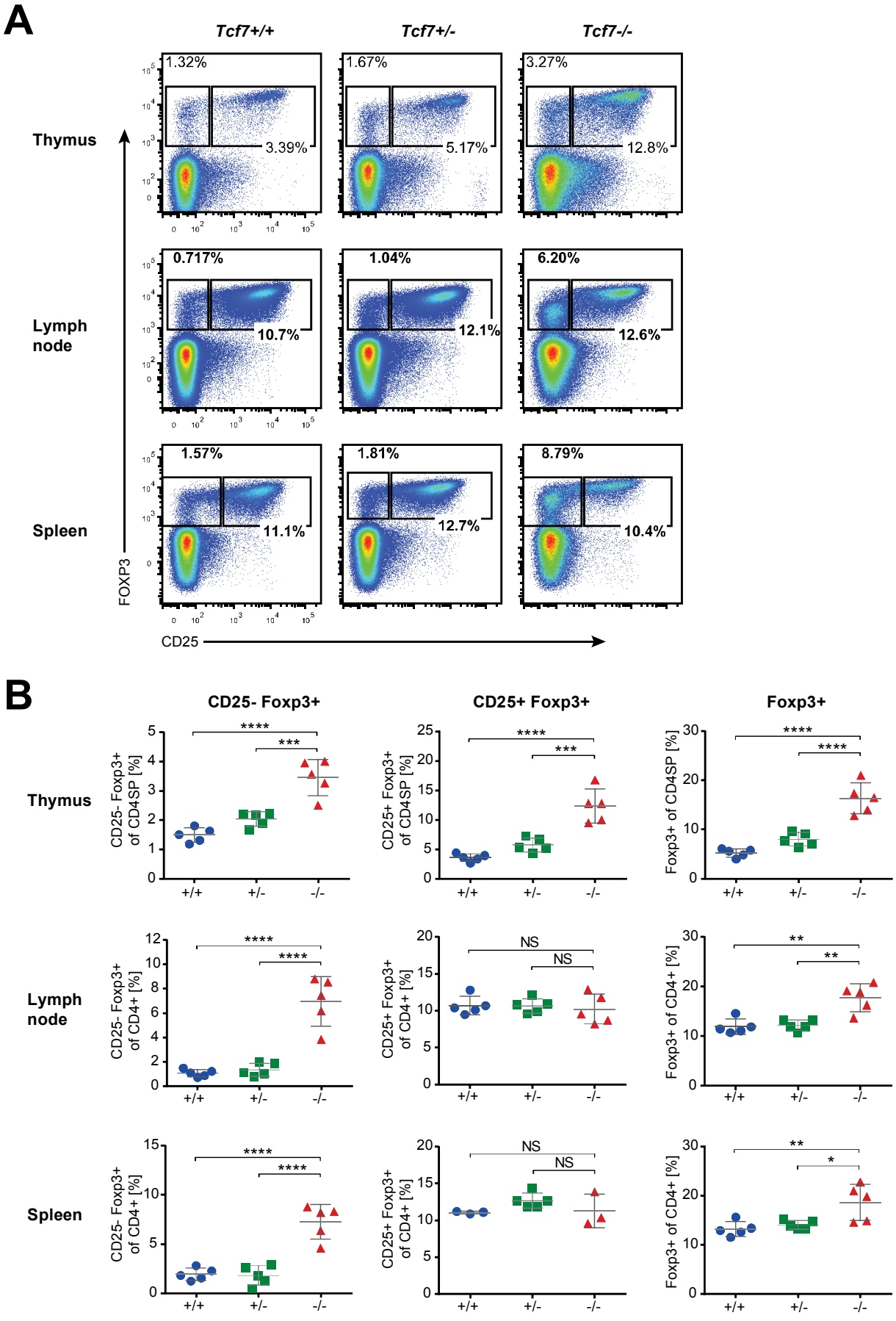
A
Tcf7+/+
Tcf7+/-
Tcf7-/-
Thymus
Lymph node
Spleen
1.32%
3.39%
1.67%
5.17%
3.27%
12.8%
0.717%
10.7%
1.04%
12.1%
6.20%
12.6%
1.57%
11.1%
1.81%
12.7%
8.79%
10.4%
FOXP3
CD25
B
CD25- Foxp3+
CD25+ Foxp3+
Foxp3+
CD25- Foxp3+ of CD4SP [%]
CD25+ Foxp3+ of CD4SP [%]
Foxp3+ of CD4SP [%]
CD25- Foxp3+ of CD4+ [%]
CD25+ Foxp3+ of CD4+ [%]
Foxp3+ of CD4+ [%]
****
***
NS
**
*
+/+
+/-
-/-

Figure 42: Comparative analysis of the T_{reg} cell CD25 and FOXP3 expression in thymus LN and spleen. Flow cytometric analysis of CD25 and FOXP3 expression in $CD4^+$ cells from thymus LN and spleen of *Tcf7*$^{+/+}$, *Tcf7*$^{+/-}$ and *Tcf7*$^{-/-}$ mice. (A) Representative histograms CD86 expression. Numbers in dot plots show percentages of cells within the indicated box. (B) Representative dot plots of CTLA-4 expression. (C) Left panel: representative dot plots of CTLA-4 and FOXP3 expression. Gate R1: CTLA-4^- $FOXP3^+$ cells. Right panel: quantified percentages of R1 with mean +SD. Each symbol represents an individual animal.
NS P > 0.05, * P < 0.05, ** P < 0.01, *** P < 0.001, **** P < 0.0001 (unpaired t test).

7.12 *Tcf7* deficiency massively decreases NKT frequencies in the thymus and in the periphery.

In addition to the effects that *Tcf7* deficiency had on T_{conv} and T_{reg} cells, we were also interested in the special T cell lineage of NKT cells which form a link between the innate and the adaptive immune system. NKT cells develop in the thymus and express a semi-invariant αβ-TCR that recognizes peptides presented by CD1d, a MHC class I-like molecule that has a specialized role in lipid antigen presentation. Besides the TCR, they also express CD4 and often NK cell markers like NK1.1. Upon stimulation, NKT cells can release T_H1 and T_H2 cytokines and chemokines (Bendelac et al., 2007).

We used fluorochrome coupled CD1d tetramers complexed to PBS-57, an analogue to the natural lipid ligand of CD1d, to detect NKT cells in the *Tcf7*$^{+/+}$ and *Tcf7*$^{-/-}$ mice. To control for unspecific binding of the PBS-57-loaded CD1d tetramer, we used an unloaded CD1d tetramer (Kawano et al., 1997; Klenerman et al., 2002).

Analysis of the thymus showed a massive reduction of $CD4^+$ $CD3^+$ mCD1d tetramer binding NKT cells in the *Tcf7*$^{-/-}$ compared to the *Tcf7*$^{+/+}$ thymus (Figure 43A-B). The average frequency of NKT cells in the thymus was about 5 times lower in the *Tcf7*$^{-/-}$ mice. While we were still able to detect low numbers of NKT cells in the thymus of *Tcf7*$^{-/-}$ mice, we were surprised to see that in the spleen the fraction of NKT cells detected was only slightly above the background detected with the unloaded CD1d tetramer (Figure 43C-D).

From these results we concluded that TCF7 is of great importance for the survival of NKT cells.

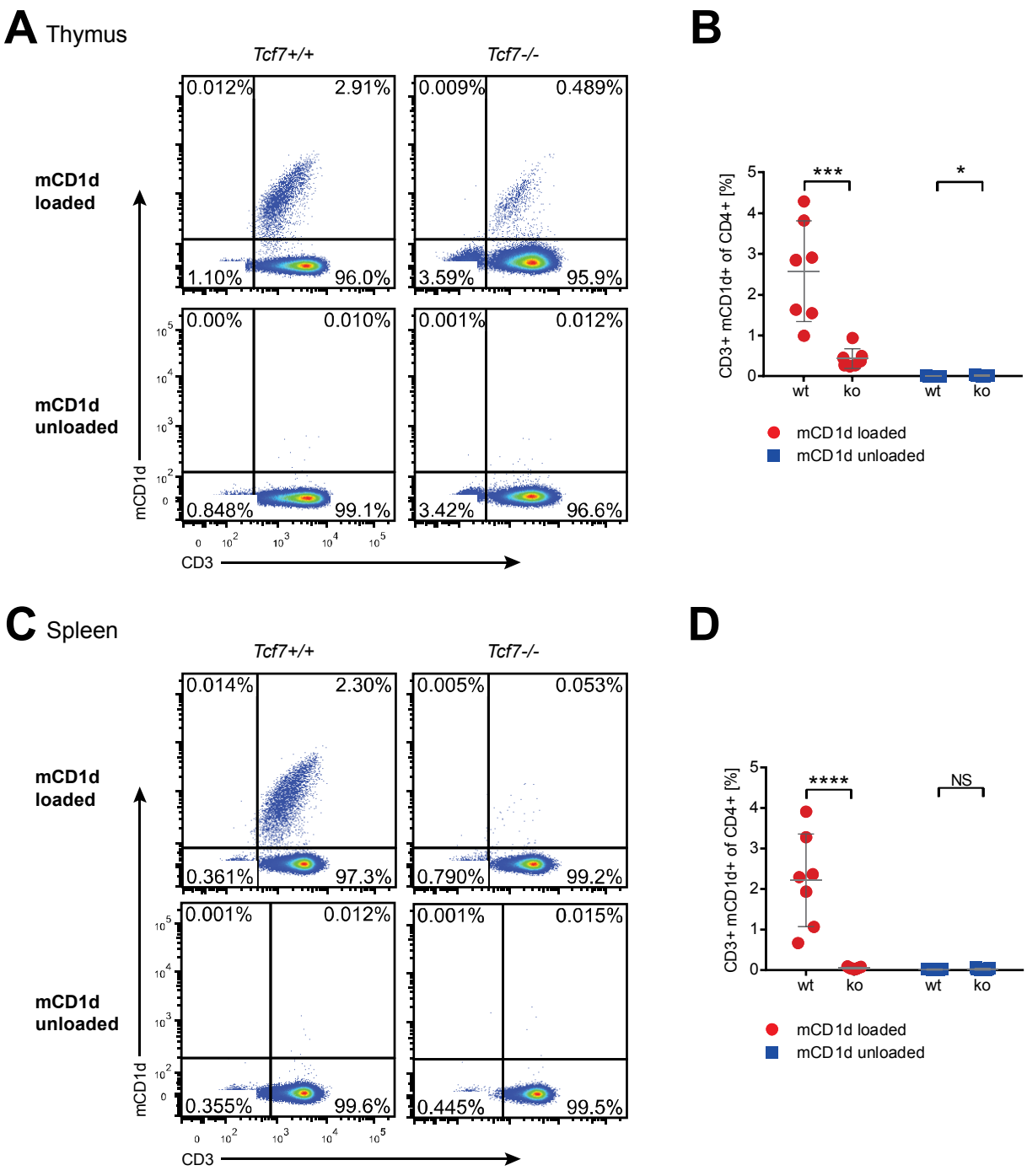

Figure 43: Detection of NKT cells with mCD1d tetramers. (A-D) Flow cytometric detection of $CD4^+$ NKT cells from thymus and spleen of *Tcf7*$^{+/+}$ and *Tcf7*$^{-/-}$ mice identified by CD3 expression and mCD1d tetramers binding. mCD1d tetramers were loaded with PBS-57. Unloaded mCD1d tetramers were used as a negative control. Numbers in dot plots show percentages of cells within the indicated box. For all quantified data mean + SD is shown. (A and C) Representative dot plots of CD3 expression and mCD1d tetramer binding in $CD4^+$ cells from (A) thymus and (C) spleen. (B and D) Quantified percentages of $CD3^+$ and tetramer binding cells among $CD4^+$ cells from (B) the thymus as depicted in A and (D) the spleen as depicted in C (n=7).

NS $P > 0.05$, * $P < 0.05$, *** $P < 0.001$, **** $P < 0.0001$ (unpaired t test).

8 Discussion

8.1 Quantitative differential mass spectrometry of the T_{reg} cell proteome

In this study we aimed to analyze the proteome of T_{reg} in comparison to T_{conv} cells to validate known, and to identify new proteins that are differentially regulated in T_{reg} cells. We achieved the detection of 5225 proteins and identification 164 that were significantly differentially regulated between T_{reg} and T_{conv} cells. The MS data was validated on the protein level by flow cytometry and compared to existing gene expression data.

The previously published T_{reg} and T_{conv} cells transcriptome data (Feuerer et al., 2010; Hill et al., 2007) allowed us to directly compare gene expression to our MS derived data. Expression of most proteins mirrored mRNA expression, however, direct comparison of T_{reg}/T_{conv} fold changes helped to recognize candidates with low to moderate fold changes on the mRNA level but high changes on the protein level or vice versa. Gene and protein expression do not always correlate, since both mRNA and protein expression are often modulated by post-transcriptional and post-translational mechanisms, e.g. RNAi or protein degradation. This kind of comparative analysis can be of great help to identify new targets that will not be recognized by only looking at the transcriptome or proteome data.

Proteomics were in fact used in the past to analyze T_{reg} cells. A previous study used differential gel-blotting to screen for proteins specifically expressed by human T_{reg} cells and identify galectin-10, a glycan binding molecule, as an essential factor for the function of T_{reg} cells (Kubach et al., 2007). In contrast to this study, we were not able to detect galectin-10 through our MS analysis. Another study performed on human T_{reg} cells identified proteins that were highly expressed on the surface of human T_{reg} cells (Solstad et al., 2011). Among them, they particularly emphasized CD71, CD95, CD147 and CD148. In line with these data, we detected an over-representation of the transferrin receptor CD71 and BASIGIN (CD147). CD95 and CD148 on the other hand were not detected by our analysis. A third data set that provided information about human T_{reg} cell proteomics concentrated on differentially expressed kinases in

T_{reg} cells (Konig et al., 2012). Comparison of their list of 11 differentially expressed kinases to our data set showed only little overlap. Since our analysis was done in mice and the here-described studies were done in humans, their moderate compliance might reflect the species differences. One other recent report used proteomics to investigate the murine FOXP3 interaction complex (Rudra et al., 2012). This work gives many new insights into the FOXP3 interaction network but does not provide information about proteins that are differentially expressed in T_{reg} cells. A big advantage of our approach to proteomics is that we do not focus on a specific cellular location, but rather look at the whole cell, which gives as the chance to capture the full unbiased picture.

The quality of the proteomics data set can be internally controlled for by looking at different aspects. One feature of good data quality is reproducibility. We detected a total of 5225 proteins. 4859 proteins were detected in at least two and 3756 proteins in all four replicates. This resulted in a solid recovery rate of 72 percent between the four replicates. Another way to look at the quality of proteomics data is to look at the expression of classical T_{reg} cell markers. In line with our expectations, we detected FOXP3, IL-2Rβ, GITR and NRP1 as highly over-represented in T_{reg} cells compared to T_{conv} cells. Additionally, SATB1 and PDE3b were detected as under-represented in T_{reg} cells. Some of the classic T_{reg} cell markers, e.g. FOXP3, were not detected in all 4 replicates or were even not detected, e.g. CD25 or GARP. Detection of proteins through MS is usually limited by sample handling, protein isolation, digestion or efficiency of the measurement itself. In retrospect it cannot be finally determined why some classical proteins were not detected, but it was most likely due to the low number of $6x10^5$ cells, used for the experiments, which limits recovery after protein extraction from the sample. The generated data represents, despite small shortcomings, the first full comprehensive quantitative and differential proteome of murine T_{reg} and T_{conv} cells.

The T_{reg} and T_{conv} cell proteomics data set, together with our comparative analysis of the transcriptome and proteome, will be a valuable source for future research in the field, since they help to understand the uniqueness of T_{reg} cells.

8.2 Identification and relevance of TCF7 for the development and function of T_{reg} cells

Based on proteomics and gene expression data comparing T_{reg} and T_{conv} cells, we intended to find candidates to further investigate their role in the development and function of T_{reg} cells. We were particularly interested in the proteins that were selectively under-represented in T_{reg} cells and identified TCF7 as a promising transcription factor for the regulation of tT_{reg} cell generation and function. Antibody staining validated the decreased *Tcf7* expression in T_{reg} compared to T_{conv} cells in different organs as predicted by our MS analysis. Different selection processes helped to decide on TCF7 as a candidate for further investigations.

Matching of the significantly under-represented proteins onto gene expression data (Feuerer et al., 2010; Hill et al., 2007) identified a prominently under-represented mRNA cluster. Alongside with *Tcf7* the cluster included *Pde3b*, *Satb1* and *Itk*. For all 3 genes, previous studies showed that their down regulation was essential for proper T_{reg} cell function. FOXP3 actively down regulates the expression of *Pde3B*, which leads to enhanced T_{reg} cell metabolic and proliferative fitness (Gavin et al., 2007). Expression of SATB1, a genome organizer, is also actively repressed by FOXP3. Forced expression of SATB1 in T_{reg} cells leads to the loss of the T_{reg} cell suppressive function (Beyer et al., 2011). A recent report demonstrated that functional $FOXP3^+$ T_{reg} cells develop at a higher frequency in an *Itk*-deficient environment (Gomez-Rodriguez et al., 2014). Association of *Tcf7* with this cluster served as an indication for its potential impact on T_{reg} cells that led us to further investigations.

The ImmGen consortium described a *Tcf7-Lef1* co-regulated cluster (Mingueneau et al., 2013). We matched this data to our proteomics data set and found that the whole cluster was significantly under-represented in T_{reg} cells. The down regulated cluster included, besides TCF7 and LEF1, also ITK, THEMIS, BCL11b and several CD3 family members. THEMIS and CD3 are both involved with TCR signaling in T cells. During T cell development THEMIS has a role in setting the TCR signal threshold for positive and negative selection (Fu et al., 2013). CD3γ, CD3δ and CD3ε are part of the TCR complex. The zinc finger protein BCL11b was found to be essential for T cell lineage commitment (Ikawa et al., 2010; Li et al., 2010). The observation that several of the *Tcf7-Lef1* co-regulated cluster members were involved in TCR signaling and thymic T cell differentiation further implied a role of TCF7 in these events. In the

future, the under–representation of these *Tcf7-Lef1* cluster proteins might help to explain how T_{reg} cells are differentially regulated compared to T_{conv} cells.

Regarding the role of TCF7 in T_{reg} cell function in the periphery, one recent report stated an association of TCF7 and FOXP3. The same study also demonstrated that activation of Wnt signaling, and thereby induction of TCF7, interfered with the suppressive activity of T_{reg} cells (van Loosdregt et al., 2013). The role of TCF7 in thymic T cell development was the subject of various studies, but surprisingly none of those made a distinction between T_{conv} and T_{reg} subsets (Kovalovsky et al., 2009; Staal et al., 2008; Steinke et al., 2014; Verbeek et al., 1995; Weber et al., 2011). The novelty of the subject made *Tcf7* an even more attractive candidate for our investigation of thymic T_{reg} development.

Comparison of our proteomics data set to existing gene expression data and analysis of the *Tcf7-Lef1* co-regulated cluster led us to further investigations regarding the role of TCF7 in T_{reg} cell function and development. While a negative impact of TCF7 on the suppressive activity of peripheral T_{reg} cells was recently demonstrated, virtually nothing is known about the role of TCF7 in thymic T_{reg} cell differentiation.

8.3 Differentiation of T_{reg} cells in the *Tcf7*-deficient mouse model

After the identification of TCF7 as our candidate, we intended to characterize the role of TCF7 in thymic T_{reg} cell differentiation. Using the *Tcf7*$^{-/-}$ mouse model (Verbeek et al., 1995), we studied FOXP3^{+} T_{reg} cells at the DP and CD4SP stage. In addition, we analyzed FOXP3 expression at the DN stage in the *Tcf7*$^{-/-}$ mice and in the TCR-transgenic TEa *Tcf7*$^{-/-}$ model.

The *Tcf7*$^{-/-}$ mouse model was first described in 1995 and since then it has been used for numerous studies of T cell differentiation. *Tcf7*-deficient mice are healthy, fertile and show no signs of autoimmune disease. However, total cell numbers in the thymus are significantly reduced and defects in the development of T cells have been described (Steinke et al., 2014; Verbeek et al., 1995). Despite these restrictions in T cell development, the *Tcf7*$^{-/-}$ thymus generates functional T cells. Thus, we considered the *Tcf7*-deficient mice suitable to study the differentiation of tT_{reg} cells.

Our analysis of the *Tcf7*$^{-/-}$ CD4SP and DP compartments demonstrated that *Tcf7* deficiency increased the fraction of FOXP3^{+} T_{reg} cells among CD4SP and DP cells.

This finding indicates that under wild-type conditions the presence of TCF7 inhibits the generation of T_{reg} cells. One could argue that the increase in T_{reg} cell frequencies is a result of the previously described defects in in the T cell compartment. Mixed BM chimeras of *Tcf7*$^{-/-}$ and *Tcf7*$^{+/+}$ could clarify this issue, but unfortunately development of *Tcf7*$^{-/-}$ T cells is almost completely arrested at early progenitor stages if placed in competition to *Tcf7*$^{+/+}$ cells. *Tcf7*$^{-/-}$ progenitors cannot compete with the *Tcf7*$^{+/+}$ progenitors and BM chimeras can therefore not be used to investigate the matter (Weber et al., 2011).

As stated above, we detect FOXP3^{+} cells at the DP stage and we assume that these cells are T_{reg} precursors. However, the topic of *Foxp3* expression at the DP stage is controversially discussed. Hsieh and colleagues describe that the major part of the detected FOXP3^{+} DP population consists of CD4SP/DP cell doublets and that real FOXP3^{+} DP cells rarely exist. They suggest that further maturation is needed for induction of *Foxp3* expression in thymocytes (Lee and Hsieh, 2009). Since we always used flow cytometric height and width parameters to exclude doublets in our experiment we assume that the detected FOXP3^{+} DP cells are authentic. Another view on the subject is that induction of *Foxp3* expression occurs after the first TCR engagement and can be detected starting at the DP stage of thymocyte development (Fontenot et al., 2005b).

Even though we believe that *Foxp3* induction usually occurs after TCR engagement, we performed, based on the profound impact of TCF7 on T cell lineage commitment (Weber et al., 2011), analysis of the DN compartment for the presence of FOXP3^{+} cells. To our surprise, we observed CD3^{-} and TCR^{-} FOXP3^{+} DN cells in the *Tcf7*$^{-/-}$ mice. In depth analysis of this population for CD5 expression and in the TCR-transgenic TEa *Tcf7*$^{-/-}$ setting indicated that the premature *Foxp3* expression at this stage occurred independent of TCR signaling. Interestingly, we demonstrated that the majority of the FOXP3^{+} DN cells were found in a DN1-DN2 transition state. Previous studies described this DN1-DN2 transition state as a T cell lineage committed population, more abundant in neonatal mice, that is exported from the thymus prior to TCR rearrangement. These immature cells migrate, expand and colonize lymphoid organs and the gut (Lambolez et al., 2006; Peaudecerf et al., 2011). The further fate of our DN1-DN2 FOXP3^{+} transition cells remains unclear. One possibility is that they migrate out from the thymus to other lymphoid organs to colonize them, but this is unlikely, since we did not detect FOXP3^{+} TCR^{-} cells in the

periphery. *Tcf7*$^{-/-}$ mice have an incomplete block at the DN1 and DN2 stages of thymocyte development (Verbeek et al., 1995). It is therefore quite possible that these transition cells do not proceed in their development. Whether TCF7 directly inhibits *Foxp3* expression in DN cells under wild-type conditions or if *de novo* induction of *Foxp3* expression occurs due to the prolonged DN1-DN2 transition is currently unclear. Expression of FOXP3 in non-hematopoietic thymic epithelial cells, other epithelial cells and tumor cells has been suggested (Chang et al., 2005; Chen et al., 2008; Triulzi et al., 2013), although this issue is still controversial (Liston et al., 2007). These previous studies suggested that *Foxp3* expression can occur outside of the lymphoid system and thus independent of TCR signaling. Our finding that *Foxp3* expression arises independently of TCR engagement in *Tcf7*$^{-/-}$ DN thymocytes is astonishing and might help to reveal the mechanisms that regulate *Foxp3* induction.
Our studies of thymic T_{reg} differentiation under *Tcf7*-deficient conditions revealed new aspects about the role of TCF7 in thymocyte development. Distinction between T_{conv} and T_{reg} cell differentiation leads to the finding that TCF7 suppresses T_{reg} cell generation at the CD4SP and DP stages. In addition, we detected premature *Foxp3* expression in *Tcf7*$^{-/-}$ DN cells that occurred in the absence of a TCR. These findings will contribute to a better understanding of T_{reg} and T_{conv} cell differentiation in the thymus.

8.4 The dosage effect of TCF7 and refinement of an *in vitro* T_{reg} cell differentiation assay

On the basis of our intriguing findings about the role of TCF7 in T_{reg} cell differentiation, we aimed to study this process in more detail *in vitro*. In order to do so, we analyzed the differentiation of T_{reg} precursors from *Tcf7*$^{+/-}$ and *Tcf7*$^{+/+}$ mice in a differentiation assay.
Since the T cell development under *Tcf7*-deficient conditions was associated with several defects, and due to major difficulties with the *in vitro* culture of *Tcf7*$^{-/-}$ T_{reg} precursors, we decided to use the *Tcf7*$^{+/-}$ mice instead. T cell development in the heterozygous mouse was normal (Verbeek et al., 1995) but levels of TCF7 were significantly reduced. We detected significantly elevated fractions of early and late T_{reg} precursors as well as CD4SP T_{reg} cells in the *Tcf7*$^{+/-}$ thymus. These observations

were in line with the results that we obtained from the *Tcf7*$^{-/-}$ thymus and indicated that reduced levels of TCF7 were sufficient to enhance T_{reg} cell generation in the thymus.

To study T_{reg} cell differentiation *in vitro,* we made use of a T_{reg} precursor differentiation assay that had been previously introduced by Wirnsberger and colleagues (Wirnsberger et al., 2009). We purposefully chose an APC free system to avoid influence from APCs and to control the amount of TCR signal in the culture. The previous study used 3 day culture with a plate-bound anti-CD3 stimulus and IL-2. As a result they generated about 10 percent of FOXP3^{+} T_{reg} cells. We introduced an anti-CD3/CD28 bead-based stimulation and used different combinations of the cytokines IL-2 and IL-15. These refinements were able to boost the efficacy of T_{reg} cell commitment to up to 80 percent. As it was previously demonstrated that CD28 co-stimulation is an important factor for the generation of T_{reg} cells (Tai et al., 2005), it is likely that the addition of CD28 to the system made the biggest difference in the generation efficiency. Anyhow, we hereby demonstrated that TCR signaling (anti-CD3), co-stimulation (anti-CD28) and common-γ-chain signaling (IL2 and IL-15) were sufficient for T_{reg} cell differentiation from the early T_{reg} precursor. For differentiation from the late T_{reg} precursor, common-γ-chain signaling alone was sufficient and resulted in up to 40 percent T_{reg} cells after 1 day of culture. Notably, we also showed that mature CD69^{-} CD4SP cells had generally lost the ability to differentiate into T_{reg} cells under these conditions, indicating that commitment into T_{reg} cell lineage is restricted to a narrow developmental window.

When we compared the ability of *Tcf7*$^{+/-}$ and *Tcf7*$^{+/+}$ precursors to differentiate into T_{reg} cells in our *in vitro* differentiation assay we observed that *Tcf7*$^{+/-}$ precursors committed into the T_{reg} cell lineage at a higher frequency and generated more T_{reg} cells by numbers. Since the endogenous TCF7 levels in precursors restrict T_{reg} cell development under these conditions, we concluded that TCF7 has to interfere either with TCR signaling, co-stimulation or common-γ-chain signaling.

Our analysis of the *Tcf7*$^{+/-}$ thymus demonstrated a dosage effect of TCF7 regarding the commitment to the T_{reg} cell lineage. Reduced levels of TCF7 lead to elevated frequencies of CD4SP T_{reg} cells and T_{reg} precursors. Furthermore, decreased expression of TCF7 results in enhanced *in vitro* T_{reg} differentiation capacity of precursors. Our refined T_{reg} cell differentiation assay will serve as valuable tool for future investigations in the field of tT_{reg} cell development.

8.5 Limiting T_{reg} cell generation capacity

Based on our findings that T_{reg} cell differentiation capacity was limited by TCF7, we intended to examine this process in more detail. In order to do so, we analyzed the influence of TCF7 on different aspects of T_{reg} cell development.

To simulate different strengths of TCR stimulus we modified our T_{reg} cell differentiation assay by using different concentrations of plate-bound anti-CD3, instead of the anti-CD3/CD28 beads. Titration of the TCR stimulus showed that reduction of TCF7 levels led to a T_{reg} cell generation advantage in terms of frequencies and cell count over a broad range of stimuli. These results indicated that during the critical window of T_{reg} cell commitment, TCF7 can function as a modulator of TCR stimulus and thereby restricts the access to the T_{reg} cell lineage. Such modulatory effects on TCR signaling have been previously suggested for other factors. THEMIS has been proposed to establish the signal threshold during T cell positive and negative selection (Fu et al., 2013). However, this study did not look at T_{reg} cell development. Another recent report suggested that expression of the members of the tumor-necrosis factor receptor (TNFR) family GITR, OX40 and TNFR2 on T_{reg} precursors translated strong TCR signals into molecular parameters that promoted T_{reg} cell differentiation (Mahmud et al., 2014). In contrast to these TNFR family members that facilitate the development of T_{reg} cells, TCF7 limits T_{reg} cell differentiation capacity and might be involved in shaping the T_{reg} cell TCR repertoire towards higher affinity. This assumption is furthermore supported by our observation that *Tcf7*-deficient mice harbored a higher frequency of $CD5^{low}$ cells. We observed a progressive decrease in the $CD5^{low}$ cells from the early to the late precursor and to the mature tT_{reg} cells under $Tcf7^{+/+}$ conditions. *Tcf7*-deficient mice showed constant levels of $CD5^{low}$ cells over the course of tT_{reg} cell generation, suggesting that the tT_{reg} cell pool from the *Tcf7*-deficient mice contains more cells with a low affinity TCR. By implications, these results indicate that under wild-type conditions most T_{reg} precursor with a low affinity TCR eventually do not commit to the T_{reg} lineage in a process that might be mediated by TCF7. Since these important findings about TCR avidities under *Tcf7*-deficient conditions are largely based on CD5 surface expression, confirmation of these findings in a different model could strengthen our conclusion. Previous studies described the *Nr4a1*-GFP mouse as a tool to look at the TCR avidities in developing T cells, since the level of GFP

expressed during activation correlates to the TCR signaling strength (Moran et al., 2011). The transcription factor *Nr4a1* is part of the immediate-early response after TCR activation and has been implicated in negative selection (Fassett et al., 2012). Generation of a *Tcf7*$^{-/-}$-*Nr4a1*-GFP mouse would give further insight into the relation between TCR affinities in T_{reg} cell development and TCF7.

To investigate the influence of TCF7 activation on T_{reg} cell differentiation, we activated the β-catenin/TCF7 pathway through Wnt signaling (Staal et al., 2008). By using two different Wnt activators (BIO and CHIR99021), both of them negative regulators of GSK3, we showed that β-catenin/TCF7 activation led to a decreased T_{reg} cell differentiation potential. Previous studies demonstrated that Axin-2, a direct TCF7 transcriptional target (Jho et al., 2002), was increased after treatment of T_{reg} cells with BIO, indicating that Wnt signaling pathway indeed got activated through BIO (van Loosdregt et al., 2013). The importance of the β-catenin/TCF7 activation for T cell development was previously demonstrated. Reconstitution of *Tcf7*$^{-/-}$ mice with a β-catenin interacting isoform of TCF7 restored T cell development in those mice (Ioannidis et al., 2001). Although Wnt signaling is one way that leads to TCF7 activation in the thymus, other pathways are involved. Notch signaling was shown to trigger TCF7 in early T cells precursors (Weber et al., 2011). Another report described that β-catenin/TCF7 were activated down-stream of TCR signaling (Kovalovsky et al., 2009). It is currently unclear whether Wnt, Notch or TCR signaling is more critical in facilitating the events that lead to TCF7 induction and thereby to limitation of T_{reg} cell differentiation. While there are so far no links between thymic T_{reg} cell differentiation and TCF7 signaling, controversial reports have been published about the role of TCF7 signaling in peripheral T_{reg} cells. The most recent report stated that TCF7/Wnt signaling interferes with proper function of T_{reg} cells (van Loosdregt et al., 2013). Another report described that upon stabilization of β-catenin and hence activation of TCF7, they observed increased T_{reg} cell survival (Ding et al., 2008). Stabilization of β-catenin in the thymus inhibited the DP to SP transition and predisposed to thymic lymphomas (Guo et al., 2007).

A closer look at the expression of TCF7 in T_{reg} precursors and T_{reg} cells demonstrated that the observed lower expression in T_{reg} compared to T_{conv} cells coincided with the first expression of FOXP3. These results indicated a link between *Foxp3* expression and down regulation of *Tcf7*. To test this hypothesis we retrovirally over-expressed *Foxp3* in isolated T cells *in vitro*, which resulted in decreased

expression levels of *Tcf7*, suggesting an influence of FOXP3 on *Tcf7* expression. How FOXP3 influences *Tcf7* expression is still unclear. Direct interaction between FOXP3 and TCF7 was previously demonstrated on the protein level (van Loosdregt et al., 2013). Controversially, another report that performed proteomics to look at FOXP3 interaction partners did not detect TCF7 as one of the partners (Rudra et al., 2012). Interestingly, the same report cross compared GATA3 and FOXP3 ChiP-sequencing data sets and identified *Tcf7* as a possibly co-regulated target (Rudra et al., 2012).

For normal thymocyte development, apoptosis is a crucial process. Negative selection depends on apoptosis regulated by pro-and anti-apoptotic members of the BCL-2 family. Upon death signaling, anti-apoptotic BCL-2 is inhibited by the pro-apoptotic BIM which triggers the mitochondrial apoptosis pathway (Strasser, 2005). TCF7 was previously linked to the regulation of BCL-2. Previous studies reported that TCF7 reduced the level of BCL-2 in DP cells after selection (Kovalovsky et al., 2009). Moreover, *Tcf7*$^{-/-}$ DP cells were rescued from apoptosis by transgenic expression of BCL-2 (Ioannidis et al., 2001). Our analysis of BCL-2 expression in early and late T_{reg} precursors of *Tcf7*$^{-/-}$ mice detected higher levels of BCL-2 in both precursors. The increased levels of BCL-2 in the *Tcf7*$^{-/-}$ precursors might enhance their survival and thereby account for the higher frequency of FOXP3^{+} cells among the DP and CD4SP thymocytes.

While we currently do not know the exact mechanism behind how TCF7 limits the access to the T_{reg} cell lineage we revealed many aspects of this process. Our results suggest that TCF7 modulates TCR signals and thereby shapes the T_{reg} cell TCR repertoire towards higher affinity clones. In addition, TCF7 seems to negatively influence T_{reg} precursor expansion and survival through the reduction of BCL-2 levels. In line with this, T_{reg} cell differentiation capacity was reduced by the activation of the β-catenin/TCF7 pathway. Interestingly, forced expression of FOXP3 facilitated the reduction of *Tcf7* levels and thus may induce a survival advantage in committed T_{reg} cells. The next step for future research in this field would now be to identify the molecular mechanisms that underlie this process.

8.6 TCF7 and its effects on peripheral T cells

After in detail analysis of the T_{reg} cell generation under *Tcf7*-deficient conditions we were interested in investigating the function of *Tcf7*$^{-/-}$ peripheral T_{conv} and T_{reg} cells. To this end, we analyzed the iT_{reg} and T_H17 cell *in vitro* generation potential of *Tcf7*$^{-/-}$ cells, characterized the marker expression patterns of *Tcf7*$^{-/-}$ T_{conv} and T_{reg} cells, and looked at the specialized T cell lineage subset of NK T cells.

Although the role of TCF7 in the function of peripheral T_{conv} and T_{reg} cells was so far not subject to extensive research, there are some reports about the role of TCF7 in those cells. The first description of the *Tcf7*-deficient mouse did mainly focus on the thymic defects, but mentioned that T cell numbers in the LNs and spleen of *Tcf7*$^{-/-}$ mice were slightly reduced, however animals showed no sign of autoimmune disease (Verbeek et al., 1995). One previous report stated that TCF7 associated with FOXP3 in T_{reg} cells and that activation of β-catenin/TCF7 through Wnt signaling impaired FOXP3 transcriptional activity and suppressive function (van Loosdregt et al., 2013). In contrast, stabilization of β-catenin, the interaction partner of TCF7 in Wnt signaling, was described to extend the survival of T_{reg} cells (Ding et al., 2008). For $CD8^+$ effector T cells, a previous report demonstrated that TCF7 was needed for proliferation and transition to the central memory phenotype (Zhou et al., 2010). TCF7 was shown to be a critical suppressor of the IL-17 gene locus which resulted in increased gene expression in *Tcf7*$^{-/-}$ cells (Ma et al., 2011; Yu et al., 2011). TCF7 was also associated with the initiation of T_H2 cell fate through the induction of GATA-3 expression and suppression of IFNγ (Yu et al., 2009).

Since we observed such a profound impact of *Tcf7* deficiency on the differentiation of T_{reg} cells in thymus, we got interested in the iT_{reg} cell generation capacity of peripheral T cells (Chen et al., 2003). Surprisingly, we detected no difference in the iT_{reg} cell generation capacity of *Tcf7*$^{-/-}$ compared to *Tcf7*$^{+/+}$ T cells over a broad range of different TGFβ concentrations. These results show that the tT_{reg} cell generation advantage observed in the *Tcf7*$^{-/-}$ thymus does not apply to the periphery, indicating that TCF7 is not involved in the process of iT_{reg} cell generation. iT_{reg} and tT_{reg} cells are in general quite distinct subsets, which is reflected in their different gene expression profiles and in the requirements needed for their generation (Feuerer et al., 2010; Horwitz et al., 2008).

In line with previous results (Ma et al., 2011; Yu et al., 2011), the induction of IL-17 under *Tcf7*$^{-/-}$ conditions was greatly favored in our *in vitro* assay. Interestingly, we also detected the generation of an IL-17^{+} and FOXP3^{+} double-positive subset in the absence of TCF7 and it is possible that those cells are an artifact of the *in vitro* cell culture conditions. However, such FOXP3^{+}IL-17^{+} cells have been previously described as suppressive peripherally derived subset of T_{reg} cells that might play a role in the control of anti-microbial inflammation (Voo et al., 2009). Closer analysis of the phenomenon might lead to a better understanding of the T_{reg} T_H17 cell balance. The kinase ITK is in part involved in controlling the balance between T_H17 and T_{reg} cells (Gomez-Rodriguez et al., 2014). ITK is also one of the proteins found in the TCF7/LEF1 co-regulated cluster described previously (Mingueneau et al., 2013). This observation raises the possibility that ITK functions differently in the absence of regulation through TCF7, which might result in a disturbed balance between T_H17 and T_{reg} cells. Therefore, it would be interesting to examine if ITK expression is changed under TCF7-deficient conditions.

For a better characterization of peripheral T_{conv} and T_{reg} cells under *Tcf7*$^{-/-}$ conditions, we compared the expression of different markers between *Tcf7*$^{-/-}$ and *Tcf7*$^{+/+}$ cells. CD86 and CD103 were detected as over-represented on both *Tcf7*$^{-/-}$ T_{conv} and T_{reg} cells, while HELIOS was detected as under-represented in both cell types. The fact that all 3 of them were influenced in the same way by the absence of TCF7 indicates that TCF7 might be directly or indirectly involved in their regulation. CD86, the ligand for CD28 and CTLA-4, is mainly expressed on APCs, but there are also reports that state the expression of functional CD86 on effector memory T cells (Carreno and Collins, 2002; Jeannin et al., 1999). Our MS analysis detected CD86 as over-represented on T_{reg} cells. However, this is not the first such finding since CD86 is also over-represented in T_{reg} cells on the level of mRNA expression, as detected by the ImmGen consortium (Heng and Painter, 2008). Apparently, the frequency of cells with an effector memory phenotype among both T_{conv} and T_{reg} cells is increased in the absence of TCF7. Interestingly, we detected an increased proportion of integrin CD103 expressing *Tcf7*$^{-/-}$ T_{conv} and T_{reg} cells. This marker was previously described as expressed on cells at mucosal sites and as a marker for potent epithelial T_{reg} cells (Annacker et al., 2005; Lehmann et al., 2002). Whether the greatly elevated frequencies of CD103^{+} T_{reg} and T_{conv} cells are due to increased proliferation of the CD103^{+} population or to a shift of the whole T cell population towards expression of

CD103 is not clear. HELIOS, the transcription factor and marker of tT_{reg} cells was significantly under-represented in *Tcf7*$^{-/-}$ T_{conv} and T_{reg} cells (Thornton et al., 2010). For T_{reg} cells this could indicate that, in the periphery of *Tcf7*$^{-/-}$ mice a smaller fraction of FOXP3^{+} T_{reg} cells is thymus derived. It is quite possible that due to the lower output of cells from the thymus of those mice, peripheral T cells show a higher proliferation rate. Controversially, we did not detect a higher rate of proliferating Ki67^{+} cells in *Tcf7*$^{-/-}$ mice. HELIOS was only expressed by a small percentage of T_{conv} cells and a function for HELIOS in these cells is so far not known.

In addition to the changes described above, we detected among T_{conv} cells from *Tcf7*$^{-/-}$ mice a lower fraction of activated cells, characterized by the expression of CD69 (Bjorndahl et al., 1988), indicating that the T_{conv} cells from *Tcf7*-deficient mice show a less activated phenotype.

For T_{reg} cells, our screen detected several changes in marker expression between the *Tcf7*$^{-/-}$ and *Tcf7*$^{+/+}$ mice. The transmembrane glycoprotein CD44 is a marker of activation and memory in T cells (Dutton et al., 1998). T_{reg} cells from *Tcf7*-deficient animals showed a slightly more memory-like phenotype, as determined by expression of CD44. The ectoenzyme CD39 is one of the mediators of T_{reg} cell suppressive function (Borsellino et al., 2007; Deaglio et al., 2007). Hence, a higher frequency of CD39^{+} T_{reg} cells in *Tcf7*$^{-/-}$ mice indicates an enhanced suppressive capacity of the T_{reg} cells. In contrast, another mediator of T_{reg} cell suppressive function, the surface receptor GARP, was detected on a lower frequency of T_{reg} cells in the *Tcf7*-deficient mice (Probst-Kepper and Buer, 2010). The T cell co-stimulatory molecule CTLA-4 is also an essential molecule for T_{reg} cell suppressive function (Rudd et al., 2009; Wing et al., 2008). Around 80 percent of T_{reg} cells are CTLA-4^{+}. We detected a higher frequency of Foxp3^{+} CTLA-4^{-} T_{reg} cells in Tcf7$^{-/-}$ compared to Tcf7$^{+/+}$ mice, indicating that the mechanism of CTLA-4-mediated suppression is used to a lesser extend in the T_{reg} cell population.

Besides FOXP3, the IL-2 receptor molecule CD25 is one of the hallmarks that characterize murine T_{reg} cells (Fontenot et al., 2003; Hori et al., 2003; Khattri et al., 2003). Our analysis detected an increased CD4^{+} CD25^{-}FOXP3^{+} T_{reg} cell population from thymus, LN and spleen. For FACS purification, FOXP3 staining cannot be applied and differentiation between T_{conv} and T_{reg} cells has to rely on CD25 staining. This is usually not a problem, the contamination rate of Foxp3^{+} cells in the T_{conv} population stays typically below 2 percent. In the case of *Tcf7*$^{-/-}$ T_{conv} cell sorting, a

contamination rate of about 5 percent would be realistic. To avoid the problem, we used a Foxp3-YFP mouse for sorting experiments. $CD25^{-}FOXP3^{+}$ T_{reg} cell had suppressive function and showed elevated levels of CD103 expression (Nishioka et al., 2006). Interestingly, we also observed elevated frequencies of $CD103^{+}$ *Tcf7*$^{-/-}$ T_{reg} cells. Together these results indicate that the *Tcf7*$^{-/-}$ T_{reg} cells had a more aged phenotype compared to the *Tcf7*$^{+/+}$. In addition, studies in humans reported that increased numbers of $CD25^{-}FOXP3^{+}$ T cells were associated with the autoimmune disease systemic lupus erythematosus (SLE) (Horwitz, 2010). In contrast to these studies, it was so far not described that *Tcf7*-deficient mice endogenously develop autoimmune disease. However, one report states that *Tcf7*$^{-/-}$ mice are more prone to the induction of autoimmune encephalomyelitis (Yu et al., 2011).

NKT cells, which form a link between the innate and the adaptive immune system, carry an αβ-TCR that recognizes lipids presented by the MHC class I-like molecule CD1d (Bendelac et al., 2007). Detection of NKT cells in the thymus and spleen of *Tcf7*$^{-/-}$ mice revealed that the numbers of NKT cells in the thymus were greatly reduced and NKT cells were almost absent in the spleen. These results indicated that TCF7 is of particular importance for the survival of NKT cells. The consequences of the observed NKT cell deficiency are currently unclear. In the past, deficiency of NKT has been linked to different autoimmune conditions, especially Diabetes type I in NOD mice, but so far this is still controversial and hard evidence is missing (Bendelac et al., 2007). However, the NKT cell deficiency might represent a link to the result that *Tcf7*$^{-/-}$ mice are more susceptible to the induction of autoimmune disease (Yu et al., 2011). Also, the finding that TCF7 seems to be of great importance for the survival of NKT cells might in the future help to better understand their development.

Analysis of the role of TCF7 in the periphery led to some intriguing findings. First, we noticed that *Tcf7* deficiency does not influence iT_{reg} cell generation *in vitro* and concluded that different mechanisms are involved in tT_{reg} versus iT_{reg} cell generation. Second, we described a $FOXP3^{+}IL\text{-}17^{+}$ cell that was generated *in vitro* under *Tcf7*$^{-/-}$ conditions only. Third, we detected changed phenotypes of T_{conv} and T_{reg} cells in *Tcf7*-deficient mice. For T_{conv} cells we observed a less activated but more effector memory like phenotype. T_{reg} cells from *Tcf7*$^{-/-}$ mice might be to a lesser extend thymus derived and had a more (effector) memory like phenotype. In addition, we observed changes in the expression of T_{reg} cell markers needed for their suppressive activity. As *Tcf7*$^{-/-}$ T_{reg} cells were described to have enhanced suppressive function

(van Loosdregt et al., 2013), these changes might explain how this is regulated. Some observed changes pointed toward a T_{reg} cell phenotype found in aged mice. Last, we described the deficiency of NKT cells in *Tcf7*$^{-/-}$ mice. In conclusion, we described a broad spectrum of changes in cells of the T cell lineage that are all linked to *Tcf7* deficiency. On the other hand, it cannot be excluded that the observed changes are caused by peripheral homeostatic expansion due to reduced T cell output from the thymus.

8.7 Conclusions and perspectives

The results of this thesis now demonstrate the involvement of the transcription factor TCF7 in the process of thymic T_{reg} cell differentiation. In addition, this thesis increases our knowledge about the effects of TCF7 on peripheral T_{reg} cells and other members of the T cell lineage.

TCF7 was identified as a promising candidate for the regulation of T_{reg} cell generation based on our differential quantitative study of the T_{reg} and T_{conv} cell proteome and comparative analysis to gene expression data. The proteomics data set itself, with its 5225 identified proteins, will be an important source for future studies in the field. Analysis demonstrated that TCF7 suppressed T_{reg} cell generation at the CD4SP and DP stage. To our surprise, we observed that absence of TCF7 led to TCR independent premature expression of FOXP3 at the DN stage. It was further demonstrated that reduced levels of TCF7 elevated frequencies of T_{reg} cells and precursors and led to increased differentiation potential of these precursors after TCR stimulation. In line with this data, activation of TCF7/β-catenin signaling had an inhibitory effect on the differentiation of T_{reg} precursors. Finally it was shown that TCF7 reduced BCL-2 levels in T_{reg} precursors and that expression of *Foxp3* decreased *Tcf7* levels.

Based our results we now propose a model in which TCF7 limits the generation of T_{reg} cells in the thymus (Figure 44).

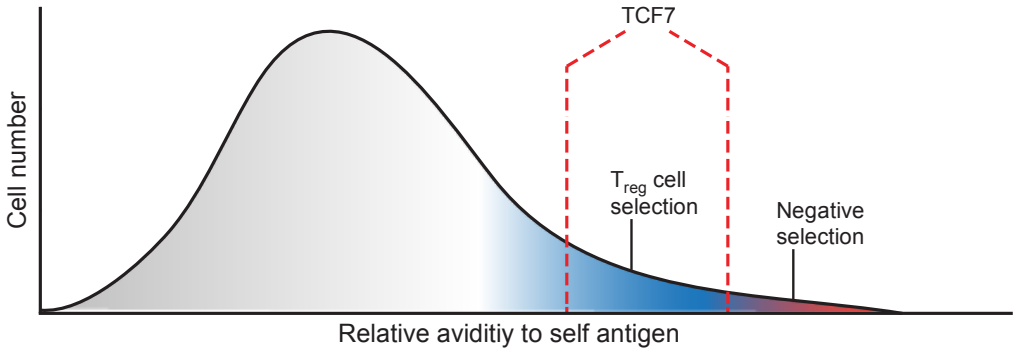

Figure 44: Model of T_{reg} selection in the thymus. The model of T_{reg} cell selection in the thymus shows the relationship between the relative avidity to self-antigen (x-axis) and the number of cells (y-axis). Areas of T_{reg} cell selection and negative selection are shown in blue and red, respectively. The red dotted line marks the area where T_{reg} cell selection is restricted by TCF7.

We suggest that TCF7 might restrict the access to the T_{reg} lineage through modulation of the TCR signals which shapes the TCR repertoire toward higher affinity clones and through the reduction of BCL-2 levels in T_{reg} precursors. Once expressed FOXP3 seems to inhibit *Tcf7* expression. This study establishes for the first time the role of TCF7 in T_{reg} cell differentiation and additional work is needed to elucidate the molecular mechanisms behind this process.

Furthermore, we studied the influence of TCF7 on different peripheral T cell subsets. Analysis of iT_{reg} generation showed that, in contrast to tT_{reg} generation, this process was not influenced by TCF7. T_H17 generation by *Tcf7*$^{-/-}$ T cells on the other hand was enhanced and also resulted in the development of $IL17^+Foxp3^+$ cells. Expression pattern analysis of T_{conv} and T_{reg} cells showed that TCF7 deficiency changed the phenotype of these cells. Additionally, we noticed that the absence of TCF7 led to NKT cell deficiency. These results extend our knowledge about the influence of TCF7 on peripheral T cell subsets.

9 References

Akira, S., Uematsu, S., and Takeuchi, O. (2006). Pathogen recognition and innate immunity. Cell *124*, 783-801.

Andersson, J., Tran, D.Q., Pesu, M., Davidson, T.S., Ramsey, H., O'Shea, J.J., and Shevach, E.M. (2008). CD4+ FoxP3+ regulatory T cells confer infectious tolerance in a TGF-beta-dependent manner. The Journal of experimental medicine *205*, 1975-1981.

Annacker, O., Coombes, J.L., Malmstrom, V., Uhlig, H.H., Bourne, T., Johansson-Lindbom, B., Agace, W.W., Parker, C.M., and Powrie, F. (2005). Essential role for CD103 in the T cell-mediated regulation of experimental colitis. The Journal of experimental medicine *202*, 1051-1061.

Apostolou, I., Sarukhan, A., Klein, L., and von Boehmer, H. (2002). Origin of regulatory T cells with known specificity for antigen. Nature immunology *3*, 756-763.

Asano, M., Toda, M., Sakaguchi, N., and Sakaguchi, S. (1996). Autoimmune disease as a consequence of developmental abnormality of a T cell subpopulation. The Journal of experimental medicine *184*, 387-396.

Azzam, H.S., Grinberg, A., Lui, K., Shen, H., Shores, E.W., and Love, P.E. (1998). CD5 expression is developmentally regulated by T cell receptor (TCR) signals and TCR avidity. The Journal of experimental medicine *188*, 2301-2311.

Bautista, J.L., Lio, C.W., Lathrop, S.K., Forbush, K., Liang, Y., Luo, J., Rudensky, A.Y., and Hsieh, C.S. (2009). Intraclonal competition limits the fate determination of regulatory T cells in the thymus. Nature immunology *10*, 610-617.

Bendelac, A., Savage, P.B., and Teyton, L. (2007). The biology of NKT cells. Annual review of immunology *25*, 297-336.

Bennett, C.L., Christie, J., Ramsdell, F., Brunkow, M.E., Ferguson, P.J., Whitesell, L., Kelly, T.E., Saulsbury, F.T., Chance, P.F., and Ochs, H.D. (2001). The immune dysregulation, polyendocrinopathy, enteropathy, X-linked syndrome (IPEX) is caused by mutations of FOXP3. Nat Genet *27*, 20-21.

Bettelli, E., Carrier, Y., Gao, W., Korn, T., Strom, T.B., Oukka, M., Weiner, H.L., and Kuchroo, V.K. (2006). Reciprocal developmental pathways for the generation of pathogenic effector TH17 and regulatory T cells. Nature *441*, 235-238.

Beyer, M., Thabet, Y., Muller, R.U., Sadlon, T., Classen, S., Lahl, K., Basu, S., Zhou, X., Bailey-Bucktrout, S.L., Krebs, W.*, et al.* (2011). Repression of the genome organizer SATB1 in regulatory T cells is required for suppressive function and inhibition of effector differentiation. Nature immunology *12*, 898-907.

Beyersdorf, N., Ding, X., Tietze, J.K., and Hanke, T. (2007). Characterization of mouse CD4 T cell subsets defined by expression of KLRG1. European journal of immunology *37*, 3445-3454.

Bjorndahl, J.M., Nakamura, S., Hara, T., Jung, L.K., and Fu, S.M. (1988). The 28-kDa/32-kDa activation antigen EA 1. Further characterization and signal requirements for its expression. J Immunol *141*, 4094-4100.

Boersema, P.J., Raijmakers, R., Lemeer, S., Mohammed, S., and Heck, A.J. (2009). Multiplex peptide stable isotope dimethyl labeling for quantitative proteomics. Nat Protoc *4*, 484-494.

Bopp, T., Becker, C., Klein, M., Klein-Hessling, S., Palmetshofer, A., Serfling, E., Heib, V., Becker, M., Kubach, J., Schmitt, S.*, et al.* (2007). Cyclic adenosine monophosphate is a key component of regulatory T cell-mediated suppression. The Journal of experimental medicine *204*, 1303-1310.

Borsellino, G., Kleinewietfeld, M., Di Mitri, D., Sternjak, A., Diamantini, A., Giometto, R., Hopner, S., Centonze, D., Bernardi, G., Dell'Acqua, M.L*., et al.* (2007). Expression of ectonucleotidase CD39 by Foxp3+ Treg cells: hydrolysis of extracellular ATP and immune suppression. Blood *110*, 1225-1232.

Brunkow, M.E., Jeffery, E.W., Hjerrild, K.A., Paeper, B., Clark, L.B., Yasayko, S.A., Wilkinson, J.E., Galas, D., Ziegler, S.F., and Ramsdell, F. (2001). Disruption of a new forkhead/winged-helix protein, scurfin, results in the fatal lymphoproliferative disorder of the scurfy mouse. Nat Genet *27*, 68-73.

Campbell, D.J., and Koch, M.A. (2011). Phenotypical and functional specialization of FOXP3+ regulatory T cells. Nature reviews Immunology *11*, 119-130.

Carreno, B.M., and Collins, M. (2002). The B7 family of ligands and its receptors: new pathways for costimulation and inhibition of immune responses. Annual review of immunology *20*, 29-53.

Ceredig, R., and Rolink, T. (2002). A positive look at double-negative thymocytes. Nature reviews Immunology *2*, 888-897.

Chang, X., Gao, J.X., Jiang, Q., Wen, J., Seifers, N., Su, L., Godfrey, V.L., Zuo, T., Zheng, P., and Liu, Y. (2005). The Scurfy mutation of FoxP3 in the thymus stroma leads to defective thymopoiesis. The Journal of experimental medicine *202*, 1141-1151.

Chaudhry, A., Rudra, D., Treuting, P., Samstein, R.M., Liang, Y., Kas, A., and Rudensky, A.Y. (2009). CD4+ regulatory T cells control TH17 responses in a Stat3-dependent manner. Science (New York, NY) *326*, 986-991.

Chen, G.Y., Chen, C., Wang, L., Chang, X., Zheng, P., and Liu, Y. (2008). Cutting edge: Broad expression of the FoxP3 locus in epithelial cells: a caution against early interpretation of fatal inflammatory diseases following in vivo depletion of FoxP3-expressing cells. J Immunol *180*, 5163-5166.

Chen, W., Jin, W., Hardegen, N., Lei, K.J., Li, L., Marinos, N., McGrady, G., and Wahl, S.M. (2003). Conversion of peripheral CD4+CD25- naive T cells to CD4+CD25+ regulatory T cells by TGF-beta induction of transcription factor Foxp3. The Journal of experimental medicine *198*, 1875-1886.

Collison, L.W., Workman, C.J., Kuo, T.T., Boyd, K., Wang, Y., Vignali, K.M., Cross, R., Sehy, D., Blumberg, R.S., and Vignali, D.A. (2007). The inhibitory cytokine IL-35 contributes to regulatory T-cell function. Nature *450*, 566-569.

Cox, J., and Mann, M. (2008). MaxQuant enables high peptide identification rates, individualized p.p.b.-range mass accuracies and proteome-wide protein quantification. Nat Biotechnol *26*, 1367-1372.

Cozzo Picca, C., Simons, D.M., Oh, S., Aitken, M., Perng, O.A., Mergenthaler, C., Kropf, E., Erikson, J., and Caton, A.J. (2011). CD4(+)CD25(+)Foxp3(+) regulatory T cell formation requires more specific recognition of a self-peptide than thymocyte deletion. Proceedings of the National Academy of Sciences of the United States of America *108*, 14890-14895.

Deaglio, S., Dwyer, K.M., Gao, W., Friedman, D., Usheva, A., Erat, A., Chen, J.F., Enjyoji, K., Linden, J., Oukka, M*., et al.* (2007). Adenosine generation catalyzed by CD39 and CD73 expressed on regulatory T cells mediates immune suppression. The Journal of experimental medicine *204*, 1257-1265.

Delacher, M., Schreiber, L., Richards, D.M., Farah, C., Feuerer, M., and Huehn, J. (2014). Transcriptional Control of Regulatory T cells. Curr Top Microbiol Immunol.

Ding, Y., Shen, S., Lino, A.C., Curotto de Lafaille, M.A., and Lafaille, J.J. (2008). Beta-catenin stabilization extends regulatory T cell survival and induces anergy in nonregulatory T cells. Nat Med *14*, 162-169.

Duarte, J.H., Zelenay, S., Bergman, M.L., Martins, A.C., and Demengeot, J. (2009). Natural Treg cells spontaneously differentiate into pathogenic helper cells in lymphopenic conditions. European journal of immunology *39*, 948-955.

Dutton, R.W., Bradley, L.M., and Swain, S.L. (1998). T cell memory. Annual review of immunology *16*, 201-223.

Ehrenstein, M.R., Evans, J.G., Singh, A., Moore, S., Warnes, G., Isenberg, D.A., and Mauri, C. (2004). Compromised function of regulatory T cells in rheumatoid arthritis and reversal by anti-TNFalpha therapy. The Journal of experimental medicine *200*, 277-285.

Fassett, M.S., Jiang, W., D'Alise, A.M., Mathis, D., and Benoist, C. (2012). Nuclear receptor Nr4a1 modulates both regulatory T-cell (Treg) differentiation and clonal deletion. Proceedings of the National Academy of Sciences of the United States of America *109*, 3891-3896.

Feng, C., Woodside, K.J., Vance, B.A., El-Khoury, D., Canelles, M., Lee, J., Gress, R., Fowlkes, B.J., Shores, E.W., and Love, P.E. (2002). A potential role for CD69 in thymocyte emigration. International immunology *14*, 535-544.

Feuerer, M., Hill, J.A., Kretschmer, K., von Boehmer, H., Mathis, D., and Benoist, C. (2010). Genomic definition of multiple ex vivo regulatory T cell subphenotypes. Proceedings of the National Academy of Sciences of the United States of America *107*, 5919-5924.

Feuerer, M., Hill, J.A., Mathis, D., and Benoist, C. (2009). Foxp3+ regulatory T cells: differentiation, specification, subphenotypes. Nature immunology *10*, 689-695.

Fontenot, J.D., Dooley, J.L., Farr, A.G., and Rudensky, A.Y. (2005a). Developmental regulation of Foxp3 expression during ontogeny. The Journal of experimental medicine *202*, 901-906.

Fontenot, J.D., Gavin, M.A., and Rudensky, A.Y. (2003). Foxp3 programs the development and function of CD4+CD25+ regulatory T cells. Nature immunology *4*, 330-336.

Fontenot, J.D., Rasmussen, J.P., Williams, L.M., Dooley, J.L., Farr, A.G., and Rudensky, A.Y. (2005b). Regulatory T cell lineage specification by the forkhead transcription factor foxp3. Immunity *22*, 329-341.

Fu, G., Casas, J., Rigaud, S., Rybakin, V., Lambolez, F., Brzostek, J., Hoerter, J.A., Paster, W., Acuto, O., Cheroutre, H.*, et al.* (2013). Themis sets the signal threshold for positive and negative selection in T-cell development. Nature *504*, 441-445.

Fu, W., Ergun, A., Lu, T., Hill, J.A., Haxhinasto, S., Fassett, M.S., Gazit, R., Adoro, S., Glimcher, L., Chan, S.*, et al.* (2012). A multiply redundant genetic switch 'locks in' the transcriptional signature of regulatory T cells. Nature immunology *13*, 972-980.

Ganz, T. (2003). The role of antimicrobial peptides in innate immunity. Integr Comp Biol *43*, 300-304.

Gavin, M.A., Rasmussen, J.P., Fontenot, J.D., Vasta, V., Manganiello, V.C., Beavo, J.A., and Rudensky, A.Y. (2007). Foxp3-dependent programme of regulatory T-cell differentiation. Nature *445*, 771-775.

Gentleman, R.C., Carey, V.J., Bates, D.M., Bolstad, B., Dettling, M., Dudoit, S., Ellis, B., Gautier, L., Ge, Y., Gentry, J.*, et al.* (2004). Bioconductor: open software development for computational biology and bioinformatics. Genome Biol *5*, R80.

Godfrey, D.I., Kennedy, J., Suda, T., and Zlotnik, A. (1993). A developmental pathway involving four phenotypically and functionally distinct subsets of CD3-CD4-CD8- triple-negative adult mouse thymocytes defined by CD44 and CD25 expression. J Immunol *150*, 4244-4252.

Gomez-Rodriguez, J., Wohlfert, E.A., Handon, R., Meylan, F., Wu, J.Z., Anderson, S.M., Kirby, M.R., Belkaid, Y., and Schwartzberg, P.L. (2014). Itk-mediated integration of T cell receptor and cytokine

signaling regulates the balance between Th17 and regulatory T cells. The Journal of experimental medicine *211*, 529-543.

Gondek, D.C., Lu, L.F., Quezada, S.A., Sakaguchi, S., and Noelle, R.J. (2005). Cutting edge: contact-mediated suppression by CD4+CD25+ regulatory cells involves a granzyme B-dependent, perforin-independent mechanism. J Immunol *174*, 1783-1786.

Grossman, W.J., Verbsky, J.W., Tollefsen, B.L., Kemper, C., Atkinson, J.P., and Ley, T.J. (2004). Differential expression of granzymes A and B in human cytotoxic lymphocyte subsets and T regulatory cells. Blood *104*, 2840-2848.

Grubin, C.E., Kovats, S., deRoos, P., and Rudensky, A.Y. (1997). Deficient positive selection of CD4 T cells in mice displaying altered repertoires of MHC class II-bound self-peptides. Immunity *7*, 197-208.

Guo, Z., Dose, M., Kovalovsky, D., Chang, R., O'Neil, J., Look, A.T., von Boehmer, H., Khazaie, K., and Gounari, F. (2007). Beta-catenin stabilization stalls the transition from double-positive to single-positive stage and predisposes thymocytes to malignant transformation. Blood *109*, 5463-5472.

Haxhinasto, S., Mathis, D., and Benoist, C. (2008). The AKT-mTOR axis regulates de novo differentiation of CD4+Foxp3+ cells. The Journal of experimental medicine *205*, 565-574.

Held, W., Clevers, H., and Grosschedl, R. (2003). Redundant functions of TCF-1 and LEF-1 during T and NK cell development, but unique role of TCF-1 for Ly49 NK cell receptor acquisition. European journal of immunology *33*, 1393-1398.

Heng, T.S., and Painter, M.W. (2008). The Immunological Genome Project: networks of gene expression in immune cells. Nature immunology *9*, 1091-1094.

Hill, J.A., Feuerer, M., Tash, K., Haxhinasto, S., Perez, J., Melamed, R., Mathis, D., and Benoist, C. (2007). Foxp3 transcription-factor-dependent and -independent regulation of the regulatory T cell transcriptional signature. Immunity *27*, 786-800.

Hogquist, K.A. (2001). Signal strength in thymic selection and lineage commitment. Current opinion in immunology *13*, 225-231.

Hori, S. (2011). Stability of regulatory T-cell lineage. Adv Immunol *112*, 1-24.

Hori, S., Nomura, T., and Sakaguchi, S. (2003). Control of regulatory T cell development by the transcription factor Foxp3. Science (New York, NY) *299*, 1057-1061.

Horwitz, D.A. (2010). Identity of mysterious CD4+CD25-Foxp3+ cells in SLE. Arthritis research & therapy *12*, 101.

Horwitz, D.A., Zheng, S.G., and Gray, J.D. (2008). Natural and TGF-beta-induced Foxp3(+)CD4(+) CD25(+) regulatory T cells are not mirror images of each other. Trends Immunol *29*, 429-435.

Hsieh, C.S., Lee, H.M., and Lio, C.W. (2012). Selection of regulatory T cells in the thymus. Nature reviews Immunology *12*, 157-167.

Hsieh, C.S., Liang, Y., Tyznik, A.J., Self, S.G., Liggitt, D., and Rudensky, A.Y. (2004). Recognition of the peripheral self by naturally arising CD25+ CD4+ T cell receptors. Immunity *21*, 267-277.

Ikawa, T., Hirose, S., Masuda, K., Kakugawa, K., Satoh, R., Shibano-Satoh, A., Kominami, R., Katsura, Y., and Kawamoto, H. (2010). An essential developmental checkpoint for production of the T cell lineage. Science (New York, NY) *329*, 93-96.

Ioannidis, V., Beermann, F., Clevers, H., and Held, W. (2001). The beta-catenin--TCF-1 pathway ensures CD4(+)CD8(+) thymocyte survival. Nature immunology *2*, 691-697.

Itoh, M., Takahashi, T., Sakaguchi, N., Kuniyasu, Y., Shimizu, J., Otsuka, F., and Sakaguchi, S. (1999). Thymus and autoimmunity: production of CD25+CD4+ naturally anergic and suppressive T

cells as a key function of the thymus in maintaining immunologic self-tolerance. J Immunol *162*, 5317-5326.

Jeannin, P., Herbault, N., Delneste, Y., Magistrelli, G., Lecoanet-Henchoz, S., Caron, G., Aubry, J.P., and Bonnefoy, J.Y. (1999). Human effector memory T cells express CD86: a functional role in naive T cell priming. J Immunol *162*, 2044-2048.

Jenkins, M.R., and Griffiths, G.M. (2010). The synapse and cytolytic machinery of cytotoxic T cells. Current opinion in immunology *22*, 308-313.

Jensen, L.J., Kuhn, M., Stark, M., Chaffron, S., Creevey, C., Muller, J., Doerks, T., Julien, P., Roth, A., Simonovic, M*., et al.* (2009). STRING 8--a global view on proteins and their functional interactions in 630 organisms. Nucleic Acids Res *37*, D412-416.

Jho, E.H., Zhang, T., Domon, C., Joo, C.K., Freund, J.N., and Costantini, F. (2002). Wnt/beta-catenin/Tcf signaling induces the transcription of Axin2, a negative regulator of the signaling pathway. Molecular and cellular biology *22*, 1172-1183.

Jordan, M.S., Boesteanu, A., Reed, A.J., Petrone, A.L., Holenbeck, A.E., Lerman, M.A., Naji, A., and Caton, A.J. (2001). Thymic selection of CD4+CD25+ regulatory T cells induced by an agonist self-peptide. Nature immunology *2*, 301-306.

Josefowicz, S.Z., Niec, R.E., Kim, H.Y., Treuting, P., Chinen, T., Zheng, Y., Umetsu, D.T., and Rudensky, A.Y. (2012). Extrathymically generated regulatory T cells control mucosal TH2 inflammation. Nature *482*, 395-399.

Kawano, T., Cui, J., Koezuka, Y., Toura, I., Kaneko, Y., Motoki, K., Ueno, H., Nakagawa, R., Sato, H., Kondo, E*., et al.* (1997). CD1d-restricted and TCR-mediated activation of valpha14 NKT cells by glycosylceramides. Science (New York, NY) *278*, 1626-1629.

Khattri, R., Cox, T., Yasayko, S.A., and Ramsdell, F. (2003). An essential role for Scurfin in CD4+CD25+ T regulatory cells. Nature immunology *4*, 337-342.

Killebrew, J.R., Perdue, N., Kwan, A., Thornton, A.M., Shevach, E.M., and Campbell, D.J. (2011). A self-reactive TCR drives the development of Foxp3+ regulatory T cells that prevent autoimmune disease. J Immunol *187*, 861-869.

Kim, J.M., Rasmussen, J.P., and Rudensky, A.Y. (2007). Regulatory T cells prevent catastrophic autoimmunity throughout the lifespan of mice. Nature immunology *8*, 191-197.

Klein, L., Kyewski, B., Allen, P.M., and Hogquist, K.A. (2014). Positive and negative selection of the T cell repertoire: what thymocytes see (and don't see). Nature reviews Immunology *14*, 377-391.

Klenerman, P., Cerundolo, V., and Dunbar, P.R. (2002). Tracking T cells with tetramers: new tales from new tools. Nature reviews Immunology *2*, 263-272.

Knoechel, B., Lohr, J., Kahn, E., Bluestone, J.A., and Abbas, A.K. (2005). Sequential development of interleukin 2-dependent effector and regulatory T cells in response to endogenous systemic antigen. The Journal of experimental medicine *202*, 1375-1386.

Koch, M.A., Tucker-Heard, G., Perdue, N.R., Killebrew, J.R., Urdahl, K.B., and Campbell, D.J. (2009). The transcription factor T-bet controls regulatory T cell homeostasis and function during type 1 inflammation. Nature immunology *10*, 595-602.

Komatsu, N., Mariotti-Ferrandiz, M.E., Wang, Y., Malissen, B., Waldmann, H., and Hori, S. (2009). Heterogeneity of natural Foxp3+ T cells: a committed regulatory T-cell lineage and an uncommitted minor population retaining plasticity. Proceedings of the National Academy of Sciences of the United States of America *106*, 1903-1908.

Konig, S., Probst-Kepper, M., Reinl, T., Jeron, A., Huehn, J., Schraven, B., and Jansch, L. (2012). First insight into the kinome of human regulatory T cells. PloS one *7*, e40896.

Korn, T., Bettelli, E., Oukka, M., and Kuchroo, V.K. (2009). IL-17 and Th17 Cells. Annual review of immunology *27*, 485-517.

Kovalovsky, D., Yu, Y., Dose, M., Emmanouilidou, A., Konstantinou, T., Germar, K., Aghajani, K., Guo, Z., Mandal, M., and Gounari, F. (2009). Beta-catenin/Tcf determines the outcome of thymic selection in response to alphabetaTCR signaling. J Immunol *183*, 3873-3884.

Kubach, J., Lutter, P., Bopp, T., Stoll, S., Becker, C., Huter, E., Richter, C., Weingarten, P., Warger, T., Knop, J.*, et al.* (2007). Human CD4+CD25+ regulatory T cells: proteome analysis identifies galectin-10 as a novel marker essential for their anergy and suppressive function. Blood *110*, 1550-1558.

Lambolez, F., Arcangeli, M.L., Joret, A.M., Pasqualetto, V., Cordier, C., Di Santo, J.P., Rocha, B., and Ezine, S. (2006). The thymus exports long-lived fully committed T cell precursors that can colonize primary lymphoid organs. Nature immunology *7*, 76-82.

Lee, H.M., and Hsieh, C.S. (2009). Rare development of Foxp3+ thymocytes in the CD4+CD8+ subset. J Immunol *183*, 2261-2266.

Lehmann, J., Huehn, J., de la Rosa, M., Maszyna, F., Kretschmer, U., Krenn, V., Brunner, M., Scheffold, A., and Hamann, A. (2002). Expression of the integrin alpha Ebeta 7 identifies unique subsets of CD25+ as well as CD25- regulatory T cells. Proceedings of the National Academy of Sciences of the United States of America *99*, 13031-13036.

Leung, M.W., Shen, S., and Lafaille, J.J. (2009). TCR-dependent differentiation of thymic Foxp3+ cells is limited to small clonal sizes. The Journal of experimental medicine *206*, 2121-2130.

Li, L., Leid, M., and Rothenberg, E.V. (2010). An early T cell lineage commitment checkpoint dependent on the transcription factor Bcl11b. Science (New York, NY) *329*, 89-93.

Liang, B., Workman, C., Lee, J., Chew, C., Dale, B.M., Colonna, L., Flores, M., Li, N., Schweighoffer, E., Greenberg, S.*, et al.* (2008). Regulatory T cells inhibit dendritic cells by lymphocyte activation gene-3 engagement of MHC class II. J Immunol *180*, 5916-5926.

Lindley, S., Dayan, C.M., Bishop, A., Roep, B.O., Peakman, M., and Tree, T.I. (2005). Defective suppressor function in CD4(+)CD25(+) T-cells from patients with type 1 diabetes. Diabetes *54*, 92-99.

Lio, C.W., and Hsieh, C.S. (2008). A two-step process for thymic regulatory T cell development. Immunity *28*, 100-111.

Liston, A., Farr, A.G., Chen, Z., Benoist, C., Mathis, D., Manley, N.R., and Rudensky, A.Y. (2007). Lack of Foxp3 function and expression in the thymic epithelium. The Journal of experimental medicine *204*, 475-480.

Ma, J., Wang, R., Fang, X., Ding, Y., and Sun, Z. (2011). Critical role of TCF-1 in repression of the IL-17 gene. PloS one *6*, e24768.

Mahmud, S.A., Manlove, L.S., Schmitz, H.M., Xing, Y., Wang, Y., Owen, D.L., Schenkel, J.M., Boomer, J.S., Green, J.M., Yagita, H.*, et al.* (2014). Costimulation via the tumor-necrosis factor receptor superfamily couples TCR signal strength to the thymic differentiation of regulatory T cells. Nature immunology *15*, 473-481.

Maier, E., Hebenstreit, D., Posselt, G., Hammerl, P., Duschl, A., and Horejs-Hoeck, J. (2011). Inhibition of suppressive T cell factor 1 (TCF-1) isoforms in naive CD4+ T cells is mediated by IL-4/STAT6 signaling. J Biol Chem *286*, 919-928.

Mellor, A.L., and Munn, D.H. (2004). IDO expression by dendritic cells: tolerance and tryptophan catabolism. Nature reviews Immunology *4*, 762-774.

Mingueneau, M., Kreslavsky, T., Gray, D., Heng, T., Cruse, R., Ericson, J., Bendall, S., Spitzer, M.H., Nolan, G.P., Kobayashi, K.*, et al.* (2013). The transcriptional landscape of alphabeta T cell differentiation. Nature immunology *14*, 619-632.

Miyao, T., Floess, S., Setoguchi, R., Luche, H., Fehling, H.J., Waldmann, H., Huehn, J., and Hori, S. (2012). Plasticity of Foxp3(+) T cells reflects promiscuous Foxp3 expression in conventional T cells but not reprogramming of regulatory T cells. Immunity *36*, 262-275.

Moran, A.E., Holzapfel, K.L., Xing, Y., Cunningham, N.R., Maltzman, J.S., Punt, J., and Hogquist, K.A. (2011). T cell receptor signal strength in Treg and iNKT cell development demonstrated by a novel fluorescent reporter mouse. The Journal of experimental medicine *208*, 1279-1289.

Murphy, K., Travers, P., and Walport, M. (2008). Janeway's Immuno Biology, 7 edn (Garland Science).

Nakayama, T., Kasprowicz, D.J., Yamashita, M., Schubert, L.A., Gillard, G., Kimura, M., Didierlaurent, A., Koseki, H., and Ziegler, S.F. (2002). The generation of mature, single-positive thymocytes in vivo is dysregulated by CD69 blockade or overexpression. J Immunol *168*, 87-94.

Nishioka, T., Shimizu, J., Iida, R., Yamazaki, S., and Sakaguchi, S. (2006). CD4+CD25+Foxp3+ T cells and CD4+CD25-Foxp3+ T cells in aged mice. J Immunol *176*, 6586-6593.

Oberle, N., Eberhardt, N., Falk, C.S., Krammer, P.H., and Suri-Payer, E. (2007). Rapid suppression of cytokine transcription in human CD4+CD25 T cells by CD4+Foxp3+ regulatory T cells: independence of IL-2 consumption, TGF-beta, and various inhibitors of TCR signaling. J Immunol *179*, 3578-3587.

Oh-Hora, M., Komatsu, N., Pishyareh, M., Feske, S., Hori, S., Taniguchi, M., Rao, A., and Takayanagi, H. (2013). Agonist-selected T cell development requires strong T cell receptor signaling and store-operated calcium entry. Immunity *38*, 881-895.

Ohkura, N., Hamaguchi, M., Morikawa, H., Sugimura, K., Tanaka, A., Ito, Y., Osaki, M., Tanaka, Y., Yamashita, R., Nakano, N.*, et al.* (2012). T cell receptor stimulation-induced epigenetic changes and Foxp3 expression are independent and complementary events required for Treg cell development. Immunity *37*, 785-799.

Okamura, R.M., Sigvardsson, M., Galceran, J., Verbeek, S., Clevers, H., and Grosschedl, R. (1998). Redundant regulation of T cell differentiation and TCRalpha gene expression by the transcription factors LEF-1 and TCF-1. Immunity *8*, 11-20.

Pacholczyk, R., Ignatowicz, H., Kraj, P., and Ignatowicz, L. (2006). Origin and T cell receptor diversity of Foxp3+CD4+CD25+ T cells. Immunity *25*, 249-259.

Pacholczyk, R., Kern, J., Singh, N., Iwashima, M., Kraj, P., and Ignatowicz, L. (2007). Nonself-antigens are the cognate specificities of Foxp3+ regulatory T cells. Immunity *27*, 493-504.

Peaudecerf, L., dos Santos, P.R., Boudil, A., Ezine, S., Pardigon, N., and Rocha, B. (2011). The role of the gut as a primary lymphoid organ: CD8alphaalpha intraepithelial T lymphocytes in euthymic mice derive from very immature CD44+ thymocyte precursors. Mucosal Immunol *4*, 93-101.

Pennington, D.J., Silva-Santos, B., Silberzahn, T., Escorcio-Correia, M., Woodward, M.J., Roberts, S.J., Smith, A.L., Dyson, P.J., and Hayday, A.C. (2006). Early events in the thymus affect the balance of effector and regulatory T cells. Nature *444*, 1073-1077.

Polansky, J.K., Kretschmer, K., Freyer, J., Floess, S., Garbe, A., Baron, U., Olek, S., Hamann, A., von Boehmer, H., and Huehn, J. (2008). DNA methylation controls Foxp3 gene expression. European journal of immunology *38*, 1654-1663.

Probst-Kepper, M., and Buer, J. (2010). FOXP3 and GARP (LRRC32): the master and its minion. Biol Direct *5*, 8.

Qureshi, O.S., Zheng, Y., Nakamura, K., Attridge, K., Manzotti, C., Schmidt, E.M., Baker, J., Jeffery, L.E., Kaur, S., Briggs, Z*., et al.* (2011). Trans-endocytosis of CD80 and CD86: a molecular basis for the cell-extrinsic function of CTLA-4. Science (New York, NY) *332*, 600-603.

Rubtsov, Y.P., Rasmussen, J.P., Chi, E.Y., Fontenot, J., Castelli, L., Ye, X., Treuting, P., Siewe, L., Roers, A., Henderson, W.R., Jr*., et al.* (2008). Regulatory T cell-derived interleukin-10 limits inflammation at environmental interfaces. Immunity *28*, 546-558.

Rudd, C.E., Taylor, A., and Schneider, H. (2009). CD28 and CTLA-4 coreceptor expression and signal transduction. Immunological reviews *229*, 12-26.

Rudra, D., deRoos, P., Chaudhry, A., Niec, R.E., Arvey, A., Samstein, R.M., Leslie, C., Shaffer, S.A., Goodlett, D.R., and Rudensky, A.Y. (2012). Transcription factor Foxp3 and its protein partners form a complex regulatory network. Nature immunology *13*, 1010-1019.

Rus, H., Cudrici, C., and Niculescu, F. (2005). The role of the complement system in innate immunity. Immunol Res *33*, 103-112.

Sakaguchi, S., Miyara, M., Costantino, C.M., and Hafler, D.A. (2010). FOXP3+ regulatory T cells in the human immune system. Nature reviews Immunology *10*, 490-500.

Salomon, B., Lenschow, D.J., Rhee, L., Ashourian, N., Singh, B., Sharpe, A., and Bluestone, J.A. (2000). B7/CD28 costimulation is essential for the homeostasis of the CD4+CD25+ immunoregulatory T cells that control autoimmune diabetes. Immunity *12*, 431-440.

Samstein, R.M., Josefowicz, S.Z., Arvey, A., Treuting, P.M., and Rudensky, A.Y. (2012). Extrathymic generation of regulatory T cells in placental mammals mitigates maternal-fetal conflict. Cell *150*, 29-38.

Sarris, M., Andersen, K.G., Randow, F., Mayr, L., and Betz, A.G. (2008). Neuropilin-1 expression on regulatory T cells enhances their interactions with dendritic cells during antigen recognition. Immunity *28*, 402-413.

Schilham, M.W., Wilson, A., Moerer, P., Benaissa-Trouw, B.J., Cumano, A., and Clevers, H.C. (1998). Critical involvement of Tcf-1 in expansion of thymocytes. J Immunol *161*, 3984-3991.

Schuster, M., Glauben, R., Plaza-Sirvent, C., Schreiber, L., Annemann, M., Floess, S., Kuhl, A.A., Clayton, L.K., Sparwasser, T., Schulze-Osthoff, K*., et al.* (2012). IkappaB(NS) protein mediates regulatory T cell development via induction of the Foxp3 transcription factor. Immunity *37*, 998-1008.

Sekiya, T., Kashiwagi, I., Yoshida, R., Fukaya, T., Morita, R., Kimura, A., Ichinose, H., Metzger, D., Chambon, P., and Yoshimura, A. (2013). Nr4a receptors are essential for thymic regulatory T cell development and immune homeostasis. Nature immunology *14*, 230-237.

Shannon, P., Markiel, A., Ozier, O., Baliga, N.S., Wang, J.T., Ramage, D., Amin, N., Schwikowski, B., and Ideker, T. (2003). Cytoscape: a software environment for integrated models of biomolecular interaction networks. Genome Res *13*, 2498-2504.

Shih, F.F., Mandik-Nayak, L., Wipke, B.T., and Allen, P.M. (2004). Massive thymic deletion results in systemic autoimmunity through elimination of CD4+ CD25+ T regulatory cells. The Journal of experimental medicine *199*, 323-335.

Smyth, G.K. (2004). Linear models and empirical bayes methods for assessing differential expression in microarray experiments. Stat Appl Genet Mol Biol *3*, Article3.

Solomon, B.D., Mueller, C., Chae, W.J., Alabanza, L.M., and Bynoe, M.S. (2011). Neuropilin-1 attenuates autoreactivity in experimental autoimmune encephalomyelitis. Proceedings of the National Academy of Sciences of the United States of America *108*, 2040-2045.

Solstad, T., Bains, S.J., Landskron, J., Aandahl, E.M., Thiede, B., Tasken, K., and Torgersen, K.M. (2011). CD147 (Basigin/Emmprin) identifies FoxP3+CD45RO+CTLA4+-activated human regulatory T cells. Blood *118*, 5141-5151.

Staal, F.J., Luis, T.C., and Tiemessen, M.M. (2008). WNT signalling in the immune system: WNT is spreading its wings. Nature reviews Immunology *8*, 581-593.

Steinke, F.C., Yu, S., Zhou, X., He, B., Yang, W., Zhou, B., Kawamoto, H., Zhu, J., Tan, K., and Xue, H.H. (2014). TCF-1 and LEF-1 act upstream of Th-POK to promote the CD4(+) T cell fate and interact with Runx3 to silence Cd4 in CD8(+) T cells. Nature immunology *15*, 646-656.

Strasser, A. (2005). The role of BH3-only proteins in the immune system. Nature reviews Immunology *5*, 189-200.

Tai, X., Cowan, M., Feigenbaum, L., and Singer, A. (2005). CD28 costimulation of developing thymocytes induces Foxp3 expression and regulatory T cell differentiation independently of interleukin 2. Nature immunology *6*, 152-162.

Taniuchi, I. (2009). Transcriptional regulation in helper versus cytotoxic-lineage decision. Current opinion in immunology *21*, 127-132.

Thedrez, A., Sabourin, C., Gertner, J., Devilder, M.C., Allain-Maillet, S., Fournie, J.J., Scotet, E., and Bonneville, M. (2007). Self/non-self discrimination by human gammadelta T cells: simple solutions for a complex issue? Immunological reviews *215*, 123-135.

Thornton, A.M., Korty, P.E., Tran, D.Q., Wohlfert, E.A., Murray, P.E., Belkaid, Y., and Shevach, E.M. (2010). Expression of Helios, an Ikaros transcription factor family member, differentiates thymic-derived from peripherally induced Foxp3+ T regulatory cells. J Immunol *184*, 3433-3441.

Tiemessen, M.M., Baert, M.R., Schonewille, T., Brugman, M.H., Famili, F., Salvatori, D.C., Meijerink, J.P., Ozbek, U., Clevers, H., van Dongen, J.J.*, et al.* (2012). The nuclear effector of Wnt-signaling, Tcf1, functions as a T-cell-specific tumor suppressor for development of lymphomas. PLoS biology *10*, e1001430.

Triulzi, T., Tagliabue, E., Balsari, A., and Casalini, P. (2013). FOXP3 expression in tumor cells and implications for cancer progression. Journal of cellular physiology *228*, 30-35.

Vaeth, M., Schliesser, U., Muller, G., Reissig, S., Satoh, K., Tuettenberg, A., Jonuleit, H., Waisman, A., Muller, M.R., Serfling, E.*, et al.* (2012). Dependence on nuclear factor of activated T-cells (NFAT) levels discriminates conventional T cells from Foxp3+ regulatory T cells. Proceedings of the National Academy of Sciences of the United States of America *109*, 16258-16263.

Van de Wetering, M., Castrop, J., Korinek, V., and Clevers, H. (1996). Extensive alternative splicing and dual promoter usage generate Tcf-1 protein isoforms with differential transcription control properties. Molecular and cellular biology *16*, 745-752.

van de Wetering, M., Oosterwegel, M., Dooijes, D., and Clevers, H. (1991). Identification and cloning of TCF-1, a T lymphocyte-specific transcription factor containing a sequence-specific HMG box. EMBO J *10*, 123-132.

van Loosdregt, J., Fleskens, V., Tiemessen, M.M., Mokry, M., van Boxtel, R., Meerding, J., Pals, C.E., Kurek, D., Baert, M.R., Delemarre, E.M.*, et al.* (2013). Canonical Wnt signaling negatively modulates regulatory T cell function. Immunity *39*, 298-310.

van Santen, H.M., Benoist, C., and Mathis, D. (2004). Number of T reg cells that differentiate does not increase upon encounter of agonist ligand on thymic epithelial cells. The Journal of experimental medicine *200*, 1221-1230.

Verbeek, S., Izon, D., Hofhuis, F., Robanus-Maandag, E., te Riele, H., van de Wetering, M., Oosterwegel, M., Wilson, A., MacDonald, H.R., and Clevers, H. (1995). An HMG-box-containing T-cell factor required for thymocyte differentiation. Nature *374*, 70-74.

Viglietta, V., Baecher-Allan, C., Weiner, H.L., and Hafler, D.A. (2004). Loss of functional suppression by CD4+CD25+ regulatory T cells in patients with multiple sclerosis. The Journal of experimental medicine *199*, 971-979.

Vignali, D.A., Collison, L.W., and Workman, C.J. (2008). How regulatory T cells work. Nature reviews Immunology *8*, 523-532.

Vivier, E., Tomasello, E., Baratin, M., Walzer, T., and Ugolini, S. (2008). Functions of natural killer cells. Nature immunology *9*, 503-510.

Vizcaino, J.A., Cote, R.G., Csordas, A., Dianes, J.A., Fabregat, A., Foster, J.M., Griss, J., Alpi, E., Birim, M., Contell, J.*, et al.* (2013). The PRoteomics IDEntifications (PRIDE) database and associated tools: status in 2013. Nucleic Acids Res *41*, D1063-1069.

von Boehmer, H. (2005). Unique features of the pre-T-cell receptor alpha-chain: not just a surrogate. Nature reviews Immunology *5*, 571-577.

von Boehmer, H., and Melchers, F. (2010). Checkpoints in lymphocyte development and autoimmune disease. Nature immunology *11*, 14-20.

Voo, K.S., Wang, Y.H., Santori, F.R., Boggiano, C., Arima, K., Bover, L., Hanabuchi, S., Khalili, J., Marinova, E., Zheng, B.*, et al.* (2009). Identification of IL-17-producing FOXP3+ regulatory T cells in humans. Proceedings of the National Academy of Sciences of the United States of America *106*, 4793-4798.

Weber, B.N., Chi, A.W., Chavez, A., Yashiro-Ohtani, Y., Yang, Q., Shestova, O., and Bhandoola, A. (2011). A critical role for TCF-1 in T-lineage specification and differentiation. Nature *476*, 63-68.

Wing, K., Onishi, Y., Prieto-Martin, P., Yamaguchi, T., Miyara, M., Fehervari, Z., Nomura, T., and Sakaguchi, S. (2008). CTLA-4 control over Foxp3+ regulatory T cell function. Science (New York, NY) *322*, 271-275.

Wirnsberger, G., Mair, F., and Klein, L. (2009). Regulatory T cell differentiation of thymocytes does not require a dedicated antigen-presenting cell but is under T cell-intrinsic developmental control. Proceedings of the National Academy of Sciences of the United States of America *106*, 10278-10283.

Wong, J., Obst, R., Correia-Neves, M., Losyev, G., Mathis, D., and Benoist, C. (2007). Adaptation of TCR repertoires to self-peptides in regulatory and nonregulatory CD4+ T cells. J Immunol *178*, 7032-7041.

Xu, Y., Banerjee, D., Huelsken, J., Birchmeier, W., and Sen, J.M. (2003). Deletion of beta-catenin impairs T cell development. Nature immunology *4*, 1177-1182.

Yadav, M., Stephan, S., and Bluestone, J.A. (2013). Peripherally induced tregs - role in immune homeostasis and autoimmunity. Front Immunol *4*, 232.

Yago, T., Shao, B., Miner, J.J., Yao, L., Klopocki, A.G., Maeda, K., Coggeshall, K.M., and McEver, R.P. (2010). E-selectin engages PSGL-1 and CD44 through a common signaling pathway to induce integrin alphaLbeta2-mediated slow leukocyte rolling. Blood *116*, 485-494.

Yang, Q., Monticelli, L.A., Saenz, S.A., Chi, A.W., Sonnenberg, G.F., Tang, J., De Obaldia, M.E., Bailis, W., Bryson, J.L., Toscano, K.*, et al.* (2013). T cell factor 1 is required for group 2 innate lymphoid cell generation. Immunity *38*, 694-704.

Yu, Q., Sharma, A., Ghosh, A., and Sen, J.M. (2011). T cell factor-1 negatively regulates expression of IL-17 family of cytokines and protects mice from experimental autoimmune encephalomyelitis. J Immunol *186*, 3946-3952.

Yu, Q., Sharma, A., Oh, S.Y., Moon, H.G., Hossain, M.Z., Salay, T.M., Leeds, K.E., Du, H., Wu, B., Waterman, M.L.*, et al.* (2009). T cell factor 1 initiates the T helper type 2 fate by inducing the transcription factor GATA-3 and repressing interferon-gamma. Nature immunology *10*, 992-999.

Yu, S., Zhou, X., Steinke, F.C., Liu, C., Chen, S.C., Zagorodna, O., Jing, X., Yokota, Y., Meyerholz, D.K., Mullighan, C.G.*, et al.* (2012). The TCF-1 and LEF-1 transcription factors have cooperative and opposing roles in T cell development and malignancy. Immunity *37*, 813-826.

Zhao, D.M., Thornton, A.M., DiPaolo, R.J., and Shevach, E.M. (2006). Activated CD4+CD25+ T cells selectively kill B lymphocytes. Blood *107*, 3925-3932.

Zheng, Y., Chaudhry, A., Kas, A., deRoos, P., Kim, J.M., Chu, T.T., Corcoran, L., Treuting, P., Klein, U., and Rudensky, A.Y. (2009). Regulatory T-cell suppressor program co-opts transcription factor IRF4 to control T(H)2 responses. Nature *458*, 351-356.

Zheng, Y., Josefowicz, S., Chaudhry, A., Peng, X.P., Forbush, K., and Rudensky, A.Y. (2010). Role of conserved non-coding DNA elements in the Foxp3 gene in regulatory T-cell fate. Nature *463*, 808-812.

Zhou, X., Bailey-Bucktrout, S.L., Jeker, L.T., Penaranda, C., Martinez-Llordella, M., Ashby, M., Nakayama, M., Rosenthal, W., and Bluestone, J.A. (2009). Instability of the transcription factor Foxp3 leads to the generation of pathogenic memory T cells in vivo. Nature immunology *10*, 1000-1007.

Zhou, X., Yu, S., Zhao, D.M., Harty, J.T., Badovinac, V.P., and Xue, H.H. (2010). Differentiation and persistence of memory CD8(+) T cells depend on T cell factor 1. Immunity *33*, 229-240.

10 Appendix

Table 1: Proteins significantly under-represented in T_{reg} cells. 51 significantly ($p < 0.05$, t-test) under-represented proteins in T_{reg} compared to T_{conv} cells identified via quantitative differential MS. All proteins have an average fold change of more than 1.5 and are sorted by p-value. If protein name was missing gene accession number was indicated.

	Protein name or Gene accession number	P-value	Average fold change T_{reg}/T_{conv} cells
1	Q8C5P7	0.0043	-9.58
2	THEMIS	0.0073	-4.12
3	SATB1	0.0074	-2.61
4	TCF7	0.0074	-2.62
5	SLC4A1	0.0074	-25.38
6	IDH2	0.0081	-2.28
7	ACTN1	0.0107	-2.04
8	PDK1	0.0118	-2.51
9	CKB	0.0118	-2.81
10	NME4	0.0118	-11.30
11	GPD2	0.0130	-1.93
12	RASGRP2	0.0130	-2.14
13	PDE3B	0.0130	-22.43
14	RASSF2	0.0135	-1.93
15	DNM2	0.0135	-14.54
16	CLYBL	0.0137	-2.80
17	SPTAN1	0.0153	-1.74
18	PADI2	0.0178	-5.29
19	DGKA	0.0193	-1.80
20	SPTBN1	0.0198	-1.71
21	FLNA	0.0203	-1.68
22	ARHGAP1	0.0204	-1.69
23	ITPR1	0.0235	-1.84
24	ITGB3	0.0235	-2.09
25	CLIP1	0.0236	-2.04
26	IKZF1	0.0239	-1.67
27	TTLL12	0.0293	-1.85

28	MADD	0.0312	-1.70
29	RANBP10	0.0312	-1.84
30	STK4	0.0327	-1.59
31	THY1	0.0327	-1.60
32	ADD1	0.0327	-1.71
33	STIM1	0.0336	-1.63
34	DENND2D	0.0339	-2.19
35	PRDX6	0.0343	-1.64
36	EPB4.1	0.0343	-1.71
37	HPCAL1	0.0358	-1.76
38	GPR132	0.0361	-1.77
39	EMB	0.0361	-1.88
40	MSRA	0.0375	-1.70
41	BPNT1	0.0378	-1.73
42	ACSF2	0.0378	-1.80
43	ACSS2	0.0419	-1.81
44	ADD3	0.0437	-1.75
45	ITK	0.0437	-2.57
46	GRAP2	0.0445	-1.54
47	GSN	0.0445	-2.27
48	EHD3	0.0453	-2.23
49	ARHGEF18	0.0473	-1.62
50	PAOX	0.0473	-1.85
51	FAM65B	0.0473	-1.85

Table 2: Proteins significantly over-represented in T_{reg} cells. 113 significantly ($p < 0.05$, t-test) over-represented proteins in T_{reg} compared to T_{conv} cells identified via quantitative differential MS. All proteins have an average fold change of more than 1.5 and are sorted by p-value. If protein name was missing gene accession number was indicated

	Protein name or Gene accession number	P-value	Average fold change T_{reg}/T_{conv} cells
1	NRP1	0.0016	18.04
2	CAPG	0.0016	7.23
3	ERGIC1	0.0035	6.33
4	LAD1	0.0043	15.70
5	FAM129A	0.0043	9.73
6	GSTO1	0.0043	8.96
7	GBP5	0.0043	4.41
8	SH3BGRL	0.0045	3.18
9	EPHX1	0.0073	2.78
10	IL2RB	0.0074	10.29
11	TNFRSF18	0.0074	9.99
12	Q4FZC9	0.0074	2.91
13	GALM	0.0074	2.72
14	SAMHD1	0.0074	2.62
15	DECR1	0.0081	3.26
16	NT5E	0.0094	7.28
17	PTMS	0.0094	2.36
18	SLC2A3	0.0107	3.97
19	SERPINB1A	0.0118	3.64
20	SNX18	0.0118	3.46
21	AHNAK	0.0118	3.25
22	S100A10	0.0118	3.05
23	H2-Q6	0.0118	2.36
24	CTSS	0.0118	2.14
25	LXN	0.0118	2.07
26	GSTA4	0.0125	17.27
27	ITGA6	0.0125	2.48
28	IIGP1	0.0129	2.43
29	HDGFRP3	0.0129	2.23
30	N6AMT2	0.0130	2.41

31	RLTPR	0.0130	2.19
32	REL	0.0131	2.37
33	AHCYL2	0.0131	2.14
34	NFKB2	0.0131	2.36
35	ALAD	0.0131	2.20
36	VWA5A	0.0134	2.16
37	PLP2	0.0135	2.86
38	ENO2	0.0137	12.93
39	CORO2A	0.0137	11.42
40	RCN1	0.0137	4.02
41	PAFAH1B3	0.0137	2.48
42	FOXP3	0.0174	9.80
43	CD86	0.0174	3.16
44	SAMHD1	0.0178	4.47
45	ENO3	0.0185	7.88
46	MYO18A	0.0185	1.88
47	GBP7	0.0196	1.88
48	PRKCA	0.0198	1.88
49	FABP5	0.0203	2.87
50	IKZF3	0.0205	2.44
51	GPHN	0.0213	2.13
52	GVIN1	0.0217	2.41
53	PLEKHO2	0.0219	2.54
54	LMNA	0.0219	1.79
55	IGTP	0.0219	1.78
56	HSPA4L	0.0236	2.05
57	TREX1	0.0236	1.85
58	TMEM173	0.0239	1.94
59	ISG20	0.0241	2.10
60	STAT5A	0.0241	1.97
61	GIMAP7	0.0241	1.88
62	NUCB2	0.0243	2.85
63	CLEC2D	0.0247	1.94
64	MARCKSL1	0.0281	2.54
65	ACOT9	0.0281	1.80
66	SHMT1	0.0291	1.63

67	LPXN	0.0312	2.53
68	SCAMP2	0.0312	1.68
69	SNX9	0.0321	4.83
70	SLAMF1	0.0329	2.63
71	TUBB2B	0.0329	2.38
72	HK2	0.0336	4.61
73	PRKRA	0.0337	2.49
74	RAB8B	0.0337	1.71
75	CD38	0.0339	6.68
76	SLC25A24	0.0339	2.09
77	REXO2	0.0343	1.88
78	STIM2	0.0358	2.88
79	NCF4	0.0358	2.85
80	ADPRH	0.0361	2.00
81	APOBEC3	0.0369	1.76
82	SERPINB6A	0.0378	2.12
83	CRMP1	0.0378	2.01
84	CCL21A	0.0378	1.95
85	CYB5A	0.0378	1.59
86	CCS	0.0381	1.77
87	TTC39B	0.0397	2.23
88	MGMT	0.0397	1.97
89	NFKB1	0.0397	1.56
90	LRRC8C	0.0403	1.57
91	HIP1R	0.0407	3.17
92	P2RX7	0.0419	5.43
93	NEK7	0.0419	1.62
94	HRSP12	0.0426	1.63
95	SAMSN1	0.0437	3.83
96	STAT5B	0.0437	1.52
97	LTA4H	0.0443	1.64
98	GATA3	0.0445	3.75
99	CD44	0.0445	2.52
100	POU2F2	0.0453	7.59
101	COMT	0.0453	1.95
102	LIG1	0.0453	1.86

103	RLTPR	0.0453	2.12
104	MYO1C	0.0456	2.81
105	AKNA	0.0458	1.65
106	UHRF2	0.0473	1.90
107	ALDH18A1	0.0473	1.63
108	ICAM1	0.0473	3.34
109	TRP53I11	0.0480	2.60
110	SIGIRR	0.0488	3.24
111	CD69	0.0493	3.23
112	LIPE	0.0498	2.09
113	SWAP70	0.0499	7.71

11 Abbreviations

%	Percent
α	alpha
β	beta
γ	gamma
δ	delta
°C	Degree Celsius
µg	Micro gram
µl	Micro liter
µm	Micro meter
µM	Micro Molar
$A_{2A}R$	adenosine receptor 2A
ACK buffer	Ammonium chloride–potassium bicarbonate cell lysis buffer
Ag	Antigen
APC	Antigen presenting cell
BCL-2	B cell lymphoma 2
BIO	6-Bromoindirubin-3′-oxime
BSA	*Bovine serum albumin*
Ca^{2+}	Calcium
cAMP	Cyclic adenosine monophosphate
CD	Clusters of differentiation
CDR	Complementarity determining region

CHIR99021	6-(2-(4-(2,4-Dichlorophenyl)-5-(4-methyl-1H-imidazol-2-yl)-pyrimidin-2-ylamino)ethyl-amino)-nicotinonitrile
CNS	Conserved non-coding region
CTL	Cytotoxic T lymphocyte
CTLA-4	Cytotoxic T lymphocyte associated antigen 4
Ctrl	Control
cTEC	Cortical thymic epithelial cell
DAPI	4’,6-Diamidino-2-Phenylindole
DC	Dendritic cell
DMEM	Dulbecco‘s Modified Eagle‘s Medium
DMSO	Dimethyl sulfoxide
DNA	Deoxyribonucleic acid
DN cell	CD4 and CD8 double-negative cell
DP cell	CD4 and CD8 double-positive cell
DTR	Diphteria toxin receptor
EDTA	Ethylenediaminetetraacetic acid
FACS	Fluorescence activated cell sorting
FBS	Fetal bovine serum
FDR	False discovery rate
FITC	Fluorescein isothiocyanate
FOXP3	Forkhead box 3
FRET	Förster resonance energy transfer
GARP	Glycoprotein-A repetitions predominant
GFP	Green fluorescent protein

GSK-3	Glycogen synthase kinase 3
HEPES	4-(2-hydroxylethyl)-1-piperazineethanesulfonic acid
HMG	High mobility group
IDO	Indoleamine 2, 3-dioxygenase
IFNγ	Interferon γ
Ig	Immunoglobulin
IL	Interleukin
ILC2	Innate group 2 innate lymphoid
IPEX	Immunodysregulation polyendocrinopathy, enteropathy X‑linked
iT_{reg} cell	(*in vitro*) Induced regulatory T cell
kD	Kilo dalton
LC-ESI-MS/MS	Liquid chromatography-electrospray ionization - tandem MS
LEF1	Lymphoid enhancer binding factor 1
LAG3	Lymphocyte associated gene 3
LN	Lymph node
MHC	Major histocompatibility complex
min	Minutes
ml	Milliliter
mM	Milli Molar
mRNA	Messenger RNA
mTEC	Medullary thymic epithelial cell
MS	Mass spectrometry
MSCV	Murine stem cell virus

NFAT	Nuclear factor of activated T cells
NLS	Nuclear localization signal
NK cell	Natural killer cell
NKT cell	Natural killer T cell
NRP1	Neuropilin 1
PBS	Phosphate buffered saline
PCR	Polymerase chain reaction
pT_{reg} cell	Peripheral induced regulatory T cell
qPCR	quantitative real-time PCR
RNA	Ribonucleic acid
RNAi	RNA interference
rpm	Rounds per minute
RT	Room temperature
SP cell	CD4 or CD8 single-positive cell
TCF1	T cell specific transcription factor 1
TCF7	Transcription factor 7
T_{conv} cell	Conventional T cell
TCR	T cell receptor
TG	Transgenic
TGFβ	Transforming growth factor β
T_H cell	T helper cell
T_{reg} cell	Regulatory T cell
tT_{reg} cell	Thymic derived regulatory T cell
YFP	Yellow fluorescent protein

12 Acknowledgments

Many people and institutions contributed to the success of my PhD studies and I want to take the opportunity to say THANK YOU:

- First, I want to thank my advisor Dr. Markus Feuerer for the support and advice that I received during my PhD project. Thank you for always finding the time to talk, discuss and analyze.
- Thanks to the current and past members of the Immune tolerance group, it was always a pleasure to work with you on a professional as well as on a personal level: Dr. David Richards, Kristin Lobbes, Dr. Jan Hettinger, Michael Delacher, Elke Lederer, Ann-Cathrin Joschko and Dr. Ulrike Träger.
- I want to thank our collaborators for their knowledge and support. We received expert assistance with the mass spectrometry experiments by Dr. Jenny Hansson and Dr. Jeroen Krijgsveld from the Genome Biology Unit at the EMBL in Heidelberg. The *Tcf7*$^{-/-}$ mouse was kindly provided by H. Clevers (Hubrecht Institute, Utrecht). A. Rudensky (Memorial Sloan Kettering Cancer Center, New York) provided us with Foxp3 YFP/Cre and Foxp3 DTR/GFP mice. J. Marie (Cancer Research Center, Lyon) contributed the TEa mice. The NIH tetramer core facility provided us with the CD1d tetramer.
- I also want to thank the members of my thesis defense and thesis advisory committees for their support: Prof. Dr. Viktor Umansky, Dr. Jeroen Krijgsveld, Prof. Dr. Ana Martin-Villalba and Prof. Dr. Stefan Wiemann.
- This work was financially supported by a stipend from the Helmholtz International Graduate School for Cancer research at the DKFZ.
- The Flow Cytometry and Animal core facilities at the DKFZ always provided excellent assistance.
- Last but not least, I want to thank my family and Michael for their continued support throughout the years. You are the best!